University of Alberta

Molecular Characterization of Human Phosphatidylethanolamine *N*-methyltransferase

by

David J. Shields ©

A thesis submitted to the Faculty of Graduate Studies and Research in partial fulfillment of the requirements for the degree of Doctor of Philosophy

Department of Biochemistry

Edmonton, Alberta

Spring 2003

National Library
of Canada

Acquisitions and
Bibliographic Services

395 Wellington Street
Ottawa ON K1A 0N4
Canada

Bibliothèque nationale
du Canada

Acquisisitons et
services bibliographiques

395, rue Wellington
Ottawa ON K1A 0N4
Canada

Your file Votre référence
ISBN: 0-612-82165-X
Our file Notre référence
ISBN: 0-612-82165-X

The author has granted a non-exclusive licence allowing the National Library of Canada to reproduce, loan, distribute or sell copies of this thesis in microform, paper or electronic formats.

The author retains ownership of the copyright in this thesis. Neither the thesis nor substantial extracts from it may be printed or otherwise reproduced without the author's permission.

L'auteur a accordé une licence non exclusive permettant à la Bibliothèque nationale du Canada de reproduire, prêter, distribuer ou vendre des copies de cette thèse sous la forme de microfiche/film, de reproduction sur papier ou sur format électronique.

L'auteur conserve la propriété du droit d'auteur qui protège cette thèse. Ni la thèse ni des extraits substantiels de celle-ci ne doivent être imprimés ou aturement reproduits sans son autorisation.

Canada

University of Alberta

Library Release Form

Name of Author: *David J. Shields*

Title of Thesis: *Molecular Characterization of Human Phosphatidylethanolamine N-methyltransferase*

Degree: *Doctor of Philosophy*

Year this Degree Granted: *2003*

Permission is hereby granted to the University of Alberta Library to reproduce single copies of this thesis and to lend or sell such copies for private, scholarly or scientific research purposes only.

The author reserves all other publication and other rights in association with the copyright in the thesis, and except as herein before provided, neither the thesis nor any substantial portion thereof may be printed or otherwise reproduced in any material form whatever without the author's prior written permission.

Crosses,
Innishannon,
Co. Cork,
Ireland

Date: Dec 23/2002.

University of Alberta

Faculty of Graduate Studies and Research

The undersigned certify that they have read, and recommend to the Faculty of Graduate Studies and Research for acceptance, a thesis entitled Molecular Characterization of Human Phosphatidylethanolamine *N*-methyltransferase submitted by David J. Shields in partial fulfillment of the requirements for the degree of Doctor of Philosophy.

Dennis E. Vance, Supervisor

Neale D. Ridgway, External Examiner

Luis B. Agellon

Roseline Godbout

Marek Michalak

Date: Dec. 09/2002

Abstract

Phosphatidylethanolamine *N*-methyltransferase (PEMT) catalyzes three sequential transmethylation reactions to produce phosphatidylcholine from phosphatidylethanolamine. *S*-adenosylmethionine (AdoMet) is the methyl group donor for each reaction. PEMT has been purified from rat liver and the encoding genes have been cloned, characterized and even disrupted in the mouse. This thesis details the first in depth study of human PEMT.

Spanning approximately 85 kB of a locus on the short arm of human chromosome 17, the *PEMT* gene contains 9 exons, 3 of which are untranslated. Differential processing yields 3 distinct transcripts, each of which contains a distinct untranslated exon at the 5' end. Liver is the primary site of *PEMT* expression while heart and testis contain a lower abundance of PEMT transcripts. Whereas the liver contains three different PEMT transcripts, in varying abundance, heart and testis contain only one and two transcripts respectively.

PEMT is primarily localized to the endoplasmic reticulum and mitochondrial-associated membranes of human liver. Four transmembrane regions span the membrane such that both the N- and C- termini of the enzyme are oriented towards the cytosol. Two intervening hydrophilic loops are localized in the ER lumen while the third connecting loop protrudes into the cytosol.

Using bioinformatic analysis of the predicted amino acid sequence of human PEMT, we identified two putative AdoMet binding motifs (^{98}Gx^{100}G &

^{180}E^{181}E). Site-directed mutagenesis experiments demonstrated the importance of the conserved motifs for PEMT specific activity. AdoMet binding assays of mutant recombinant PEMT derivatives established a role for the motifs in binding of the AdoMet moiety.

In summary, we have conducted a multi-faceted investigation of PEMT in the human species. Genomic characterization elucidated the structure of the PEMT gene and revealed that the gene is differentially processed in a tissue-specific manner. Biochemical analysis of human liver defined the subcellular distribution of PEMT and topographical studies resolved the orientation of the enzyme in the ER membranes. Using bioinformatic and biochemical approaches we identified two novel motifs that are essential for binding of the methyl group donor, AdoMet. Combined, these studies represent the first in depth examination of the methylation-based biosynthesis of PC in humans.

Table of Contents

1. Introduction 1

1.1 Phosphatidylcholine: an overview 2

1.1.1 Phosphatidylcholine: the molecule 2

1.1.2 PC as a Component of Membranes 2

1.1.3 PC as a Precursor of Signaling Molecules 3

1.1.4 PC and Lung Surfactant 4

1.1.5 Fates of Hepatic Phosphatidylcholine 4

1.1.5(a) Bile 4

1.1.5(b) Lipoproteins 5

1.1.6 Routes of PC Biosynthesis 6

1.2 The CDP-Choline Pathway for PC biosynthesis 7

1.2.1 Choline 7

1.2.2 Choline Transporter 9

1.2.3 Choline kinase 9

1.2.4 CTP:Phosphocholine Cytidylyltransferase 11

1.2.5 Cholinephosphotransferase 13

1.3 Transmethylation of PE: the PEMT pathway 14

1.3.1 PEMT 14

1.3.2 Substrates 14

1.3.3 Methyl group donor 17

1.3.4 Purification of PEMT 18

1.3.5 cDNA and gene cloning 20

1.3.6 Hepatic expression of PEMT 21

1.3.7 Subcellular localization of PEMT 22

1.3.8 Membrane topography 24

1.3.9 Regulation of PEMT activity 24

1.3.10 Genetic ablation of *Pemt* 25

1.3.10(a) The importance of choline 26

1.3.10(b) VLDL secretion 27

1.3.10(c) Bile PC composition 29

1.3.10(d) Regulation of plasma homocysteine levels 29

1.4 Thesis objectives 32

References 42

2. Genomic characterization of human PEMT 59

2.1 Introduction 60

2.2 Materials and Methods 63

2.2.1 Reagents 63

2.2.2 DNA isolation and Southern analysis 63

2.2.3 Cloning of the gene 64

2.2.4 Chromosomal mapping of the human PEMT gene 64

2.2.5 Gene structure 65

2.2.6 Distribution of PEMT transcripts 65

2.2.7 RNA extraction and RT-PCR analysis 66

2.2.8 Transcription start sites 67

2.2.9 Transcription factor binding sites 68

2.3 Results and discussion 69

2.3.1 Gene cloning 69

2.3.2 Chromosomal mapping of the human PEMT gene 69

2.2.3 Structure of the gene 70

2.3.4 Tissue distribution of PEMT transcripts 71

2.3.5 Transcript profile of PEMT 73

2.3.6 Identification of transcription start sites 75

2.3.7 Analysis of the putative promoter region 76

References 93

3. Membrane topography of human PEMT 96

3.1 Introduction 97

3.2 Materials and Methods 100

3.2.1 Reagents 100

3.2.2 Subcellular fractionation 100

3.2.3 Bioinformatic analysis 101

3.2.4 Recombinant plasmid construction 102

3.2.5 Cell culture and Transfections 103

3.2.6 PEMT activity assays 104

3.2.7 Immunoblot analysis 104

3.2.8 Endoproteinase LysC protection assays` 105

3.3 Results 107

3.3.1 Subcellular localization of PEMT 107

3.3.2 Predicted membrane topography of PEMT 107

3.3.3 Characterization of HA-tagged PEMT protein 108

3.3.4 Protease analysis of epitope-tagged PEMT 109

3.3.5 Evaluation of HA-tagged PEMT mutants 112

3.3.6 Protease protection analysis of HA-PEMT mutants 113

3.4 Discussion 116

References 135

4. Molecular dissection of the AdoMet binding site of PEMT 139

4.1 Introduction 140

4.2 Materials and Methods 143

4.2.1 Reagents 143

4.2.2 Bioinformatic analysis 143

4.2.3 Recombinant plasmid construction 144

4.2.4 Cell culture and Transfections 146

4.2.5 PEMT activity assays and Immunoblots 146

4.2.6 AdoMet binding assays 147

4.3 Results 149

4.3.1 Identification of a putative AdoMet binding motif 149

4.3.2 Conservative mutagenesis of the GxG motif 149

4.3.3 Conservative mutagenesis of ^{100}G abolishes AdoMet binding activity 150

4.3.4 Non-conservative and combinatorial mutations of the GXG motif 151

4.3.5 Non-conservative mutagenesis of ^{98}G reduces AdoMet binding activity 152

4.3.6 Identification of a second putative AdoMet binding motif 153

4.3.7 Mutagenesis of the di-glutamate motif decreases PEMT activity 154

4.3.8 Mutagenesis of the di-glutamate motif diminishes AdoMet binding activity 155

4.4 Discussion 156

References 175

5. Summary and Future Directions 178

References 184

List of Tables

Table 2.1	Oligonucleotides used in the genomic characterization of human PEMT	80
Table 2.2	Genomic Structure of Human PEMT	82

List of Figures

Fig. 1.1	Hepatic phosphatidylcholine biosynthesis	35
Fig. 1.2	Fates of choline	37
Fig. 1.3	CDP-choline pathway of PC biosynthesis	39
Fig. 1.4	PE biosynthetic pathways	41
Fig. 2.1	Chromosomal localization of the human PEMT gene as determined by FISH mapping	84
Fig. 2.2	Genomic organization of human PEMT	86
Fig. 2.3	Tissue-specific expression profile of PEMT	88
Fig. 2.4	Relative abundance of different PEMT mRNA isoforms in human liver, heart & testis	90
Fig. 2.5	Identification of the transcription start site and putative promoter region of the major PEMT transcript	92
Fig. 3.1	Subcellular localization of PEMT in human liver	122
Fig. 3.2	Hydropathy plot and predicted membrane topography of PEMT	124
Fig 3.3	Epitope-tagged PEMT protein is enzymatically active in transfected Cos-7 cells	126
Fig. 3.4	Luminal orientation of loop A and cytosolic orientation of the C-terminus as determined by protease protection analysis	128

Fig. 3.5	Epitope-tagged mutant PEMT derivatives retain enzymatic activity in transfected Cos-7 cells	130
Fig. 3.6	Protease protection analysis of the PEMT mutant CK2R2 confirms the cytosolic orientation of the C-terminus	132
Fig. 3.7	Luminal orientation of loops A and C demonstrated by protease protection analysis of PEMT mutant, AK2R2	134
Fig. 4.1	Interrelationships between the PEMT-catalyzed biosynthesis of PC and Hcy metabolism	162
Fig. 4.2	A putative AdoMet binding motif (GXG) is conserved in PEMT orthologues	164
Fig. 4.3	Conservative mutagenesis of the GXG motif alters PEMT specific activity and AdoMet-binding activity	166
Fig. 4.4	Non-Conservative and combinatorial mutagenesis of the GXG motif decreases PEMT specific activity and AdoMet-binding activity	168
Fig. 4.5	A putative AdoMet-binding motif (EE) is conserved in PEMT orthologues	170
Fig. 4.6	Site-directed mutagenesis of the di-glutamate motif decreases the enzymatic and AdoMet-binding activities of PEMT	172
Fig. 4.7	Model of the topographical organization of the AdoMet binding site of PEMT	174

Abbreviations

ACS	acyl-CoA synthetase
AdoHcy	*S*-adenosyl-homocysteine
AdoMet	*S*-adenosyl-L-methionine
ATP	adenosine triphosphate
BAC	bacterial artificial chromosome
cAMP	cyclic adenosine monophosphate
CD	choline deficient
cDNA	DNA complementary to mRNA
ChPT	cholinephosphotransferase
CK	choline kinase
CPT1	carnitine palmitoyltransferase I
CT	CTP:phosphocholine cytidylyltransferase
CTP	cytidine triphosphate
DAPI	4', 6-diamidin-2 phenylin-dol-dihydrochloride
dbEST	EST data base
DG	diacylglycerol
DNA	deoxyribonucleic acid
ER	endoplasmic reticulum
EST	expressed sequence tag
FISH	fluorescence in situ hybridization
GNMT	glycine *N*-methyltransferase
h	human

HA	haemagglutinin
Hcy	homocysteine
HDL	high density lipoprotein particles
ICMT	isoprenylcysteine carboxyl methyltransferase.
IP3	inositol triphosphate
kDa	kilodalton
LDL	low density lipoproteins
m	mouse
MAM	mitochondria-associated membranes
mRNA	messenger RNA
ORF	open reading frame
PAGE	polyacrylamide gel electrophoresis
PBS	phosphate buffered saline
PC	phosphatidylcholine
PCR	polymerase chain reaction
PDI	protein disulphide isomerase
PDME	phosphatidyldimethylethanolamine
PE	phosphatidylethanolamine
PEMT	phosphatidylethanolamine *N*-methyltransferase
PFGE	pulse field gel electrophoresis
PMME	phosphatidylmonomethylethanolamine
PKC	protein kinase C
PS	phosphatidylserine
PSS	phosphatidylserine synthase

RNA	ribonucleic acid
RT-PCR	reverse transcriptase-mediated PCR
SCAP	(SREBP) cleavage-activating protein
SDS	sodium dodecyl sulphate
SREBP	sterol regulatory element binding protein
TG	triacylglycerol
VLDL	very low density lipoprotein
5'UTR	5'untranslated region

Chapter 1

Introduction

1.1 Phosphatidylcholine: an overview

1.1.1 Phosphatidylcholine: the molecule

Phosphatidylcholine (PC) is the most abundant phospholipid in eukaryotic cells (1). Initially described in the 19th century as a component of egg yolk and named lecithin, PC has been the subject of intensive research since the 1950s when chemical synthesis of the molecule facilitated the resolution of its structure (2,3). This provided the impetus, and raw material, for future study. Structurally, this amphipathic phospholipid is composed of a glycerol backbone, to which are attached two fatty acyl chains, and a choline headgroup linked via a phosphodiester linkage (4,5).

Thus far, more than 100 different species of phospholipids have been found in mammalian cells (6). Differences in the specific combination of fatty acyl chains attached at the sn-1 and sn-2 positions of the glycerol moiety may contribute, at least in part, to determining the ultimate fate of each phospholipid species. It is now known that PC serves as the principal component of eukaryotic cellular membranes, as a precursor of signal transduction molecules, and as a key element of lipoproteins, bile and lung surfactant (7-10).

1.1.2 PC as a Component of Membranes

A primary function of PC is as a component of eukaryotic cellular membranes (7,11). PC constitutes between 25 and 55% of the eukaryotic membrane phospholipids, but in contrast, the majority of prokaryotes contain little if any PC in their membranes (12,13). Within eukaryotes, the PC content of different subcellular membranes varies widely. Whereas PC comprises as much as 60% of nuclear membranes, it may account for as little as 35% of the plasma membrane (14). This stark disparity in PC content may reflect differences in the properties of individual membranes such as fluidity and thickness, as well as the specific lipid and protein content that are requisite for the function of specific organelles.

1.1.3 PC as a Precursor of Signaling Molecules

The study of lipid mediators is an area of signal transduction that has exploded in recent years. The signaling roles of the inositol lipids and derivatives thereof, such as inositol triphosphate (IP3) and diacylglycerol (DG) have been well characterized and the focus of much investigation (15). However, PC is also a major precursor of signal transducing molecules, reviewed in (16). Cleavage by different phospholipases generates distinct signaling molecules that mediate specific downstream effects. For example, cleavage by phospholipase A_2 at the sn-2 position of PC may yield arachidonic acid and lysoPC (16). While arachidonic acid is a precursor of the eicosanoids, lysoPC is itself proposed to be a key molecule in signal transduction (17,18). Alternatively, phospholipase C-mediated hydrolysis of

PC yields DG, which activates the ubiquitous protein kinase, PKC (16). PC may also serve as a precursor for numerous other molecules implicated in signaling including, phosphatidic acid, lysophosphatidic acid, platelet activating factor and sphingomyelin (16,19-21).

1.1.4 PC and Lung Surfactant

PC serves as a crucial component of lung surfactant, which functions to maintain the alveolar structure during exhalation (22). Specifically, PC is proposed to reduce the surface tension at the air liquid interface on the surface of the alveoli (23). One distinctive characteristic of lung surfactant PC is that it is exclusively of the dipalmitoyl species, suggesting a specific role for this species of PC in lung function (23).

1.1.5 Fates of Hepatic Phosphatidylcholine

Although all nucleated metazoan cells synthesize PC to fulfill the structural and signal transducing requirements for this phospholipid, PC biosynthesis is highest in the liver (24). This increased PC biosynthetic capacity is necessary because the liver is the site of production of two PC-rich components, bile and VLDL particles (10,25).

1.1.5 (a) Bile

Bile is an integral component of the lipid metabolic process. Produced by the liver and secreted from the gall bladder, bile functions as a detergent in the intestinal tract where it enables the digestion and absorption of lipids, and fat-soluble molecules such as vitamins A, D, E and K (26). Intestinal digestion of lipids also provides a means to supply the surrounding tissues with essential fatty acids (27). While the primary active components of bile are the sterol-derived bile acids, other constituents include water (82%), phospholipids (4%), unesterified cholesterol (1%) and other solutes (1%) (26).

PC is the major phospholipid in bile while phosphatidylethanolamine and sphingomyelin are also present in smaller quantities (26,28). A member of the ATP-binding cassette-type transporters, mdr2, transports PC across the canalicular membrane of the liver and into bile. Genetic ablation of *Abcb4* that encodes mdr2, revealed that the biliary secretion of cholesterol, but not bile acids, is dependent on PC (29). Once secreted, the micellar action of PC protects the bile duct from the detergent action of the bile acids (30). Formation of PC-bile acid micelles also promotes the digestion of intestinal lipids (27).

1.1.5 (b) Lipoproteins

Lipoprotein particles are the other major fate of PC in the liver. Triacylglycerol (TG) and cholesteryl esters are transported in the peripheral

bloodstream as components of lipoprotein particles (25). PC and a derivative, lysoPC, facilitate the solubilization of lipoprotein particles by the formation of a surface monolayer that encompasses the TG and cholesteryl ester core (31). PC is the major phospholipid in lipoproteins, with levels varying from 60% in VLDL particles to 80% in HDL particles (32). Phosphatidylethanolamine, phosphatidylinositol, phosphatidylserine, sphingomyelin and ceramide are also found as components of VLDL particles (25). In addition to the structural role of PC in lipoproteins, the molecule also serves as a donor of fatty acyl groups for the formation of cholesteryl esters. In a reaction catalyzed by lecithin:cholesterol acyltransferase, fatty acyl moieties are transferred from the sn-2 position of PC to cholesterol to generate cholesteryl esters, which are components of the neutral lipid core in lipoproteins (33).

1.1.6 Routes of PC Biosynthesis

PC is primarily synthesized from one of two substrates, either from choline in a series of reactions catalyzed by the enzymes of the CDP choline pathway, or from phosphatidylethanolamine via three consecutive PEMT-catalyzed transmethylation reactions (7,34). Production of PC may also occur through base exchange of the choline head group or by the reacylation of lysoPC (35,36). However, the latter two routes are quantitatively insignificant compared to the primary biosynthetic pathways.

As organisms have evolved, the relative proportion of PC derived from the CDP-choline and PEMT pathways has changed significantly. For example, in prokaryotes, although PC is not a commonly synthesized phospholipid, the methylation based pathway accounts for the majority of PC synthesis (37-41). In yeast, both the CDP-choline and PEMT pathways are present and functional but the primary biosynthetic route for PC is still the PEMT pathway (42,43). This contrasts with rodents in which the CDP-choline pathway mediates the majority of PC biosynthesis (44). In fact, whereas the enzymes of the CDP-choline pathway are active in all nucleated cells, the PEMT-controlled pathway only contributes significantly to PC synthesis in liver (7,34). Nevertheless, even in the liver of rodents, the CDP-choline pathway accounts for up to 70% of PC synthesis (Fig. 1.1)(45-48).

1.2 The CDP-Choline Pathway for PC biosynthesis

1.2.1 Choline

Choline is the initial substrate for the CDP-choline pathway (Fig. 1.2). This quaternary amine is a common dietary component that is found in numerous foods, but is particularly enriched in beef liver, lettuce, cauliflower and peanuts (49). In 1998, the Food and Nutrition Board of the Institute of Medicine of the National Academy of Sciences classified choline as an

essential human nutrient (50). Dietary intake of choline is essential as the molecule is not synthesized *de novo* (51). Choline deficiency may arise during pregnancy or lactation, or in the starving or cirrhotic individual (52).

Although choline is the initial substrate for the CDP-choline biosynthesis pathway, PC is but one of the important fates of this soluble molecule (Fig. 1.3). Acetylation of choline in cells of the neuronal lineage produces the neurotransmitter acetylcholine. This reaction is catalyzed by the enzyme choline acetyltransferase. Upon intake, choline is preferentially directed to PC, and to acetylcholine in neurons, but quantitatively, acetylcholine is not a major fate of choline (53).

Excess choline undergoes oxidation to yield betaine, which serves as an osmolyte in the kidney, and as a methyl group donor in the liver (53). Betaine:homocysteine methyltransferase (BHMT) subsequently catalyzes the transfer of a methyl group from betaine to homocysteine, producing methionine (53). This reaction serves to replenish the methionine pool and facilitates the synthesis of *S*-adenosylmethionine, which provides methyl groups for the majority of methylation reactions (53). Choline may also be used to synthesize the choline-derived phospholipid, sphingomyelin as well as the signaling molecules, platelet-activating factor and sphingosylphosphorylcholine (52).

1.2.2 Choline Transporter

(UniGene Clusters Rn. 10336, Hs.179902)

For choline to be used as a substrate for the CDP-choline pathway, uptake by the cell is first required. Although the mechanistic details of the transport of choline into the cell have been the subject of some controversy, current evidence suggests the existence of at least two primary choline transporters: a high affinity sodium-dependent transporter and a low affinity sodium-independent transporter (54). Recently, the cloning of a human cDNA encoding CDw92, a member of the choline-like transporter family, was described (55). Further work demonstrated that the encoding gene is alternatively processed and that the CDw92 protein is an active transporter of choline (Bakovic, M., personal communication).

1.2.3 Choline Kinase

(E.C 2.7.1.32, UniGene Cluster Hs.77221)

Following transport into the cell, choline is phosphorylated by choline kinase (CK), the first enzyme of the CDP-choline pathway, to yield phosphocholine (Fig. 1.2)(56). Inverse regulation of CK and choline acetyltransferase, which makes acetylcholine, has been described (57). Several lines of evidence suggest a role for CK in mitogenesis. Both Ras and epidermal growth factor proteins stimulate CK activity, and increased

CK activity has been reported in tumors of the breast, lung, prostate and colorectal region (58-64).

Wittenberg and Kornberg first detected CK activity in yeast extracts in the 1950s (65). CK has since been purified from rat kidney, liver and brain, and appears to exist as several isoenzymes (66-70). Analysis of the purified proteins revealed that CK displays a certain lack of substrate specificity as the enzyme also phosphorylates ethanolamine (66-68).

Two choline kinase cDNAs (Chkα1 and Chkα2) have been cloned from a rat liver library, encoding proteins with predicted sizes of 50 kDa and 52 kDa respectively (71,72). The cDNAs differ in that the α2 cDNA contains an additional internal 45 nt segment, probably as a result of alternate processing of the encoding gene. A third cDNA (Chkβ) was cloned from a rat kidney library and encodes a protein with a predicted size of 42 kDa (73). The Chkβ cDNA is 57-59% homologous to the Chkα cDNAs. Mouse orthologues of the rat Chkα1, α2 and β cDNAs have also been cloned (74).

More recently, cloning of the murine *Chkα* and *Chkβ* genes was described and while each contains 11 exons, the *Chkα* gene encompasses 40 kB of genomic sequence whereas the *Chkβ* gene spans a mere 3.5 kB of the mouse genome (75). Interestingly, the murine *Chkβ* gene is located 560 bp upstream of the gene encoding the muscle isoenzyme of carnitine palmitoyltransferase I (CPT1), a key regulator of mitochondrial fatty acid

oxidation (75). The genes are similarly contiguous in the human genome and in fact a hybrid transcript containing exons from the human *CHKβ* and *CPT1* genes has been reported (76). Genetic disruption of each of the murine *Chk* genes is currently in progress (Ishidate, K., personal communication).

1.2.4 CTP:Phosphocholine Cytidylyltransferase (E.C 2.7.7.15, UniGene Clusters Hs.273558, Hs.132794)

Once phosphocholine is generated by choline kinase, it is converted to CDP-choline in a CTP-dependent reaction catalyzed by the enzyme, CTP:phosphocholine cytidylyltransferase (CT) (Fig. 2)(7,44). This reaction is regarded as the rate-limiting step in the CDP-choline pathway (77,78). Evidence to support this notion was derived from pulse-chase experiments in which rat hepatocytes were labeled with [*methyl*-^{3}H]choline; analysis of the metabolites of the CDP-choline pathway revealed that 95% of the radioactivity in the precursors was localized in phosphocholine (79).

Kennedy first described the CDP-choline pathway in the 1950s and CT was purified to homogeneity from rat liver, as a homodimer, three decades later (80-83). This facilitated the cloning of the Pcyt1α cDNA, which encodes a protein with a predicted molecular mass of 42 kDa (84). CT typically translocates from the ER or nuclear membranes, where it exists as a membrane-bound enzyme, to the cytosol where it is a soluble enzyme

(42). Five distinct functional domains have been identified in the CT protein, namely, an N-terminal domain that contains a nuclear localization signal, a catalytic domain, a phosphorylation domain and two lipid-binding domains (85-88). Although CT activity is regulated by phosphorylation and by the binding to lipids, CT may also be regulated at the transcriptional and post-transcriptional levels (89-94). Correlations between CT activity and transcription, and the specific phase of the cell cycle have also been described (95,96).

Two genes (*Pcyt1α* and *Pcyt1β*) have been cloned, which encode at least three CT isoforms, Pcyt1α, Pcyt1β1 and Pcyt1β2 (86,97-99). All isoforms contain the catalytic domain and the helical lipid-binding domain (86). Genetic disruption of the *Pcyt1α* gene has been carried out in macrophages using the Cre-lox method (100). Macrophages lacking the *Pcyt1α* gene display enhanced sensitivity to cholesterol loading (100). More recently, a mouse was generated in which the *Pcyt1α* gene was specifically ablated in the liver (Tabas, I., Vance, D.E., collaborative project). Phenotypic analysis is ongoing. The decision to generate models with a tissue-specific ablation of *Pcyt1α* was taken when the existence of the *Pcyt1β* gene was unknown. Hence, a global genetic ablation of the *Pcyt1α* gene was expected to be lethal. Genetic disruption of the *Pcyt1β* gene is in progress (Jackowski, S., personal communication).

1.2.5 Cholinephosphotransferase

(E.C 2.7.8.2, UniGene Cluster Hs.171889)

In the third and final reaction of the CDP-choline pathway, CDP-choline:1,2 diacylglycerol cholinephosphotransferase catalyzes the transfer of phosphocholine from CDP-choline to DG, producing PC and cytidine monophosphate (CMP) (Fig. 2)(81,101,102). Attempts at purification of the enzyme have not been successful, most likely due to the membrane-bound nature of the enzyme. However, an ethanolaminephosphotransferase enzyme with choline phosphotransferase activity has recently been purified to homogeneity from rat liver microsomes (103).

Three human cholinephosphotransferase cDNAs (CEPT1, CHPT1 and CHPT1β) have been cloned based on information from the NCBI expressed sequence tag databases (104,105). CEPT1 encodes a protein with a predicted molecular mass of 46.5 kDa that recognizes both CDP-choline and CDP-ethanolamine as phospho-base donors to DG (104). Thus, it appears that the CEPT1 enzyme can catalyze the synthesis of both PC and PE. In contrast the CHPT1 enzyme encodes a protein that specifically utilizes CDP-choline as substrate (105). The CHPT1 protein has a predicted molecular mass of 45.2 kDa and is 60% identical to CEPT1 at the amino acid sequence level (105).

Cloning of the human *CHPT1* gene has also been described; it contains 10 exons and spans 32 kB of genomic sequence (105). Alternate processing of the *CHPT1* gene appears to be responsible for the existence of two different CHPT1 transcripts (105). The transcripts differ in that CPT1β contains a 27 bp insert, which introduces a premature termination codon (105). A resulting truncated protein of 24.3 kDa is predicted but whether the protein is active has not been reported (105).

1.3 Transmethylation of PE: the PEMT pathway

1.3.1 PEMT

(EC 2.1.1.17, UniGene Cluster Hs.15192)

The enzyme PEMT catalyzes three sequential methylation reactions in the production of PC from phosphatidylethanolamine (34). Phosphatidylmonomethylethanolamine (PMME) and phosphatidyldimethylethanolamine (PDME) are the reaction intermediates (34). *S*-adenosylmethionine (AdoMet) is the methyl group donor and *S*-adenosylhomocysteine (AdoHcy) is produced with each transmethylation step (34).

1.3.2 Substrates

A first insight into the substrate of the PEMT pathway was provided by the work of Stetten in 1941, who demonstrated that rats fed [^{15}N]-ethanolamine produced a labeled form of what was described as choline phosphatidate (106). The nature of the substrate was later resolved by the work of Bremer and Greenberg who showed that the methylation substrate was in fact phosphatidylethanolamine (PE) (24). Although minor amounts of the products PMME and PDME are detectable following the methylation of PE, PC has been identified as the predominant reaction product (24,107). Each of the metabolites in the PEMT pathway has been proposed to stimulate PEMT activity (45). Addition of ethanolamine, monomethylethanolamine and dimethylethanolamine to hepatocytes caused elevated levels of PE, PMME and PDME respectively, and a concomitant increase in PEMT enzymatic activity resulted (45).

PE is derived from four main pathways (Fig. 1.4) (44). De novo synthesis of PE is conducted through the CDP-ethanolamine pathway, an analogous pathway to the CDP-choline pathway, but which utilizes ethanolamine as the initial substrate (88,108-111). PE may also originate from the decarboxylation of phosphatidylserine (PS), the reacylation of lyso-PE or as a result of the reaction of ethanolamine with PS (44,112,113).

Unlike mammals, plants do not appear to recognize PE as a methylation substrate (114). Instead, phosphoethanolamine (an intermediary of the PE biosynthetic pathway) is methylated to yield

phosphomonomethylethanolamine, phosphodimethylethanolamine and phosphocholine, which may subsequently be incorporated into PC (115-118). This occurs in plants such as *Daucus carota* (carrots), *Beta vulgaris* (sugarbeet), *Lemna paucicostata* (duckweed) and *Hordeum vulgare* (barley). In other plants, such as *Apium graveolens* (celery) and *Glycine max* (soybean), as well as carrots and barley, phosphomonomethylethanolamine is converted to PMME, which in turn can be sequentially methylated to produce PC (117-119).

One feature that distinguishes PEMT pathway-derived PC from that produced by the CDP-choline pathway is the fatty acid composition of the molecule (46). Whereas PEMT-derived PC contains more of the fatty acid species, 18:0 (stearic acid) and 20:4 (arachidonic acid), PC from the CDP-choline pathway is enriched in fatty acid species such as 16:0 (palmitic acid) and 18:0 (stearic acid) (46,120,121). Such diversity in the fatty acid species has been proposed to impact on the ultimate fate of PC from each pathway, as certain fatty acid species may be targeted for a specific biological function (46). For example, PEMT pathway-derived PC is enriched in arachidonic acid, which has a key role in signal transduction (17).

However, given that the fatty acid composition of PC may be quickly remodeled by the enzymatic activities of distinct acyltransferases and transacylases, the significance of disparate fatty acid species profiles in PC from different pathways must be evaluated (6). In a recent study,

molecular analysis of bile PC did not reveal differences in the acyl chain composition of PC derived from each pathway, suggesting that remodeling of PC must have taken place prior to secretion into bile (122). Interestingly, it has also been reported that PC synthesized by the methylation pathway is more actively metabolized than PC derived from choline (46). Thus, PEMT pathway-derived PC may not be targeted to a specific biological function *per se*, but rather may be preferentially utilized by the PC-remodeling/-metabolizing enzymes or directed to a PC pool targeted for remodeling/breakdown.

1.3.3 Methyl Group Donor

In the 1940's, it was observed by Du Vigneaud *et al.* that methyl groups in various metabolites were originating from methionine, but it wasn't until a decade later that Cantoni *et al.* identified Adomet as the methyl group donor (123,124). In 1959, Bremer and Greenberg demonstrated that PE is a methyl acceptor for AdoMet (24). AdoMet-dependent methyltransferases act on a panoply of substrates including DNA, RNA, lipids, proteins and small molecules such as glycine and guanidinoacetate (125). Methylation has been shown to occur on the oxygen and nitrogen atoms of substrates, and to a lesser extent on carbon and sulphur atoms (126). Several derivatives of folate as well as betaine may also serve as methyl group donors, but AdoMet is by far the most widely used transmethylation cofactor (127,128).

AdoMet-dependent methyltransferases comprise an assorted group of enzymes that have roles in cellular processes as diverse as cellular signaling, elimination of xenobiotics, protein synthesis and stabilization of RNA, DNA and proteins, but only six of the enzymes are true biosynthetic enzymes (125). However, the products of each biosynthetic reaction are essential for biological function; creatine, epinephrine, ubiquinone/coenzyme Q, melatonin and PC.

AdoMet synthetase (or methionine adenosyltransferase) catalyzes the synthesis of AdoMet from L-methionine and ATP in a ubiquitous two-step reaction (129-131). However, the majority of dietary methionine is converted to AdoMet in the liver (132,133). Although the liver actively takes up methionine, the issue of whether the liver may also take up AdoMet is controversial and has not been definitively proven (45,134,135). AdoMet concentrations are highest in the liver and kidney with lesser amounts in the heart, pancreas, skeletal muscle and brain (130). Increments in the cellular AdoMet concentration increase the AdoMet/AdoHcy ratio, which stimulates PEMT activity (135). Conversely, increases in the cellular AdoHcy concentration decrease the AdoMet/AdoHcy ratio, which inhibits PEMT activity (125,135,136).

1.3.4 Purification of PEMT

PEMT was purified to homogeneity from rat liver in the 1980s, almost three decades after the PEMT pathway was first described (137). The purification procedure exploited the fact that Triton X-100 solubilizes PEMT but does not render the integral membrane protein inactive (138). The purified enzyme was an 18.3 kDa protein that catalyzed the transmethylation of PE to yield PC (137). The purified enzyme preferentially methylated unsaturated PE species, with species containing two or more double bonds being optimally methylated (120). A single active site was proposed based on kinetic data (139). PEMT has a pH optimum of 10-10.5 but the physiological significance of this alkaline pH optimum is unknown (107,137,140). It has been proposed that such a pH may be reflective of the ionization state of the ethanolamine headgroup of PE (pK_a ~9.5) or of catalytic residues in the active site of PEMT (141).

Subsequent work has indicated that each of the PEMT orthologues appear to be similarly membrane bound with the exception of the *Rhodobacter sphaeroides* PEMT enzyme, which is localized in the cytosol (142). Purification of a PEMT enzyme from *Rhodobacter sphaeroides* as well as *Zymonas mobilis* has been completed (143,144). A *Clostridium beijerinckii* PEMT enzyme has been identified that only catalyzes the methylation of phosphatidylethanolamine, with the result that PMME, but not PC is generated (145). Similarly, PMME is the major product of the PE methylation pathway in *Dictyostelium discoideum* (146).

1.3.5 cDNA and Gene Cloning

A rat PEMT cDNA was cloned from a rat liver cDNA library using oligonucleotides based on the N-terminal sequence of the purified rat PEMT enzyme (147,148). The encoded protein has a predicted molecular mass of 22.3 kDa, and catalyzed the synthesis of PC from PE when expressed in a cell line that lacks the endogenous PEMT enzyme (148). Comparative sequence analysis of the yeast *PEM2* gene product and the predicted rat PEMT enzyme revealed 44% identity and 68% similarity between the predicted amino acid sequences (148,149).

Using a radiolabeled rat PEMT cDNA as probe, two λ clones and three P1 clones were isolated from mouse genomic DNA libraries (150). Southern analysis demonstrated that the cloned mouse *Pemt* was a single copy gene. Genomic characterization demonstrated that the gene spans at least 35 kB of mouse chromosome 11 and contains 7 exons (150). Genetic disruption of the murine gene has been completed and phenotypic analysis of the engineered animal will be discussed in a subsequent section (151).

In the yeast *Saccharomyces cerevisiae*, the PE-methylation pathway is the predominant route for PC biosynthesis whereas the CDP-choline pathway serves in an auxiliary capacity (42,43). Two genes encoding PEMT enzymes have been cloned by genetic complementation (152). The *PEM1*-encoded PE methyltransferase catalyzes the first methylation reaction while

the *PEM2*-encoded phospholipid methyltransferase catalyzes the second and third reactions (149,153,154). The *PEM1*- and *PEM2*-encoded enzymes are predicted to be 101.2 and 23.2 kDa respectively, and are only 9.3% identical at the amino acid level (43). Genes encoding PEMT enzymes have also been cloned from *Schizosaccharomyces pombe, Rhodobacter sphaeroides, Acetobacter aceti* and *Sinorhizobium meliloti* (37,155-157)

1.3.6 Hepatic Expression of PEMT

Bremer and Greenberg first reported that the liver is the site of highest PEMT activity in the 1950s (158). Subsequent analyses confirmed the tissue-specific expression pattern of PEMT (148). Although PEMT activity has been reported in numerous extra-hepatic tissues, the activities in those tissues are a mere fraction of those reported for liver (1,159-164). Analysis of the murine PEMT gene promoter sequence identified several canonical binding sites for transcription factors that might mediate liver-specific expression, including HNF5 and C/EBP (150). However, specific factors that mediate the tissue expression profile of PEMT remain to be identified.

PEMT expression commences at birth in rats, with an attendant sharp increase in PEMT mRNA levels, protein abundance and PEMT specific activity (165). Prior to birth, when the rat liver is actively growing, PEMT protein and transcripts are absent (165). Thus, there exists an inverse

correlation between PEMT activity and the rate of liver development. Several lines of evidence have been presented that corroborate the observed inverse correlation between PEMT expression and hepatocyte growth and differentiation.

Partial hepatectomized rats display a severe decrease in both PEMT activity and immunoreactive PEMT protein (166). The observed decrement in enzymatic activity and protein abundance is most pronounced 24 h post hepatectomy, when liver regeneration is most active (166). Expression profiling studies of paired clinical hepatocellular carcinoma samples and distal non-cancerous samples from the same patients revealed a 3.54-fold reduction in PEMT mRNA levels in the tumorous samples (167).

A significant reduction in PEMT activity and protein is also evident in rat models of lead nitrate-induced hyperplasia, chemically induced hepatic tumorigenesis and aflatoxin-induced hepatocellular carcinoma (168-170). In contrast, the enzymatic activity of CT, the rate-limiting enzyme in the CDP-choline pathway, was elevated in each model (166,168,169). Thus, the enzymatic activities of the PC biosynthetic pathways may be reciprocally regulated. As yet, it is unresolved whether PEMT functions as a tumor suppressor in instances of liver carcinoma or if expression of PEMT is simply down regulated during periods of increased hepatocyte proliferation.

1.3.7 Subcellular Localization of PEMT

Early reports localized PEMT activity to the 100,000 × *g* or microsomal fraction of rat liver homogenates (24). Further biochemical analyses of liver, using sucrose and Percoll gradients indicated that the majority of PEMT activity is localized to the endoplasmic reticulum (ER) and a subfraction of the ER that cofractionates with mitochondria; mitochondria associated membranes (MAM) (148,171,172). Although PEMT activity is distributed between the ER and MAM fractions, only the isoform designated PEMT2, in the MAM fraction, is immunoreactive with an antibody raised against a C-terminal rat PEMT peptide (148). The ER-specific isoform designated PEMT1 is not immunoreactive against the anti-peptide antibody (148). The difference between the two rat PEMT isoforms is unknown.

An ER/MAM-localization for PEMT positions the enzyme at one of the major sites of lipid biosynthesis within the cell. Enzymes of several lipid biosynthetic pathways have been localized to this subcompartment, including cholinephosphotransferase, ethanolaminephosphotransferase, diacylglycerol acyltransferase, glycerol-3-phosphate acyltransferase, Acyl-CoA synthetase (ACS) 1 and ACS 4, 3-hydroxy-3-methylglutaryl-CoA reductase, phosphatidylserine synthase (PSS) 1 and PSS 2 as well as enzymes required for the synthesis of glycosylphosphatidylinositols (172-176). More recently, PEMT activity has also been reported on the bile canalicular membranes, suggesting a possible role for PEMT in bile homeostasis (177).

1.3.8 Membrane Topography

Purification of the rat PEMT enzyme confirmed the membrane-bound nature of the protein (137). Subsequent biochemical fractionation studies of rat liver revealed that the enzyme is enriched in regions of the endoplasmic reticulum (148). However, the exact topographical orientation of the protein within the membranes of the ER has not been elucidated. Early studies on the orientation of the catalytic site in rat liver microsomes yielded conflicting results. One study suggested that the first enzymatic reaction takes place on the inner leaflet while the subsequent reactions occur on the outer surface of the microsomes (178). In contrast, separate studies suggested that the PEMT reactions take place in their entirety, on the external surface of the microsomes (179,180). Thus, the membrane topography of PEMT remains unresolved. As the topographical studies were based on trypsin proteolysis of microsomal membranes, domains other than the catalytic site, which are required for the structural integrity and hence the activity of the enzyme may have been destroyed.

1.3.9 Regulation of PEMT activity

As described previously, PEMT activity is modulated at least in part by substrate concentrations and the cellular AdoMet/AdoHcy ratio (45,135). Developmental regulation of PEMT expression has also been described and PEMT mRNA and protein levels as well as PEMT specific activity are inversely correlated with the rate of hepatic growth and differentiation (165-170).

Reciprocal regulation of the CDP-choline and PEMT pathways occurs in the differentiating hepatocyte (166,168,169). Similar reciprocal regulation of the two pathways is mediated by long chain fatty acids, which inhibit PEMT activity but stimulate the translocation to membranes and enzymatic activity of CT (181).

Numerous studies in the 1980s focused on the post-translational regulation of PEMT but a series of conflicting results were generated. The role of cyclic AMP (cAMP)-dependent mechanisms was investigated extensively, using cAMP analogues, glucagon and the β-adrenergic agonist, isoprenaline. However, results "demonstrating" direct stimulation or inhibition of PEMT activity by each agonist were reported in almost equal measure, and a consensus regarding the post-translational regulation of PEMT has not been reached (182-187).

Purification of the rat PEMT enzyme facilitated in vitro phosphorylation studies of the protein (137). Although the purified enzyme was phosphorylated on a serine residue by the cAMP-dependent protein kinase *in vitro*, an associated change in PEMT activity did not result (188). Thus, a defined post-translational regulatory mechanism for PEMT has not been elucidated.

1.3.10 Genetic Ablation of Pemt

Following the cloning of the murine *Pemt* gene, a targeting vector was constructed for genetic ablation of the methyltransferase in the mouse. The targeting vector disrupted the second murine exon, which encodes the translation initiation codon (150,151). Mice homozygous for a disrupted *Pemt* allele were generated and the animals did not display any overtly abnormal phenotype (151).

1.3.10 (a) The Importance of Choline

When the *Pemt* disruptant mice were subjected to a choline deficient diet, primary liver failure resulted (189). Provision of choline to the mice on day 4, following a 3 day regimen of choline deficiency, rescued the animals from the diet-induced liver failure (190). Thus, early choline-deficiency mediated effects on the livers of *Pemt* disruptant animals may be reversible (190). Choline deficiency perturbs two major tenets of PC biosynthesis. Depletion of dietary choline reduces the levels of the initial substrate of the CDP-choline pathway, but also removes one of the methyl group donors (betaine) that facilitate replenishment of the methionine pool (49).

Under normal conditions, PC synthesized by the PEMT pathway may be hydrolyzed to produce choline but this is not an option in the PEMT deficient animal. Thus, the two primary biosynthetic routes for PC are independently disrupted and the animal cannot generate the essential phospholipid, PC.

In liver, it is estimated that 60% of free choline is oxidized to betaine (191). Subsequently, the sulfur-containing amino acid, homocysteine is remethylated (using betaine as methyl donor) to produce methionine, a precursor of AdoMet (131). Choline-derived methyl groups are incorporated into PC via the PEMT-catalyzed AdoMet-dependent transmethylation reaction (192). However, the liver is the site of numerous AdoMet-dependent methylation reactions and choline-derived methyl groups may be incorporated into substrates of these reactions also (133). It is unknown whether choline deficiency in the *Pemt* "knockout" mouse causes changes in the methylation of substrates other than PE, and if such changes may contribute to choline-deficiency induced primary liver failure.

1.3.10 (b) VLDL Secretion

Analysis of secreted lipoproteins from hepatocytes of mice with a wildtype or disrupted *Pemt* gene, revealed a 50% decrease in triacylglycerol (TG) secretion (193). Hepatocyte PC levels and PC secretion were unchanged, suggesting that PEMT activity may have a role in assembly or secretion of the lipoprotein particles as opposed to PEMT-pathway-derived PC being an essential component of the particle (193). Fractionation studies demonstrated that the reduction in TG secretion occurred in the very low density lipoprotein (VLDL) and low density lipoprotein (LDL) particles (193). ApoB100, a key structural protein in lipoproteins, was reduced by 70% in

the VLDL/LDL fractions, whereas levels of ApoB48, an RNA edited version of ApoB100, were unchanged (193).

Although VLDL/LDL secretion was diminished in hepatocytes from *Pemt* disruptant mice, it is noteworthy that changes in secretion were evident in male mice but not female mice (193). Moreover, the altered lipoprotein secretion occurred in male mice that were subjected to a high fat/high cholesterol diet, but not those fed a chow diet (193). As ablation of the *Pemt* gene caused gender-specific changes in lipoprotein secretion, this suggests that PEMT is regulated in a gender-specific fashion or it may reflect the interplay of PEMT with other gender-specific facets of lipoprotein metabolism. A gender specific role for PEMT in lipoprotein metabolism corroborates previously observed differences between the PEMT enzyme in male and female mice. Although PEMT activity is similar between male and female mice, liver homogenate protein from female mice displays approximately two-fold more immunoreactivity with the anti-peptide rat PEMT antibody than homogenates from male mice (Shields, D.J., unpublished results).

A similar dichotomy was reported in rats fed a choline deficient diet (194). Choline deficiency caused an increase of 34% in male hepatic PEMT activity but the female hepatic PEMT activity was unchanged (194). Regulation of plasma VLDL levels has also been shown to occur in a gender-specific manner in both rodents and humans (195,196). Thus, although

PEMT may be required for optimal VLDL secretion in male mice, the exact mechanism underlying this regulation remains to be elucidated.

1.3.10 (c) Bile PC Composition

PC synthesized by the liver is primarily directed to lipoprotein particles or bile. *Pemt* wildtype and *Pemt* deficient mice were examined to determine if PEMT pathway-derived PC is required to fulfill the bile PC requirements (122). However, bile PC content was unchanged whether the PEMT pathway was intact or absent (122). In contrast, wildtype mice fed a choline deficient diet displayed a 40% reduction in bile PC levels (122). As discussed earlier, administration of a choline deficient diet may have effects on both the CDP-choline and PEMT pathways, thus this result does not definitively prove that CDP-choline pathway-derived PC is necessary for bile PC content. Rather, it suggests that diminished hepatic PC biosynthesis causes a reduction in bile PC concentrations. Furthermore this can be interpreted to mean that although the liver synthesizes large amounts of PC, much of which is targeted to bile and VLDL particles, bile may not necessarily be an *a priori* fate for hepatic PC in times of dietary stress.

1.3.10 (d) Regulation of Plasma Homocysteine Levels

In the methylation–dependent synthesis of PC, the enzyme PEMT catalyzes the transfer of a methyl group from AdoMet to PE; with the result

that one molecule of AdoHcy is also generated with each transmethylation reaction (34). This AdoHcy molecule is hydrolyzed to adenosine and homocysteine (197). Subsequently, the homocysteine molecule is targeted to one of three major fates; homocysteine may enter the transsulfuration pathway to form cysteine, undergo remethylation to form methionine or be exported into the extracellular space (plasma or urine)(198).

Plasma homocysteine levels are reduced by approximately 50% in mice lacking a functional *Pemt* gene (199). Ectopic expression of PEMT in a hepatoma cell line that lacks endogenous PEMT activity resulted in a significant increase in the secretion of homocysteine into the medium (199). Combined, these results suggest a novel role for PEMT in the regulation of homocysteine levels.

Glycine *N*-methyltransferase (GNMT) comprises approximately 1% of the total soluble proteins in the liver (200). GNMT catalyzes the AdoMet-dependent synthesis of sarcosine from glycine, with the concomitant production of one AdoHcy molecule, and is proposed to exist to maintain the AdoMet/AdoHcy ratio (201). Excess methyl groups in the form of methionine, choline or betaine are metabolized to sarcosine via the GNMT-catalyzed reaction (132,202). However, a role for other AdoMet-dependent methyltransferases in the regulation of homocysteine levels was previously undocumented. Data from the PEMT-deficient animal suggest that the PE-

methyltransferase may be a significant biological modulator of hepatic one carbon metabolism.

1.4 Thesis Objectives

PEMT is an AdoMet-dependent methyltransferase that catalyzes the synthesis of the essential biomolecule, PC. Early work on PEMT focused on the methyltransferase reaction and regulation of enzymatic activity. Over the last 15 years however, significant advances have been made in our knowledge of the PEMT pathway, with the purification to homogeneity of the enzyme and the subsequent cloning of the rat cDNA and murine PEMT gene. Genetic disruption of the murine gene yielded an animal model upon which much of the recent work on PEMT has been based. This thesis represents the next major step in the advancement of this field; we sought to conduct the first detailed examination of PEMT in *Homo sapiens.* Specifically, our objective was to fulfill the following aims:

- To characterize the human PEMT genomic structure and locus.
- To elucidate the subcellular localization and membrane topography of the encoded enzyme.
- To identify specific PEMT residues that binds the methyl group donor, AdoMet.

Cloning of the human gene will enable the analysis of PEMT expression and allow us to determine if the human PEMT is also expressed in a tissue-specific manner. Characterization of the genomic locus will identify contiguous genes and allow us to evaluate the impact of the

genomic context on PEMT expression. Furthermore, resolution of the PEMT genomic structure will facilitate the design and future development of engineered models for the analysis of human PEMT expression and enzymatic activity.

Purification of PEMT revealed it to be an integral membrane enzyme but preliminary studies to elucidate the topography of the enzyme proved inconclusive. Resolution of the membrane topography of PEMT will provide the basis for the identification of the catalytic site and putative sites of post-translational regulation. A topographical model would also represent the first steps towards the structural resolution of the PEMT enzyme.

Disruption of the murine PEMT gene caused a 50% decrease in plasma homocysteine levels. Elevated plasma homocysteine levels are an independent risk factor for cardiovascular disease. Identification of residues essential for the binding of AdoMet will not only resolve one facet of the enzyme catalytic site, but will also provide insight into the mechanism by which PEMT regulates homocysteine levels. Combined, these data will greatly enhance our understanding of both the PEMT-mediated regulation of plasma homocysteine levels, and the methylation-dependent synthesis of the essential biomolecule, PC.

Figure 1.1 Hepatic PC Biosynthesis

The enzymes of the PEMT and CDP-choline pathways mediate the majority of hepatic PC biosynthesis. In the PEMT pathway, phosphatidylethanolamine is sequentially methylated to form phosphatidylmonomethylethanolamine (PMME), phosphatidyldimethylethanolamine (PDME) and PC. The enzymes of the PEMT pathway catalyze 30% of hepatic PC biosynthesis, while the CDP-choline pathway accounts for the remaining 70% of hepatic PC biosynthesis.

Choline is the substrate for the CDP-choline pathway; choline kinase catalyses the phosphorylation of choline to form phospho-choline, which is converted to CDP-choline in a CTP-dependent reaction catalyzed by the enzyme, CTP:phosphocholine cytidylyltransferase. CDP-choline:1,2 diacylglycerol cholinephosphotransferase catalyzes the final reaction of the CDP-choline pathway, in which phosphocholine is transferred from CDP-choline to DG, producing PC and cytidine monophosphate (CMP).

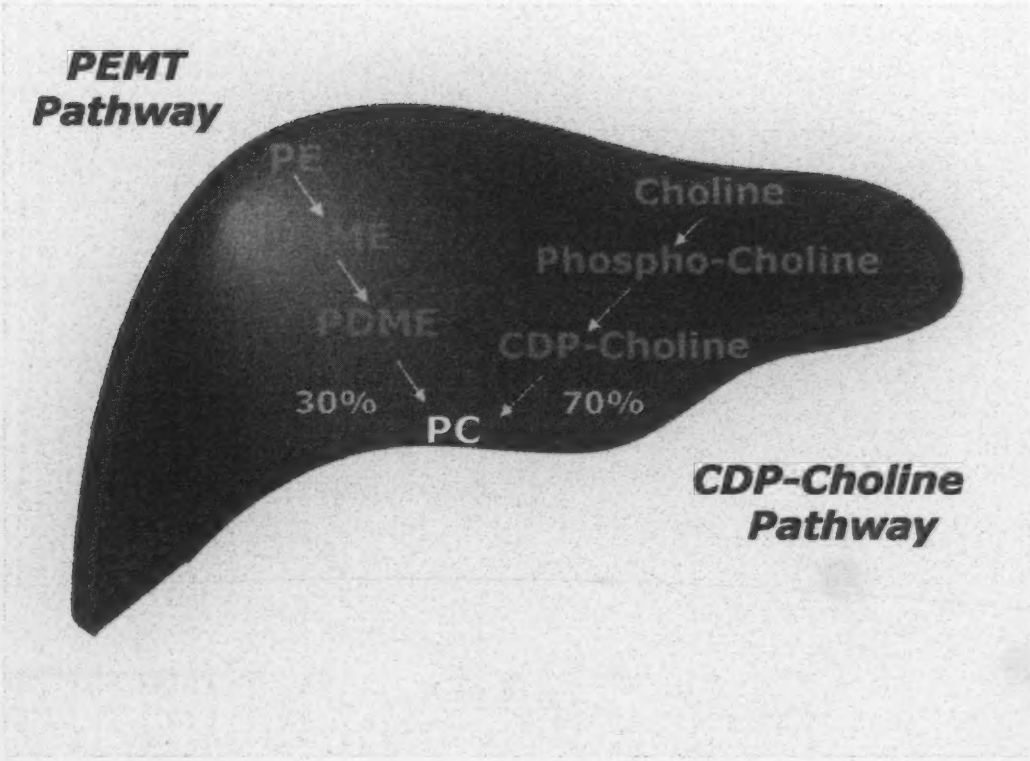
PEMT
Pathway
PE
ME
PDME
30%
PC
Choline
Phospho-Choline
CDP-Choline
70%
CDP-Choline
Pathway

Figure 1.2 Fates of Choline

Choline serves as the precursor of several distinct classes of molecules in the cell. Specific fates include the structural lipids, phosphatidylcholine and sphingomyelin, and the signaling molecules, platelet activating factor and sphingosylphosphorylcholine. Choline can also be oxidized to form the osmolyte and methyl donor, betaine, or acetylated to produce the neurotransmitter, acetylcholine. (Fig. from Blusztajn, J. K., (1998), *Science*, **281**, 794-795.)

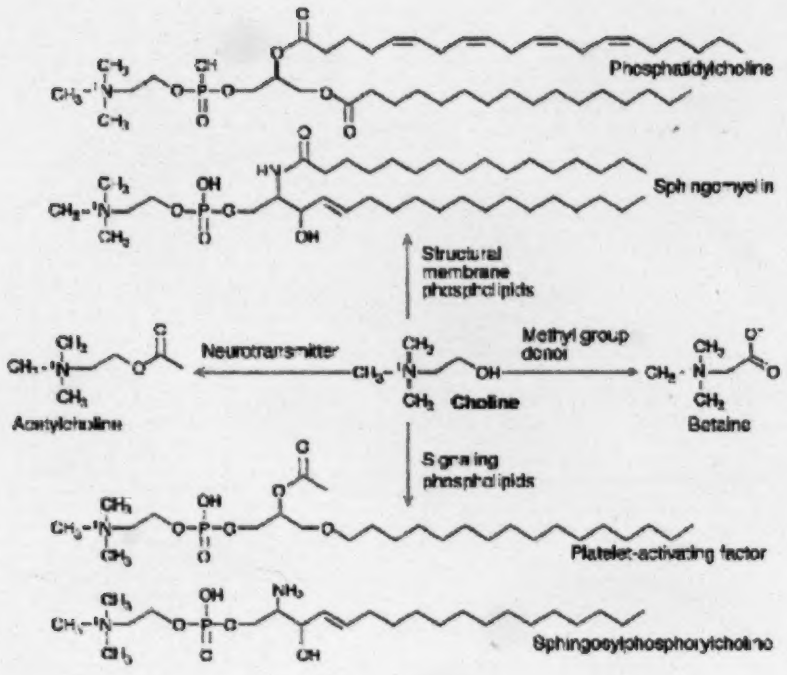
Phosphatidylcholine
Sphingomyelin
Structural membrane phospholipids
Neurotransmitter
Methyl group donor
Acetylcholine
Choline
Betaine
Signaling phospholipids
Platelet-activating factor
Sphingosylphosphorylcholine

Figure 1.3 CDP-Choline Pathway of PC Biosynthesis

Choline is phosphorylated by choline kinase (CK) to produce phosphocholine. CTP:phosphocholine cytidylyltransferase (CT) catalyzes the rate-limiting step in the pathway. Translocation of CT between membrane-bound and soluble forms is regulated as shown. The final reaction of the pathway is catalyzed by CDP-choline:1,2 diacylglycerol cholinephosphotransferase (CPT). (Fig. from Vance, D.E., (2002) in *Biochemistry of Lipids, Lipoproteins and Membranes* (Vance, D. E., and Vance, J. E., eds), 4 Ed., pp. 205-232, Elsevier, Amsterdam)

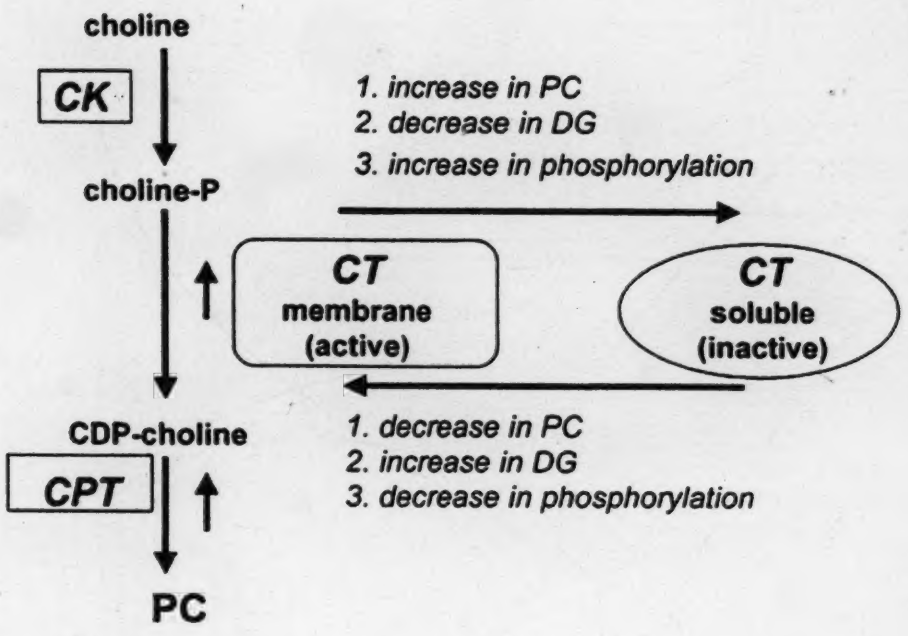
choline
CK
choline-P
CDP-choline
CPT
PC
CT
membrane
(active)
CT
soluble
(inactive)
1. increase in PC
2. decrease in DG
3. increase in phosphorylation
1. decrease in PC
2. increase in DG
3. decrease in phosphorylation

Figure 1.4 PE Biosynthetic Pathways

Four principal pathways are utilized in the synthesis of PE. Numbers denote the catalytic enzymes. 1) ethanolamine (choline) kinase, 2) CTP-phosphoethanolamine cytidylyltransferase, 3) CDP-ethanolamine: 1,2-diacylglycerol ethanolaminephosphotransferase, 4) PS synthase, 5) PS decarboxylase, 6) phospholipase A_2, 7) acyl-CoA:lyso-PE acyltransferase. (Fig. from Vance, D.E., (2002) in *Biochemistry of Lipids, Lipoproteins and Membranes* (Vance, D. E., and Vance, J. E., eds), 4 Ed., pp. 205-232, Elsevier, Amsterdam)

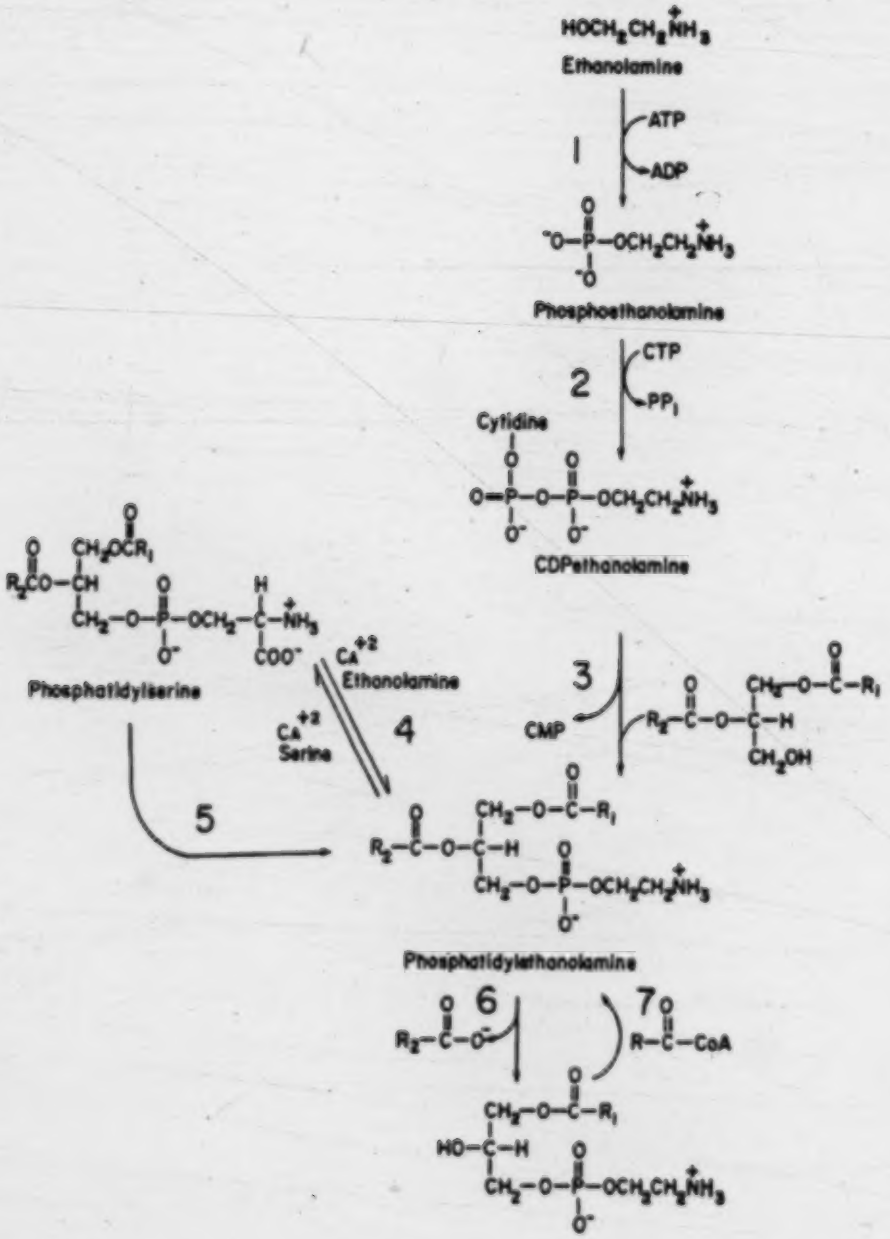
Ethanolamine
ATP
ADP
1
Phosphoethanolamine
CTP
PPi
2
Cytidine
CDPethanolamine
Phosphatidylserine
Ca+2
Ethanolamine
Ca+2
Serine
4
3
CMP
5
Phosphatidylethanolamine
6
7
CoA

References

1. Ridgway, N. D. (1989) in *Phosphatidylcholine Metabolism* (Vance, D. E., ed), pp. 103-120, CRC, Boca Raton, FL.

2. Gobley, M. (1850) *J. Pharm. Chim.* **17**, 401-407

3. Baer, E., and Kates, M. (1950) *J. Amer. Chem. Soc.* **72**, 942-949

4. Diakonow, C. (1868) *Zbl. Med. Wiss.* **2**, 434-435

5. Strecker, A. (1868) *Ann.Chem. Pharm.* **148**, 77-90

6. Yamashita, A., Sugiura, T., and Waku, K. (1997) *J. Biochem. (Tokyo)* **122**, 1-16.

7. Kent, C. (1997) *Biochim. Biophys. Acta.* **1348**, 79-90.

8. Exton, J. H. (1994) *Biochim. Biophys. Acta.* **1212**, 26-42.

9. Mathur, S. N., Born, E., Murthy, S., and Field, F. J. (1996) *Biochem. J.* **314**, 569-75.

10. Graham, J., Ahmed, H., and Northfield, T. (1989) in *Trends in Bile Acid Research.*, pp. 177-187, Kluwer Academic Publishers, Dordrecht

11. Henry, S. A., and Patton-Vogt, J. L. (1998) *Prog. Nucleic. Acid. Res. Mol. Biol.* **61**, 133-79

12. Ansell, G. B., and Spanner, S. (1982) in *Phospholipids* (Hawthorne, J. N., and Ansell, G. B., eds), pp. 1-49, Elsevier, Amsterdam

13. Heath, R. J., Jackowski, S., and Rock, C. O. (2002) in *Biochemistry of Lipids, Lipoproteins and Membranes* (Vance, D. E., and Vance, J. E., eds), 4 Ed., pp. 55-92, Elsevier, Amsterdam

14. Thompson, G. A. (1992) in *The Regulation of Membrane Lipid Metabolism*, 2 Ed., pp. 1-20, CRC, Boca Raton

15. Irvine, R. F. (2002) *Sci. STKE.* **2002**, RE13.

16. McPhail, L. C. (2002) in *Biochemistry of Lipids, Lipoproteins and Membranes* (Vance, D. E., and Vance, J. E., eds), 4 Ed., pp. 315-340, Elsevier, Amsterdam

17. Murakami, M., Nakatani, Y., Kuwata, H., and Kudo, I. (2000) *Biochim. Biophys. Acta.* **1488**, 159-66.

18. Xu, Y. (2002) *Biochim. Biophys. Acta.* **1582**, 81-8.

19. Huwiler, A., Kolter, T., Pfeilschifter, J., and Sandhoff, K. (2000) *Biochim. Biophys. Acta.* **1485**, 63-99.

20. Xie, Y., Gibbs, T. C., and Meier, K. E. (2002) *Biochim. Biophys. Acta.* **1582**, 270-81.

21. Serhan, C. N., Haeggstrom, J. Z., and Leslie, C. C. (1996) *FASEB. J.* **10**, 1147-58.

22. Veldhuizen, R., Nag, K., Orgeig, S., and Possmayer, F. (1998) *Biochim. Biophys. Acta.* **1408**, 90-108.

23. Possmayer, F. (1989) in *Phosphatidylcholine Metabolism* (Vance, D. E., ed), pp. 205-224, CRC, Boca Raton, FL.

24. Bremer, J., and Greenberg, D. M. (1959) *Biochim. Biophys. Acta.* **35**, 287-288

25. Vance, J. E. (2002) in *Biochemistry of Lipids, Lipoproteins and Membranes* (Vance, D. E., and Vance, J. E., eds), 4 Ed., pp. 505-526, Elsevier, Amsterdam

26. Agellon, L. B. (2002) in *Biochemistry of Lipids, Lipoproteins and Membranes* (Vance, D. E., and Vance, J. E., eds), 4 Ed., pp. 433-448, Elsevier, Amsterdam

27. Minich, D. M., Vonk, R. J., and Verkade, H. J. (1997) *J. Lipid. Res.* **38**, 1709-21.

28. Hay, D. W., and Carey, M. C. (1990) *Hepatology* **12**, 6S-14S; discussion 14S-16S.

29. Smit, J. J., Schinkel, A. H., Oude Elferink, R. P., Groen, A. K., Wagenaar, E., van Deemter, L., Mol, C. A., Ottenhoff, R., van der Lugt, N. M., van Roon, M. A., and et al. (1993) *Cell* **75**, 451-62.

30. Van Nieuwkerk, C. M., Elferink, R. P., Groen, A. K., Ottenhoff, R., Tytgat, G. N., Dingemans, K. P., Van Den Bergh Weerman, M. A., and Offerhaus, G. J. (1996) *Gastroenterology* **111**, 165-71.

31. Jonas, A. (2002) in *Biochemistry of Lipids, Lipoproteins and Membranes* (Vance, D. E., and Vance, J. E., eds), 4 Ed., pp. 483-504, Elsevier, Amsterdam

32. Skipski, V. P. (1972) in *Blood Lipids and Lipoproteins* (Nelson, G. J., ed), pp. 471-583, Wiley-Interscience, New York

33. Subbaiah, P. V., and Monshizadegan, H. (1988) *Biochim. Biophys. Acta.* **963**, 445-55.

34. Vance, D. E., and Ridgway, N. D. (1988) *Prog. Lipid. Res.* **27**, 61-79

35. Dils, R. R., and Hubscher, G. (1959) *Biochim. Biphys. Acta.* **32**, 293-294

36. Schmid, P. C., Deli, E., and Schmid, H. H. (1995) *Arch. Biochem. Biophys.* **319**, 168-76.

37. Arondel, V., Benning, C., and Somerville, C. R. (1993) *J. Biol. Chem.* **268**, 16002-8.

38. Johnston, N. C., and Goldfine, H. (1983) *J. Gen. Microbiol.* **129**, 1075-81.

39. Goldfine, H. (1984) *J. Lipid. Res.* **25**, 1501-7.

40. de Rudder, K. E., Sohlenkamp, C., and Geiger, O. (1999) *J. Biol. Chem.* **274**, 20011-6.

41. de Rudder, K. E., Thomas-Oates, J. E., and Geiger, O. (1997) *J. Bacteriol.* **179**, 6921-8.

42. Kent, C. (1995) *Annu. Rev. Biochem.* **64**, 315-43

43. Carman, G. M., and Henry, S. A. (1999) *Prog. Lipid. Res.* **38**, 361-99.

44. Vance, D. E. (2002) in *Biochemistry of Lipids, Lipoproteins and Membranes* (Vance, D. E., and Vance, J. E., eds), 4 Ed., pp. 205-232, Elsevier, Amsterdam

45. Sundler, R., and Akesson, B. (1975) *J. Biol. Chem.* **250**, 3359-67.

46. DeLong, C. J., Shen, Y. J., Thomas, M. J., and Cui, Z. (1999) *J. Biol. Chem.* **274**, 29683-8.

47. Reo, N. V., and Adinehzadeh, M. (2000) *Toxicol. Appl. Pharmacol.* **164**, 113-26.

48. Reo, N. V., Adinehzadeh, M., and Foy, B. D. (2002) *Biochim. Biophys. Acta.* **1580**, 171-88.

49. Zeisel, S. H. (1990) in *Choline Metabolism and Brain Function* (Wurtman, R., and Wurtman, J., eds), pp. 75-99, Raven, New York

50. Blusztajn, J. K. (1998) *Science* **281**, 794-5.

51. Best, C. H., and Huntsman, M. E. (1932) *J. Physiol. (London)* **75**, 405-412

52. Zeisel, S. H., and Blusztajn, J. K. (1994) *Annu. Rev. Nutr.* **14**, 269-96

53. Garrow, T. A. (2001) in *Homocysteine in health and disease* (Carmel, R., and Jacobsen, D. W., eds), Cambridge University Press, 145-152

54. Lockman, P. R., and Allen, D. D. (2002) *Drug. Dev. Ind. Pharm.* **28**, 749-71.

55. Wille, S., Szekeres, A., Majdic, O., Prager, E., Staffler, G., Stockl, J., Kunthalert, D., Prieschl, E. E., Baumruker, T., Burtscher, H., Zlabinger, G. J., Knapp, W., and Stockinger, H. (2001) *J. Immunol.* **167**, 5795-804.

56. Ishidate, K. (1997) *Biochim. Biophys. Acta.* **1348**, 70-8.

57. Bussiere, M., Campenot, R. B., Ure, D. R., Vance, J. E., and Vance, D. E. (1995) *Biochim Biophys Acta* **1259**, 148-54.

58. Uchida, T. (1996) *Biochim Biophys Acta* **1304**, 89-104.

59. Nakagami, K., Uchida, T., Ohwada, S., Koibuchi, Y., Suda, Y., Sekine, T., and Morishita, Y. (1999) *Jpn J Cancer Res* **90**, 419-24.

60. Nakagami, K., Uchida, T., Ohwada, S., Koibuchi, Y., and Morishita, Y. (1999) *Jpn J Cancer Res* **90**, 1212-7.

61. Ramirez de Molina, A., Penalva, V., Lucas, L., and Lacal, J. C. (2002) *Oncogene* **21**, 937-46.

62. Ramirez de Molina, A., Gutierrez, R., Ramos, M. A., Silva, J. M., Silva, J., Bonilla, F., Sanchez, J. J., and Lacal, J. C. (2002) *Oncogene* **21**, 4317-22.

63. Ramirez de Molina, A., Rodriguez-Gonzalez, A., Gutierrez, R., Martinez-Pineiro, L., Sanchez, J., Bonilla, F., Rosell, R., and Lacal, J. (2002) *Biochem Biophys Res Commun* **296**, 580-3.

64. Ratnam, S., and Kent, C. (1995) *Arch. Biochem. Biophys.* **323**, 313-22.

65. Wittenberg, J., and Kornberg, A. (1953) *J. Biol. Chem.* **202**, 431-444

66. Ishidate, K., Nakagomi, K., and Nakazawa, Y. (1984) *J. Biol. Chem.* **259**, 14706-10.

67. Porter, T. J., and Kent, C. (1990) *J. Biol. Chem.* **265**, 414-22.

68. Uchida, T., and Yamashita, S. (1990) *Biochim Biophys Acta* **1043**, 281-8.

69. Ishidate, K., Iida, K., Tadokoro, K., and Nakazawa, Y. (1985) *Biochim. Biophys. Acta.* **833**, 1-8.

70. Tadokoro, K., Ishidate, K., and Nakazawa, Y. (1985) *Biochim. Biophys. Acta.* **835**, 501-13.

71. Uchida, T., and Yamashita, S. (1992) *J. Biol. Chem.* **267**, 10156-62.

72. Uchida, T. (1994) *J. Biochem. (Tokyo)* **116**, 1241-50.

73. Aoyama, C., Nakashima, K., Matsui, M., and Ishidate, K. (1998) *Biochim. Biophys. Acta.* **1390**, 1-7.

74. Aoyama, C., Nakashima, K., and Ishidate, K. (1998) *Biochim Biophys Acta* **1393**, 179-85.

75. Aoyama, C., Yamazaki, N., Terada, H., and Ishidate, K. (2000) *J. Lipid. Res.* **41**, 452-64.

76. Yamazaki, N., Shinohara, Y., Kajimoto, K., Shindo, M., and Terada, H. (2000) *J. Biol. Chem.* **275**, 31739-46.

77. Sundler, R., Arvidson, G., and Akesson, B. (1972) *Biochim Biophys Acta* **280**, 559-68.

78. Vance, D. E., Trip, E. M., and Paddon, H. B. (1980) *J. Biol. Chem.* **255**, 1064-9.

79. Pelech, S. L., Pritchard, P. H., Brindley, D. N., and Vance, D. E. (1983) *J. Biol. Chem.* **258**, 6782-8.

80. Kennedy, E. P., and Weiss, S. B. (1955) *J. Amer. Chem. Sc.* **77**, 250-253

81. Kennedy, E. P., and Weiss, S. B. (1956) *J. Biol. Chem.* **222**, 193-214

82. Weinhold, P. A., Rounsifer, M. E., and Feldman, D. A. (1986) *J. Biol. Chem.* **261**, 5104-10.

83. Feldman, D. A., and Weinhold, P. A. (1987) *J. Biol. Chem.* **262**, 9075-81.

84. Kalmar, G. B., Kay, R. J., Lachance, A., Aebersold, R., and Cornell, R. B. (1990) *Proc. Natl. Acad. Sci. U S A.* **87**, 6029-33.

85. Yang, W., and Jackowski, S. (1995) *J. Biol. Chem.* **270**, 16503-6.

86. Lykidis, A., Murti, K. G., and Jackowski, S. (1998) *J. Biol. Chem.* **273**, 14022-9.

87. Lykidis, A., and Jackowski, S. (2001) *Prog. Nucleic. Acid. Res. Mol. Biol.* **65**, 361-93

88. Lykidis, A., Jackson, P., and Jackowski, S. (2001) *Biochemistry* **40**, 494-503.

89. MacDonald, J. I., and Kent, C. (1994) *J. Biol. Chem.* **269**, 10529-37.

90. Kent, C. (1990) *Prog. Lipid. Res.* **29**, 87-105

91. Sohal, P. S., and Cornell, R. B. (1990) *J. Biol. Chem.* **265**, 11746-50.

92. Houweling, M., Tijburg, L. B., Vaartjes, W. J., Batenburg, J. J., Kalmar, G. B., Cornell, R. B., and Van Golde, L. M. (1993) *Eur. J. Biochem.* **214**, 927-33.

93. Tessner, T. G., Rock, C. O., Kalmar, G. B., Cornell, R. B., and Jackowski, S. (1991) *J. Biol. Chem.* **266**, 16261-4.

94. Hogan, M., Kuliszewski, M., Lee, W., and Post, M. (1996) *Biochem. J.* **314**, 799-803.

95. Jackowski, S. (1994) *J. Biol. Chem.* **269**, 3858-67.

96. Golfman, L. S., Bakovic, M., and Vance, D. E. (2001) *J. Biol. Chem.* **276**, 43688-92.

97. Tang, W., Keesler, G. A., and Tabas, I. (1997) *J. Biol. Chem.* **272**, 13146-51.

98. Rutherford, M. S., Rock, C. O., Jenkins, N. A., Gilbert, D. J., Tessner, T. G., Copeland, N. G., and Jackowski, S. (1993) *Genomics* **18**, 698-701.

99. Lykidis, A., Baburina, I., and Jackowski, S. (1999) *J. Biol. Chem.* **274**, 26992-7001.

100. Zhang, D., Tang, W., Yao, P. M., Yang, C., Xie, B., Jackowski, S., and Tabas, I. (2000) *J. Biol. Chem.* **275**, 35368-76.

101. Weiss, S. B., SMith, S. W., and Kennedy, E. P. (1958) *J. Biol. Chem.* **231**, 53-64

102. McMaster, C. R., and Bell, R. M. (1997) *Biochim. Biophys. Acta.* **1348**, 100-10.

103. Mancini, A., Del Rosso, F., Roberti, R., Orvietani, P., Coletti, L., and Binaglia, L. (1999) *Biochim. Biophys. Acta.* **1437**, 80-92.

104. Henneberry, A. L., and McMaster, C. R. (1999) *Biochem. J.* **339**, 291-298

105. Henneberry, A. L., Wistow, G., and McMaster, C. R. (2000) *J. Biol. Chem.* **275**, 29808-15.

106. Stetten, D. (1941) *J. Biol. Chem.* **138**, 437-438

107. Gibson, K. D., Wilson, J. D., and Udenfriend , S. (1961) *J. Biol. Chem.* **236**, 673-679

108. Yamashita, S., and Hosaka, K. (1997) *Biochim. Biophys. Acta.* **1348**, 63-9.

109. Kim, K., Kim, K. H., Storey, M. K., Voelker, D. R., and Carman, G. M. (1999) *J. Biol. Chem.* **274**, 14857-66.

110. Bladergroen, B. A., and van Golde, L. M. (1997) *Biochim. Biophys. Acta.* **1348**, 91-9.

111. McMaster, C. R., and Bell, R. M. (1997) *Biochim. Biophys. Acta.* **1348**, 117-23.

112. Voelker, D. R. (1997) *Biochim. Biophys. Acta.* **1348**, 236-44.

113. Florin-Christensen, J., Suarez, C. E., Florin-Christensen, M., Wainszelbaum, M., Brown, W. C., McElwain, T. F., and Palmer, G. H. (2001) *Proc. Natl. Acad. Sci. U S A.* **98**, 7736-41.

114. Schmid, K. M., and Ohlrogge, J. B. (2002) in *Biochemistry of Lipids, Lipoproteins and Membranes* (Vance, D. E., and Vance, J. E., eds), 4 Ed., pp. 93-126, Elsevier, Amsterdam

115. Hanson, A. D., and Rhodes, D. (1983) *Plant Physiol.* **71**, 692-700

116. Mudd, S. H., and Datko, J. H. (1986) *Plant Physiol.* **82**, 126-135

117. Hitz, W. D., Rhodes, D., and Hanson, A. D. (1981) *Plant Physiol.* **68**, 814-822

118. Datko, A. H., and Mudd, S. H. (1988) *Plant Physiol.* **88**, 854-861

119. Rolph, C. E., and Goad, L. J. (1991) *Physiolo. Planta.* **83**, 605-610

120. Ridgway, N. D., and Vance, D. E. (1988) *J. Biol. Chem.* **263**, 16856-63.

121. Cook, H. W., and McMaster, C. R. (2002) in *Biochemistry of Lipids, Lipoproteins and Membranes* (Vance, D. E., and Vance, J. E., eds), 4 Ed., pp. 181-204, Elsevier, Amsterdam

122. Agellon, L. B., Walkey, C. J., Vance, D. E., Kuipers, F., and Verkade, H. J. (1999) *Hepatology* **30**, 725-9.

123. Du Vigneaud, V., Cohn, M., Chandler, J. P., Schenck, S., and Simmonds, S. (1941) *J. Biol. Chem.* **140**, 625-641

124. Cantoni, G. L. (1952) *J. Amer. Chem. Soc.* **74**, 2942-2943

125. Clarke, S., and Banfield, K. (2001) in *Homocysteine in health and disease* (Carmel, R., and Jacobsen, D. W., eds), Cambridge University Press, 63-78

126. Fauman, E. B., Blumenthal, R.M., Cheng, X. (1999) in *S-Adenosylmethionine-Dependent Methyltransferases: Structures and Functions* (Cheng, X., Blumenthal, R.M., ed), pp. 1-32, World Scientific Publishing, Singapore

127. Awad, W. M., Jr., Whitney, P. L., Skiba, W. E., Mangum, J. H., and Wells, M. S. (1983) *J. Biol. Chem.* **258**, 12790-2.

128. Banerjee, R. V., and Matthews, R. G. (1990) *Faseb. J.* **4**, 1450-9.

129. Chiang, P. K., Gordon, R. K., Tal, J., Zeng, G. C., Doctor, B. P., Pardhasaradhi, K., and McCann, P. P. (1996) *FASEB. J.* **10**, 471-80.

130. Fowler, B. (2001) in *Homocysteine in health and disease* (Carmel, R., and Jacobsen, D. W., eds), Cambridge University Press, 163-175

131. Mato, J. M., Corrales, F. J., Lu, S. C., and Avila, M. A. (2002) *FASEB. J.* **16**, 15-26

132. Mudd, S. H., and Poole, J. R. (1975) *Metabolism* **24**, 721-35.

133. Finkelstein, J. D., and Martin, J. J. (1986) *J. Biol. Chem.* **261**, 1582-7.

134. Van Phi, L., and Soling, H. D. (1982) *Biochem. J.* **206**, 481-7.

135. Hoffman, D. R., Marion, D. W., Cornatzer, W. E., and Duerre, J. A. (1980) *J. Biol. Chem.* **255**, 10822-7.

136. Hoffman, D. R., Haning, J. A., and Cornatzer, W. E. (1981) *Lipids* **16**, 561-7.

137. Ridgway, N. D., and Vance, D. E. (1987) *J. Biol. Chem.* **262**, 17231-9.

138. Schneider, W. J., and Vance, D. E. (1979) *J. Biol. Chem.* **254**, 3886-91.

139. Ridgway, N. D., and Vance, D. E. (1988) *J. Biol. Chem.* **263**, 16864-71.

140. Tanaka, Y., Doi, O., and Akamatsu, Y. (1979) *Biochem Biophys Res Commun* **87**, 1109-15.

141. Vance, D. E., Walkey, C. J., and Cui, Z. (1997) *Biochim Biophys Acta* **1348**, 142-50.

142. Cain, B. D., Donohue, T. J., Shepherd, W. D., and Kaplan, S. (1984) *J. Biol. Chem.* **259**, 942-8.

143. Arondel, V., Benning, C., and Somerville, C. R. (1993) *J Biol Chem* **268**, 16002-8.

144. Tahara, Y., Ogawa, Y., Sakakibara, T., and Yamada, Y. (1986) *Ag. Biol. Chem.* **50**, 257-259

145. Johnston, N. C., and Goldfine, H. (1983) *J Gen Microbiol* **129**, 1075-81.

146. van Waarde, A., and van Hoof, P. J. M. (1985) *Biochimica. Biophysica. Acta.* **836**, 27-38

147. Ridgway, N. D. (1988) in *Ph.D Thesis*, pp. 163, Dept. of Biochemistry, University of British Columbia, Vancouver

148. Cui, Z., Vance, J. E., Chen, M. H., Voelker, D. R., and Vance, D. E. (1993) *J. Biol. Chem.* **268**, 16655-63.

149. Kodaki, T., and Yamashita, S. (1987) *J. Biol. Chem.* **262**, 15428-35.

150. Walkey, C. J., Cui, Z., Agellon, L. B., and Vance, D. E. (1996) *J. Lipid. Res.* **37**, 2341-50.

151. Walkey, C. J., Donohue, L. R., Bronson, R., Agellon, L. B., and Vance, D. E. (1997) *Proc. Natl. Acad. Sci. U S A.* **94**, 12880-5.

152. Kodaki, T., and Yamashita, S. (1987) *J Biol Chem* **262**, 15428-35.

153. Summers, E. F., Letts, V. A., McGraw, P., and Henry, S. A. (1988) *Genetics* **120**, 909-22.

154. McGraw, P., and Henry, S. A. (1989) *Genetics* **122**, 317-30.

155. Kanipes, M. I., Hill, J. E., and Henry, S. A. (1998) *Genetics* **150**, 553-62.

156. Hanada, T., Kashima, Y., Kosugi, A., Koizumi, Y., Yanagida, F., and Udaka, S. (2001) *Biosci. Biotechnol. Biochem.* **65**, 2741-8.

157. de Rudder, K. E., Lopez-Lara, I. M., and Geiger, O. (2000) *Mol. Microbiol.* **37**, 763-72.

158. Bremer, J., and Greenberg, D. M. (1959) *Biochim. Biophys. Acta.* **46**, 205-216

159. Blusztajn, J. K., and Wurtman, R. J. (1981) *Nature* **290**, 417-8.

160. Yang, E. K., Blusztajn, J. K., Pomfret, E. A., and Zeisel, S. H. (1988) *Biochem J* **256**, 821-8.

161. Panagia, V., Ganguly, P. K., and Dhalla, N. S. (1984) *Biochim. Biophys. Acta.* **792**, 245-53.

162. Prasad, C., and Edwards, R. M. (1981) *J. Biol. Chem.* **256**, 1300-3.

163. Nieto, A., and Catt, K. J. (1983) *Endocrinology* **113**, 758-62.

164. Sarzale, M. G., and Pilarska, M. (1976) *Biochim. Biophys. Acta* **441**, 81-92

165. Cui, Z., Shen, Y. J., and Vance, D. E. (1997) *Biochim. Biophys. Acta.* **1346**, 10-6.

166. Houweling, M., Cui, Z., Tessitore, L., and Vance, D. E. (1997) *Biochim. Biophys. Acta.* **1346**, 1-9.

167. Xu, L., Hui, L., Wang, S., Gong, J., Jin, Y., Wang, Y., Ji, Y., Wu, X., Han, Z., and Hu, G. (2001) *Cancer. Res.* **61**, 3176-81.

168. Tessitore, L., Cui, Z., and Vance, D. E. (1997) *Biochem. J.* **322**, 151-4.

169. Tessitore, L., Dianzani, I., Cui, Z., and Vance, D. E. (1999) *Biochem. J.* **337**, 23-7.

170. Tessitore, L., Sesca, E., and Vance, D. E. (2000) *Int. J. Cancer.* **86**, 362-7.

171. Vance, J. E., and Vance, D. E. (1988) *J Biol Chem* **263**, 5898-909.

172. Vance, J. E. (1990) *J. Biol. Chem.* **265**, 7248-56.

173. Rusinol, A. E., Cui, Z., Chen, M. H., and Vance, J. E. (1994) *J. Biol. Chem.* **269**, 27494-502.

174. Lewin, T. M., Kim, J. H., Granger, D. A., Vance, J. E., and Coleman, R. A. (2001) *J. Biol. Chem.* **276**, 24674-9.

175. Stone, S. J., and Vance, J. E. (2000) *J. Biol. Chem.* **275**, 34534-40.

176. Vidugiriene, J., Sharma, D. K., Smith, T. K., Baumann, N. A., and Menon, A. K. (1999) *J. Biol. Chem.* **274**, 15203-12.

177. Verma, A., Ahmed, H. A., Davis, T., Jazrawi, R. P., and Northfield, T. C. (1999) *J. Hepatol.* **31**, 852-9.

178. Higgins, J. A. (1981) *Biochim Biophys Acta* **640**, 1-15.

179. Vance, D. E., Choy, P. C., Farren, S. B., Lim, P. H., and Schneider, W. J. (1977) *Nature* **270**, 268-9.

180. Audubert, F., and Vance, D. E. (1984) *Biochim. Biophys. Acta.* **792**, 359-62.

181. Audubert, F., Pelech, S. L., and Vance, D. E. (1984) *Biochim. Biophys. Acta.* **792**, 348-57.

182. Geelen, M. J., Groener, J. E., De Haas, C. G., and Van Golde, L. M. (1979) *FEBS. Lett.* **105**, 27-30.

183. Castano, J. G., Alemany, S., Nieto, A., and Mato, J. M. (1980) *J. Biol. Chem.* **255**, 9041-3.

184. Pritchard, P. H., Pelech, S. L., and Vance, D. E. (1981) *Biochim. Biophys. Acta.* **666**, 301-6.

185. Marin-Cao, D., Alvarez Chiva, V., and Mato, J. M. (1983) *Biochem. J.* **216**, 675-80.

186. Pelech, S. L., Pritchard, P. H., Sommerman, E. F., Percival-Smith, A., and Vance, D. E. (1984) *Can. J. Biochem. Cell. Biol.* **62**, 196-202.

187. Pelech, S. L., Ozen, N., Audubert, F., and Vance, D. E. (1986) *Biochem. Cell. Biol.* **64**, 565-74.

188. Ridgway, N. D., and Vance, D. E. (1989) *Biochim. Biophys. Acta.* **1004**, 261-70.

189. Walkey, C. J., Yu, L., Agellon, L. B., and Vance, D. E. (1998) *J. Biol. Chem.* **273**, 27043-6.

190. Waite, K. A., Cabilio, N. R., and Vance, D. E. (2002) *J. Nutr.* **132**, 68-71.

191. Zeisel, S. H., Story, D. L., Wurtman, R. J., and Brunengraber, H. (1980) *Proc. Natl. Acad. Sci. U S A.* **77**, 4417-9.

192. DeLong, C. J., Hicks, A. M., and Cui, Z. (2002) *J. Biol. Chem.* **277**, 17217-25.

193. Noga, A. A., Zhao, Y., and Vance, D. E. (2002) *J. Biol. Chem.* **277**, 42358-42365

194. Johnson, P. I., and Blusztajn, J. K. (1998) *Neurochem. Res.* **23**, 583-7.

195. Weinstein, I., Turner, F. C., Soler-Argilaga, C., and Heimberg, M. (1978) *Biochim. Biophys. Acta.* **530**, 394-401.

196. Walsh, B. W., Schiff, I., Rosner, B., Greenberg, L., Ravnikar, V., and Sacks, F. M. (1991) *N. Engl. J. Med.* **325**, 1196-204.

197. Finkelstein, J. D. (1998) *Eur. J. Pediatr.* **157 Suppl 2**, S40-4.

198. Finkelstein, J. D. (2001) in *Homocysteine in health and disease* (Carmel, R., and Jacobsen, D. W., eds), Cambridge University Press, 92-99

199. Noga, A. A., Stead, L. M., Zhao, Y., Brosnan, M. E., Brosnan, J. T., and Vance, D. E. (2003) *J. Biol. Chem.* **In Press**

200. Kerr, S. J. (1972) *J. Biol. Chem.* **247**, 4248-52.

201. Balaghi, M., Horne, D. W., and Wagner, C. (1993) *Biochem. J.* **291**, 145-9.

202. Mudd, S. H., Ebert, M. H., and Scriver, C. R. (1980) *Metabolism* **29**, 707-20.

Chapter 2

Genomic Characterization of Human Phosphatidylethanolamine *N*-methyltransferase

Portions of this chapter were published in *Biochimica Biophysica Acta*, **1436**, 405-412, (1999), and in *Biochimica Biophysica Acta*, **1532**, 105-114, (2001)

2.1 Introduction

Phosphatidylcholine (PC) is essential for eukaryotic cell viability, being an important component of membranes, lipoproteins and bile, in addition to having a role in intracellular signaling (1-4). In mammalian species, two pathways synthesize PC. All nucleated cells produce PC by the CDP-choline pathway in which the rate limiting enzyme is CTP-phosphocholine cytidylyltransferase (CT) (5). An additional pathway is utilized primarily in liver, where the enzyme phosphatidylethanolamine *N*-methyltransferase (PEMT) catalyzes three sequential methylation reactions converting phosphatidylethanolamine (PE) to PC (6).

It is estimated that the PEMT pathway accounts for up to 30% of hepatic PC production (7-9). Despite generating such a proportion of hepatic PC, a specific function for PEMT-derived PC has not yet been defined. As PEMT expression is highest in liver, a role for PEMT-derived PC in a function specific to liver such as VLDL secretion or bile production has been hypothesized (10-13). A recent study demonstrating PEMT activity in the bile canalicular membrane of hamster liver further supports a possible role for PEMT in bile production (14). However, the discovery of PEMT in canalicular membranes only serves to add further complexity to understanding the role of PEMT in hepatocytes, as PEMT has already been described heretofore in two different subcellular locations, with PEMT1 found

in endoplasmic reticulum and PEMT2 confined to mitochondria-associated membranes (15).

PEMT expression commences at birth in rodents, and is primarily liver-specific but trace activities have been reported in several other tissues (6,15-20). In addition, expression of rat PEMT2 is related to liver growth, as an inverse relationship between PEMT2 expression and hepatic growth rates has been observed (16,21-23). The significance of diminished PEMT expression during hepatocyte growth and differentiation is as yet unknown.

Disruption of the murine gene has been completed and the resulting mice do not display any overtly abnormal phenotype (24,25). However, when challenged with a choline-deficient (CD) diet that removes the substrate for the CDP-choline pathway, the mice undergo primary liver failure emphasizing the importance of the PEMT pathway in a CD state such as starvation, pregnancy or lactation (25,26). Provision of a choline supplemented diet to animals that have been subjected to a CD diet for 3 days rescues the animals from liver failure suggesting that any CD-mediated effects that occur in the first 3 days might be reversible (27).

Previously, we cloned three human PEMT (hPEMT) cDNAs from liver, each of which has a different 5′ primary structure indicating alternative splicing during processing of the human gene (28). This phenomenon has not been observed for the murine PEMT gene (29). Moreover, analysis of

ESTs corresponding to each 5' UTR revealed a differential expression profile, suggesting that transcription of the variant mRNA species may be regulated in a tissue-specific manner (28). To gain insight into the role of the PEMT pathway in humans and to study expression of the enzyme in higher mammals, a bacterial artificial chromosome (BAC) was isolated and characterized. Expression of the gene and differential processing of transcripts was investigated.

2.2 Materials and Methods

2.2.1 Reagents

Restriction endonucleases, modifying enzymes and random primer labeling kit were obtained from Life technologies Inc. Radioisotopes ([α-^{32}P]-CTP, [γ-^{32}P]-ATP) were from Amersham Biotech. *Accurase* long-range polymerase was from Biocan scientific. Topo-TA cloning kit was from Invitrogen.

2.2.2 DNA Isolation and Southern Analysis

BAC DNA was isolated using a Qiagen midi-prep kit (Tip 100), plasmid DNA was isolated with a *Wizard* miniprep kit (Promega), and genomic DNA was extracted from lymphocytes of healthy male volunteers using a Genomic DNA extraction kit (MBI Fermentas). To perform Southern blot analysis, DNA was separated by agarose gel electrophoresis and transferred to Hybond-N+ nylon membrane (Amersham) using a vacuum blotter (Biorad) as per the manufacturer's instructions. Pre-hybridization and hybridization steps were carried out at 42 °C, in 6 x SSC (1 × SSC = 0.15 M NaCl, 0.015 M trisodium citrate), 0.01 M sodium phosphate, 0.01 M EDTA, 0.5% SDS, 0.1% milk, 100 μg ml^{-1} sheared salmon testes DNA (Sigma), and 1 × 10^{6} cpm ml^{-1} of probe as required. Membranes were washed in conditions of low (1 × SSC, 0.1% SDS at room temp.) or high (0.1 × SSC,

0.1% SDS at 55°C) stringency. Blots were exposed to a phosphorimager screen and scanned using a Storm 540 phosphorimager (Molecular Dynamics).

2.2.3 Cloning of the Gene

Using primers specific for the 3′ end of hPEMT cDNA, a BAC library spanning chromosome 17p was kindly screened using PCR by Dr. H. Aburatani (University of Tokyo, Japan). To confirm the presence of *PEMT* sequence in isolated clones, BAC DNA was digested using *Hin*dIII and subjected to Southern blot analysis with a radiolabeled-hPEMT cDNA as probe. Structure of the clone was confirmed by comparison with a genomic DNA restriction pattern using the same probe. BAC insert size was determined by pulse field gel electrophoreses (PFGE) analysis of *Not*I-digested DNA.

2.2.4 Chromosomal Mapping of the Human PEMT Gene

A biotinylated probe consisting of the full-length human PEMT gene in a BAC clone was used to perform fluorescence in situ hybridization (FISH). Mapping of the probe was carried out using normal human lymphocyte chromosomes, counterstained with propidium iodide and 4′, 6-diamidin-2 phenylin-dol-dihydrochloride (DAPI). This procedure was performed under

the direction of Dr. Barbara Beatty at the CGAT FISH mapping resource center at the University of Toronto, Ontario, Canada.

2.2.5 Gene Structure

BAC DNA was digested with *Bam*HI, *Eco*RI, and *Hind*III and fragments containing exonic sequence identified by Southern blotting using a radiolabeled hPEMT cDNA, or exon-specific oligonucleotides as probes. Hybridizing fragments were subcloned into pBluescriptII/SK- (Stratagene). Using primers based on hPEMT cDNA sequence and with reference to the murine *Pemt* gene structure, exon-intron boundary sequences were determined. Synthesis of primers was performed at the DNA core facility, University of Alberta using a 394 DNA/RNA synthesizer (Applied Biosystems). PCR amplification of introns 6 (primers Ex6F-Ex7R, see Table 2.1), 7 (Ex7F-Ex8R) and 8 (Ex8F-Ex9R) was carried out using *Taq* polymerase (94°C for 30 s, 50°C for 30 s, 72°C for 1 min.). Intron 5 (Ex5F-Ex6R) was amplified using *Accurase* long-range polymerase (94°C, 20 s; 50°C, 30 s; 68°C, 4 min. for 10 cycles, followed by 20 cycles of 94°C, 20 s; 50°C, 30 s; 68°C, 4 min. +20 s per cycle, and a final extension step of 7 min. at 68°C).

2.2.6 Distribution of PEMT Transcripts

Rapid-Scan™ gene expression panels (Origene technologies) contain first strand cDNAs from different tissues that serve as template for PCR at concentrations ranging over four orders of magnitude. PCR amplification was performed using the primer pair Ex4F-Ex9R (Table 2.1), for 35 cycles (94°C for 1 min., 54°C for 30 s, 72°C for 30 s plus a final extension time of 3 min. at 72°C). Products of the reaction were analyzed by Southern blot analysis using the 36 bp radiolabeled internal probe, PEMT-int (Table 2.1). To investigate transcription of specific mRNA species in human tissues, Master Blots™ (dot blots) and Multiple Tissue Northern blots™ (Clontech) were probed with radiolabeled oligonucleotides specific for each untranslated exon (Ex1R, Ex2R, Ex3R, Table 2.1). Blots were washed as described for Southern blot analysis and analyzed using a phosphorimager.

2.2.7 RNA Extraction and RT-PCR Analysis

Normal adult liver samples obtained from the University of Alberta Hospital Dept. of Pathology were snap frozen in liquid nitrogen at resection. Total RNA was prepared from liver samples using Trizol (Life Tech. Inc.) according to the manufacturer's instructions and RNA quality was evaluated by 1% formaldehyde gel electrophoresis and ethidium bromide staining. Total RNA (3 μg), previously treated with RNase-free DNase I (Life Tech Inc.), was reverse transcribed using an 18mer oligo-dT primer and Superscript II reverse transcriptase (Life Tech, Inc) as per the manufacturer's instructions. Heart and testis poly A^+ RNA (0.5 μg)

(Clontech) was reverse transcribed as above but using a gene specific antisense primer (Ex9R, Table 2.1). PCR was performed on the reverse transcription (RT) products using an antisense primer common to each transcript (Ex9R or Ex6R, liver; Ex8R or Ex7R, heart & testis, Table 2.1) and a sense primer specific to each 5′ UTR (Ex1F, Ex2F, Ex3F, Table 2.1). Amplification was for 30 cycles (94°C for 30 s, 50°C for 30 s and an extension step of 72°C for 1 min.). Southern blot analysis was performed on products of the reaction, using the radiolabeled internal probe, PEMT-int (Table 2.1).

2.2.8 Transcription Start Sites

CapSite™ cDNA (Nippon Gene Co.) was a kind gift of Dr. Kozo Ishidate (Tokyo Dental and Medical University, Japan). Capped mRNA and hence transcripts with intact 5′ ends were isolated, and a linker was appended to the 5′ end of the transcripts after removal of the 5′ m^7GpppN cap structure. Reverse transcription generates a linker-cDNA library. Primers complementary to the attached linker (IRC, IIRC, supplied with kit, Table 2.1) are used in combination with gene-specific antisense primers to generate an amplicon that includes the 5′ end of the transcript and thereby maps the transcriptional start site. PCR was performed initially using the *PEMT*-specific antisense primer, Ex5R and a primer complementary to the attached linker, IRC (Table 2.1). Nested PCR using the *PEMT*-specific antisense primer, Ex4R and IIRC (Table 2.1) followed. Amplification was

performed as described for RT-PCR analysis above. The resulting product was cloned into pCR2.1-Topo (Invitrogen), following the manufacturer's protocol. Cloned plasmid DNA was sequenced in both directions at the University of Alberta DNA core facility using an Applied Biosystems 373A DNA Sequencer to identify the transcription start site.

2.2.9 *Transcription Factor Binding Sites*

Sequence proximal to the transcription start site was obtained by "gene walking" using the primers, WU-I, WU-II and WU-III (Table 2.1) for sequencing directly from 5 μg of BAC DNA. The putative promoter region was evaluated using the *Transfac* search engine for the identification of consensus transcription factor binding sites (http://pdap1.trc.rwcp.or.jp/research/db/TFSEARCH.html).

2.3 Results and Discussion

2.3.1 Gene Cloning

Four clones were isolated from a BAC library by PCR screening. Southern blot analysis of the clones using radiolabeled exon-specific probes indicated each exon to be present in clone 354-L4. Integrity of the cloned human DNA was confirmed by comparison with genomic DNA restriction patterns using Southern blot analysis (C.J. Walkey, personal communication). Pulse field gel electrophoresis of BAC DNA indicated an insert size of approximately 120 kb (data not shown). In accordance with a directive from the human gene nomenclature committee (http://www.gene.ucl.ac.uk/nomenclature/), the human gene shall be entitled *PEMT*, as opposed to *Pemt* as used in the mouse.

2.3.2 Chromosomal Mapping of the Human PEMT gene

FISH mapping demonstrated that the PEMT gene locus occupies a position on chromosome 17p11.2 (Fig. 2.1), corroborating previous results from radiation hybrid mapping experiments (28). Normal human lymphocyte chromosomes were probed with a biotinylated derivative of the full-length human PEMT gene in a BAC clone. Twenty well spread metaphases were analyzed and positive hybridization signals were detected in >90% of the cells. Signals were visualized on both alleles in >90% of the

positive spreads. This locus (17p11.2) is syntenic to the region of the mouse chromosome 11 that includes the *Pemt* gene (28). Gene products derived from loci in proximity to the human PEMT gene include, SREBP1 (a transcriptional regulator of lipid metabolism), a Ras-related protein of unknown function and several hypothetical proteins (data obtained from www.ncbi.nlm.nih.gov; LocusLink ID 10400).

2.3.3 Structure of the Gene

Electrophoresis and comparative Southern blot analysis of restriction fragments were performed to elucidate the gene structure. A combination of Southern blotting and sequencing identified exonic sequence, and facilitated determination of exon and intron sizes as well as sequences of splice junctions (Table 2.2). Additionally, this strategy confirmed the presence and order of each untranslated first exon in the gene. First exons of the cDNA clones rp18b2a, rp1a1a and rp3c1a, are now designated exons 1, 2 and 3, respectively, based on their 5′ to 3′ order in the gene (Fig. 2.2) (28).

As restriction fragments spanning introns 5-8 were not subcloned, PCR was used to estimate intron size. Long-range PCR was performed in the case of intron 5, as it was found to span approximately 8 kb (Table 2.1). A gene structure comprising 9 exons and eight introns was thereby elucidated (Fig. 2.2). Comparative analysis of human and rat open reading

frames revealed an identity of 82.3% but no similarity exists between any of the untranslated first exons and the first exon of rat (28). To determine if an exon with similarity to any of the three human untranslated exons is present in the mouse gene, Southern blot analysis was performed on murine genomic DNA using radiolabeled probes specific for each untranslated exon. No cross-reactivity was detected (data not shown). Thus, this may indicate that alternative processing of *PEMT* exons 1, 2 and 3 is specific to humans.

2.3.4 Tissue Distribution of PEMT Transcripts

Splicing of a 5'-untranslated exon is frequently associated with alternative tissue-specific expression. One of the most complex examples identified to date is the human neuronal nitric oxide synthase gene (*NOS1*), which has 9 different exon 1 variants that direct transcriptional initiation in different tissues (30). Several human genes encoding enzymes of lipid metabolism, including carnithine palmitoyltransferase-I β and acetyl-CoA carboxylase α are also subject to similar regulation (31,32). PEMT has been studied extensively in mouse and rat models and is predominantly expressed in liver (6). However, splicing of PEMT mRNA has not been reported in mice or rats (15,29). Thus, the expression profile of PEMT transcripts in humans was analyzed to investigate if splicing results in an expression pattern disparate from that of the homologous rodent enzyme.

PCR analysis demonstrated the existence of high levels of PEMT in human liver but transcripts were also detectable in human heart and testis, and to a lesser extent in brain and skeletal muscle (Fig. 2.3A). Direct analysis of tissue mRNA indicated that the liver is the site of major *PEMT* expression (Figs 2.3B & 2.3C). To investigate the individual transcript profiles, mRNA from each tissue was analyzed with radiolabeled oligonucleotides specific for each untranslated exon. A probe specific for exon 2 (Ex2R) cross-reacted with liver mRNA only (Figs 2.3B & 2.3C), whereas exon 1- (Ex1R) and exon 3-specific (Ex3R) probes did not cross-react with mRNA from any tissue (data not shown). Thus, exon 2-containing transcripts appear to be the major transcript of the human PEMT gene. Furthermore, the major transcript exists in both adult and fetal human liver (Figs 2.3B & 2.3C). This is in contrast to rodents where expression of the gene begins at birth (15).

Expression of the gene at high levels in human liver correlates with results from rodents and supports a hypothesis implicating the PEMT pathway in the provision of PC for VLDL secretion and/or bile formation. However, the discovery of PEMT transcripts in extra-hepatic tissues is also not without precedent as PEMT activity has been detected in each of the corresponding rat tissues albeit at a much lower level than in liver (17-20). It is noteworthy in the case of heart that studies of PEMT in cardiac sarcoplasmic reticulum have revealed elevated PEMT activity in rats with induced chronic diabetes (33). It is hypothesized that changes in PEMT

activity and hence PC synthesis may have a role in the development of cardiac dysfunction in the diabetic state (33).

In addition, a recent study of patients with Alzheimer's disease described lowered PEMT activity in the frontal cortex of Alzheimer's patient's compared with age-matched controls (34). It is postulated that diminished PEMT activity may be implicated in the abnormal brain phospholipid metabolism observed in patients with Alzheimer's disease (34).

Thus, the detection of PEMT transcripts in human heart and brain represents an important step towards understanding the mechanisms responsible for aberrant PEMT activity in these pathophysiological states. It should now be possible to distinguish if changes at the transcriptional or post-transcriptional level can account for the reported changes in PEMT activity. Moreover, as PEMT activity in heart and brain is so low compared to that of liver, the pathophysiological relevance of altered PEMT activity in human heart and brain may now be evaluated.

2.3.5 Transcript Profile of PEMT

Studies were extended to include analysis of transcripts in liver, heart and testis. RT-PCR was performed on total RNA prepared from normal human liver or poly A^+ RNA from heart and testis, using sense primers specific for each untranslated exon (Ex1F, Ex2F, Ex3F, Table 2.1) and a

common antisense primer, (Ex9R or Ex6R, liver; Ex8R or Ex7R, heart & testis, Table 2.1, Figs 2.4A & 2.4B). All PCR reactions were carried out using equal volumes of the RT products, thus providing equal amounts of template for each reaction.

Amplicons of the predicted size were obtained with each primer pair in the liver (Fig. 2.4A), supporting the existence of all three transcripts in this tissue. However, amplicons of the predicted size were only obtained using an exon 1-specific primer in heart and using both exon 1- and exon 3-specific primers in testis (Fig. 2.4A). In the case of the latter amplicon from testis (exon 3-containing transcript), this transcript appears to be present in very low abundance. Southern blot analysis of the RT-PCR products using the internal probe, PEMT-int, confirmed the authenticity of the PEMT transcripts.

RT-PCR analysis was subsequently performed using a different set of sense primers that are also specific for each untranslated exon. Similar results were obtained confirming the relative abundance of the transcripts within each tissue and excluding differential primer hybridization kinetics as a cause of the observed differences in transcript abundance in liver and testis (data not shown). Thus, differential processing of the *PEMT* gene generates alternate transcripts, the abundance of which is controlled in a tissue-specific manner. The significance of alternate transcripts in both liver and the extra-hepatic tissues may now be investigated.

Transcripts containing exon 2 as the first exon are the major PEMT transcripts in human liver (Fig. 2.3). The lack of cross-reactivity with transcripts containing exons 1 or 3 in RNA blot analysis may be explained by the lower levels of these transcripts in liver compared to those containing exon 2. Thus, detection of the transcripts by RT-PCR is likely due to the sensitive nature of the procedure.

Assays of human liver homogenates demonstrated significant PEMT activity in this organ (0.24 nmol/min. mg prot.). Based on the above results, it would thus appear that the most abundant transcript is responsible for the majority of hepatic PEMT activity given that each transcript has a common open reading frame. However, differences in the *cis*-acting elements in the 5′ UTR have been shown to confer differences in the translational efficiency of mRNA species (35). Thus, it is also possible that a pattern of enzymatic activity distinct from the transcript profile may exist.

2.3.6 Identification of Transcription Start Sites

The transcription start site of the major PEMT transcript was identified. Using the primer pair, Ex5R-IRC (Table 2.1), followed by nested PCR using primers, Ex4R-IIRC, a single amplicon was generated from a CapSite liver cDNA library (Fig. 2.5). The PCR product was cloned, and

sequenced in both directions. A single transcription start site was identified 50 bp upstream of the previously identified 5'end of exon 2 (Figs 2.5B & 2.5C). The cap-site is located 175 bp upstream of the translation initiation site of that transcript (Fig. 2.5C). Several clones were sequenced and each clone contained sequence specific to the exon 2-containing transcript. However, each PEMT transcript has a different untranslated first exon, thus three distinct transcription start sites should exist. As the antisense primers used in the analysis are common to all transcripts, the most abundant transcript has a higher probability of being amplified, hence the detection of only exon 2-containing transcripts. To specifically identify the transcriptional start site of mRNA species containing exons 1 or 3 at the 5' end, antisense primers were utilized that are specific for each transcript. However, the transcription start sites were not identified using this strategy. Attempts to identify the transcription start sites by 5' RACE were also unsuccessful (data not shown) indicating that the transcripts may be present in very low amounts, a hypothesis substantiated by results from the previous experiments (Figs 2.3B, 2.3C and 2.4A).

2.3.7 Analysis of the Putative promoter region

A combination of "gene walking", subcloning and sequencing of cloned fragments to confirm sequence fidelity elucidated the proximal promoter region sequence of the major transcript. As exon 2 is the leader exon of this transcript, the corresponding promoter is referred to as

promoter B. Sequences of each untranslated exon and the corresponding promoter are enumerated relative to the first common nucleotide, which is at the 5' end of exon 4, and are also designated the letter, A, B or C based on their structural order in the gene (Figs 2.5B & 2.5C). Using the *Transfac* search engine, sequence analysis of promoter B was performed to identify putative transcription factor binding sites. Consensus binding sites for several transcription factors including C/EBP, AP1, SREBP, GATA-1 and STATx, were identified but the major PEMT promoter was found to be devoid of TATA or CCAAT boxes (Fig. 2.5C). Factors such as C/EBP and SREBP may contribute to the high liver-specific expression of exon 2-containing transcripts. Promoter analysis of the human PEMT gene may now be undertaken to fully elucidate the elements that mediate the differential expression of the transcripts.

In summary, cloning and structural characterization of the *PEMT* gene is described for the first time. The *PEMT* gene encodes three variant transcripts generated by differential promoter usage. Three unique untranslated leading exons are alternatively spliced to a common exon 4, where translation initiates. Liver, heart and testis each have a disparate PEMT transcript profile demonstrating that differential promoter usage also mediates a tissue-specific expression pattern. The relative abundance of PEMT transcripts in liver is vastly greater than in extra-hepatic tissues signifying that higher levels of the enzyme may be important in this organ. Moreover, the existence of three distinct transcripts in liver may suggest

differential regulation of hepatic *PEMT* expression, such as during development or in periods of physiological stress.

Table 2.1 Oligonucleotides Used in the Genomic Characterization of Human PEMT

Oligonucleotides were utilized for PCR, RT-PCR, CapSite cDNA, Rapid-Scan™ analysis and sequencing of exon-intron boundaries.

Primer Name	Sequence
PEMT-specific primers	
Ex1F	GCGGATGAAGAGATCTGGGA
Ex1R	TGTTCGTTACCTCGGCTCCCGGGTTCCCAGATCTCTTCATC
Ex2F	GCGACCATAAAGCCTCTTCCT
Ex2R	GACGAATAGCCTCAGCTGTTAACACCCCAAAGCATGGGTA
Ex3F	GGATCCGCGGCGAGGAGAG
Ex3R	GAATCAGGTAAAAGCAAATTAAAACAATAGTGGTGTGCCT
Ex4F	CACCTTCAATCCGCTCTACTG
Ex4R	AAGGTGATGGTGATGACGG
Ex5F	ACCATCCTGCTCCTGAACTTCC
Ex5R	GAAGTTCAGGAGCAGGATGGTG
Ex6F	TTCTTTGCACTGGGGTTCGC
Ex6R	AACCCCAGTGCAAAGAAGCTGG
Ex7F	GGAAGCACAGCCAACTACTTGG
Ex7R	GGTTGTCCAGGATGTTGAAGGG
Ex8F	CCCTCACCTACATAATGGCTCTCC
Ex8R	GGAGAGCCATTCTGTAGGTGAGGG
Ex9R	GCAGCTCAATCAGCTCCTCTTG
PEMT-int	AGCCTGGGCCTCGCGCTCCTGGGACTGGGCGTCGTG
WU-I	AAGGAAAGGAGCTACCCACCAC
WU-II	ACCACACACAACAAAGGGC
WU-III	GGATGAGTGTGCCAGAGTCT
CapSite primers	
IRC	CAAGGTACGCCACAGCGTATG
IIRC	GTACGCCACAGCGTATGATGC

Table 2.2 Genomic Structure of Human PEMT

Exon-intron boundary sequences were determined using primers based on the cDNA sequence, with reference to the murine gene structure. Exon sequence is in upper case. Lower case bold letters indicate a consensus splicing nucleotide in the intronic sequence at the ends of introns (36). Codon phase refers to the site of splicing relative to a codon, i.e. a splice site between codons is designated "O", splicing between 1st and 2nd nucleotides of the codon as "I", and between 2nd and 3rd nucleotides as "II".

a. Position in cDNA relative to identified transcription start site.

b. Determined by bioinformatic analysis

c. Flanking exonic sequence is untranslated

Exon	Size (bp)	Position in cDNA[a]	Splice Donor	Intron Size(kb)	Splice Acceptor	Codon Phase
1	99	-	CAGgtg	15[b]	[illegible]	[illegible]
2	165	1	GTGgtg	4.0	[illegible]	[illegible]
3	60	-	CTGgta	0.5	[illegible]	[illegible]
4	108	166	GTGgta	53[b]	gcagGCA	0
5	116	274	CTGgta	8.0	ttagGTT	II
6	146	420	TAGgta	3.0	acagCTT	I
7	112	532	CATgtg	3.5	acagGTG	II
8	79	611	AGAgtg	0.6	tcagGCA	II
9	285	896	-	-	gcagGCC	-

Figure 2.1 Chromosomal Localization of the Human PEMT Gene as Determined by FISH Mapping

Human lymphocyte chromosomes were probed with a biotinylated derivative of the human PEMT gene. Avidin-fluorescein isothiocyanate was used to detect the biotinylated probe. Chromosomes were counterstained with propidium iodide and 4', 6-diamidin-2-phenylindol-dihydrochloride (DAPI).

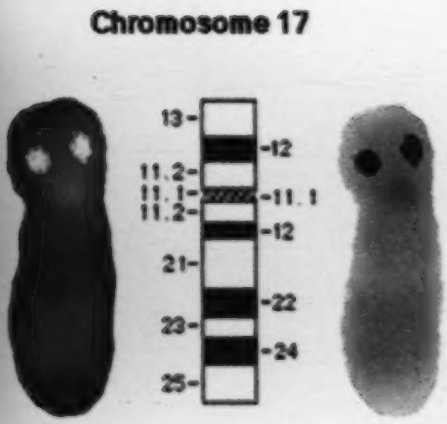
Chromosome 17
13-
-12
11.2-
11.1-
-11.1
11.2-
-12
21-
-22
23-
-24
25-

Figure 2.2 Genomic Organization of Human *PEMT*

Schematic representation of the exon-intron organization of PEMT. Boxes and the intervening spaces represent exons and introns, respectively. Shaded boxes indicate differentially processed 5' untranslated exons. Exon 4 contains the translation start site (AUG). Exons and introns are drawn to scale with the exception of the introns denoted by asterisks. The scale bar denotes 1kb. Exons and introns are enumerated as indicated in the schematic diagram. Solid lines connecting exons represent the splicing pattern of the most abundant transcript in human liver, while dashed lines between exons indicate alternative processing to generate less abundant splice variants.

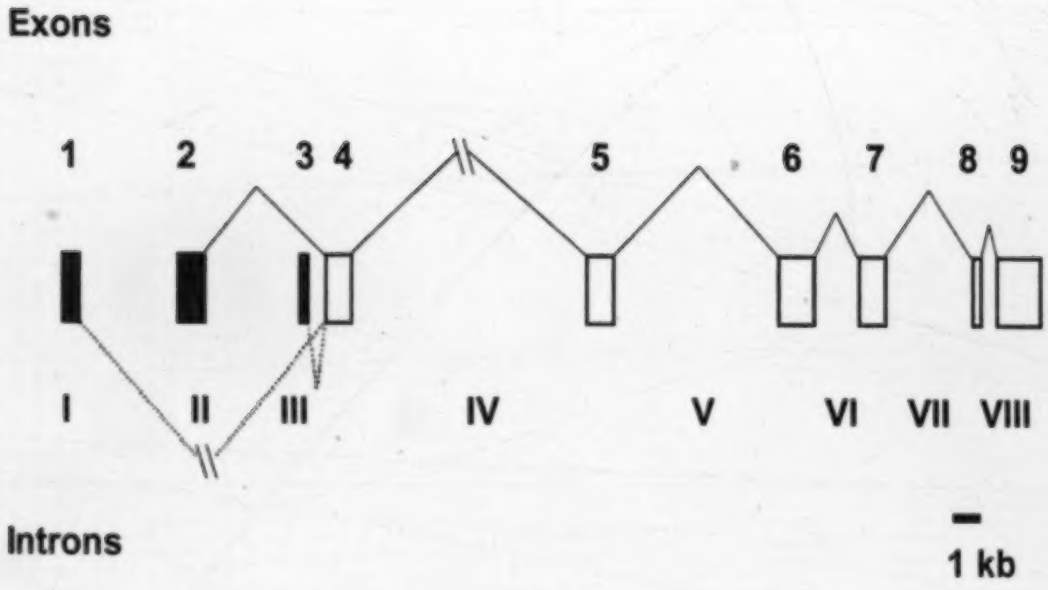
Exons
1
2
3 4
5
6
7
8 9
I
II
III
IV
V
VI
VII
VIII
Introns
1 kb

Figure 2.3 Tissue-specific Expression Profile of PEMT

A. Southern blot analysis of PCR products using a Rapid-Scan™ cDNA panel as template. Primers for amplification are specific for the hPEMT open reading frame. A panel containing cDNAs at a concentration of 1000X β-actin transcripts is shown. Amplicons were confirmed to be of PEMT origin by Southern blot analysis using the radiolabeled internal oligonucleotide, PEMT-int as probe (Table I).

B. A radiolabeled exon 2-specific oligonucleotide was used to probe a Master Blot™, to determine the transcript(s) expressed in liver. Northern blot analysis was carried out as described in detail in *Materials and Methods.* Each dot contains 100-500 ng mRNA. Key to tissue mRNA present on the Master Blot™ is as follows:

A1, whole brain; A2, amygdala; A3, caudate nucleus; A4, cerebellum; A5, cerebral cortex; A6, frontal lobe; A7, hippocampus; A8, medulla oblongata; B1, occipital lobe; B2, putamen; B3, substantia nigra; B4, temporal lobe; B5, thalamus; B6, sub-thalamic nucleus; B7, spinal cord; C1, heart; C2, aorta; C3, skeletal muscle; C4, colon; C5, bladder; C6, uterus; C7, prostate; C8, stomach; D1, testis; D2, ovary, D3, pancreas; D4, pituitary gland; D5, adrenal gland; D6,thyroid gland; D7, salivary gland; D8, mammary gland; E1, kidney; ***E2, liver;*** *E3, small intestine; E4, spleen; E5, thymus; E6, peripheral leukocyte; E7, lymph node; E8, bone marrow; F1, appendix; F2, lung; F3, trachea; F4, placenta; G1, fetal brain; G2, fetal heart; G3, fetal kidney; G4, fetal liver; G5, fetal spleen; G6, fetal thymus; G7, fetal lung; H1, yeast total RNA; H2, yeast tRNA; H3, E. coli rRNA: H4, E. coli DNA; H5, Poly r(A); H6, human C_0t1 DNA; H7, human DNA (100 ng); H8, human DNA (500 ng).*

C. Adult and fetal Multiple Tissue Northern™ blots were probed with a radiolabeled exon 2-specific oligonucleotide. Each lane contains approximately 2 μg mRNA. A band (1kb) corresponding to PEMT mRNA is detectable only in human adult (left panel) and fetal (right panel) liver mRNA. Blots were treated as described above.

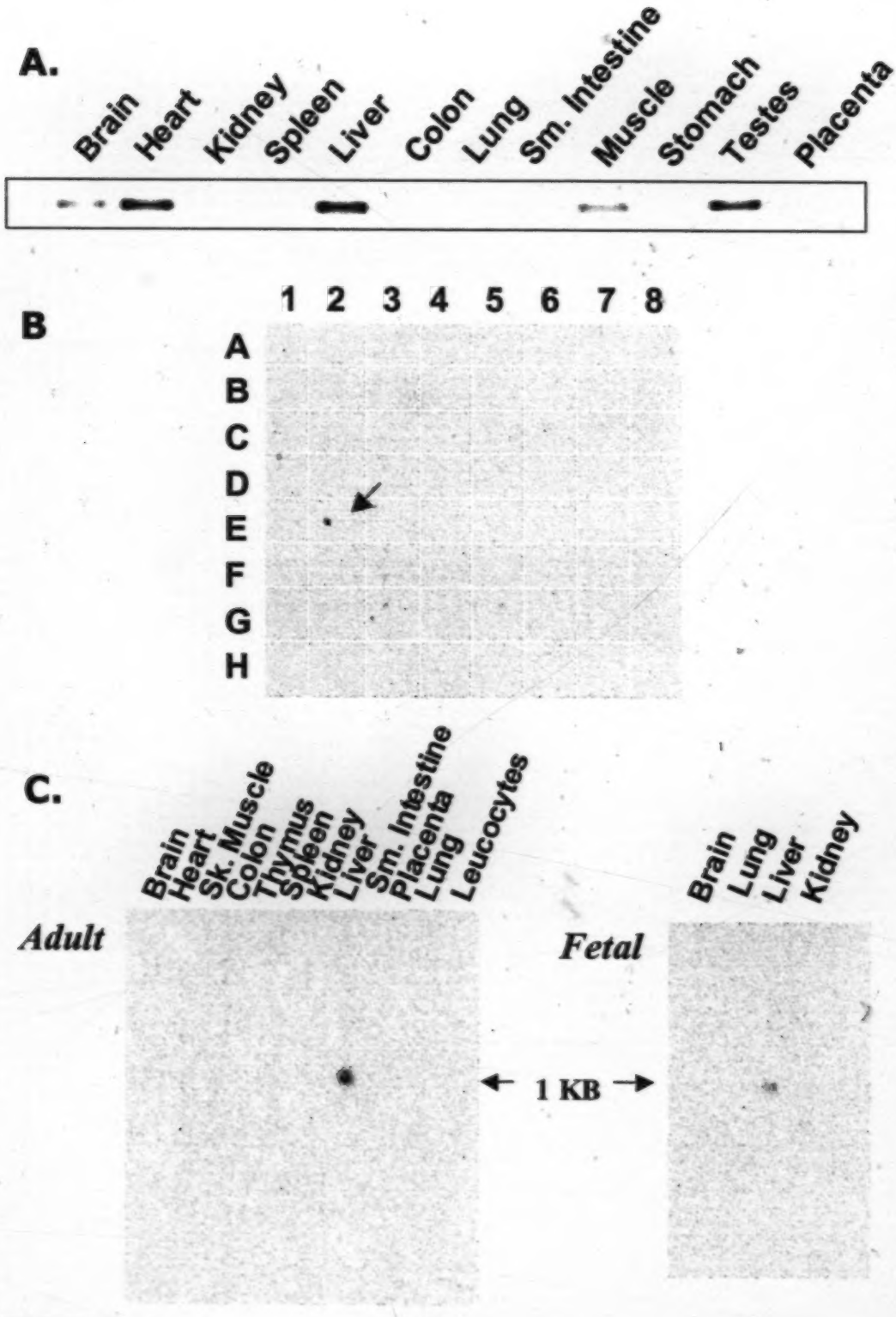
A.
Brain
Heart
Kidney
Spleen
Liver
Colon
Lung
Sm. Intestine
Muscle
Stomach
Testes
Placenta
B
1 2 3 4 5 6 7 8
A
B
C
D
E
F
G
H
C.
Brain
Heart
Sk. Muscle
Colon
Thymus
Spleen
Kidney
Liver
Sm. Intestine
Placenta
Lung
Leucocytes
Adult
Brain
Lung
Liver
Kidney
Fetal
1 KB

Figure 2.4 Relative Abundance of Different PEMT mRNA Isoforms in Human Liver, Heart & Testis

A. Southern blot analysis of RT-PCR products from total liver RNA or heart & testis poly A^+ RNA using different primer pairs. Total RNA (3μg) and poly A^+ RNA (500ng) were reverse transcribed using an 18mer oligo-dT and the gene-specific Ex9R as primer respectively. PCR was carried out with equal volumes of the same RT reaction as template for each tissue using the indicated primer sets. The PCR products were confirmed to be of PEMT origin by Southern blot analysis using the radiolabeled internal oligonucleotide, PEMT-int, as described in *Materials and Methods.*

B. Schematic representation showing locations of primers used in RT-PCR analysis of human liver RNA. Antisense (AS)-1 and -2 refer to Ex9R and Ex6R respectively for liver and to Ex8R and Ex7R for heart and testis. Crosshatched boxes represent untranslated variable exons and open boxes represent translated common exons.

A

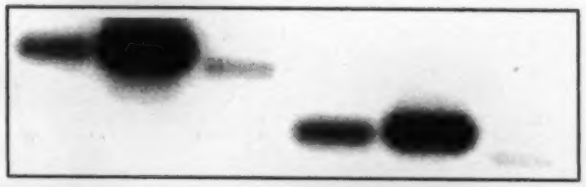

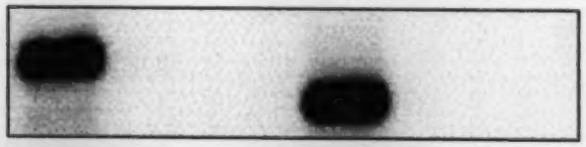

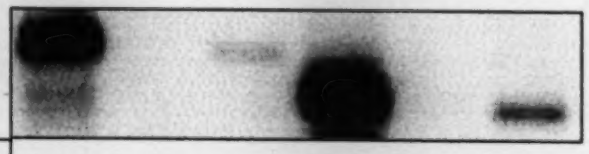

Primer						
Ex1F	+			+		
Ex2F		+			+	
Ex3F			+			+
AS1				+	+	+
AS2	+	+	+			

B

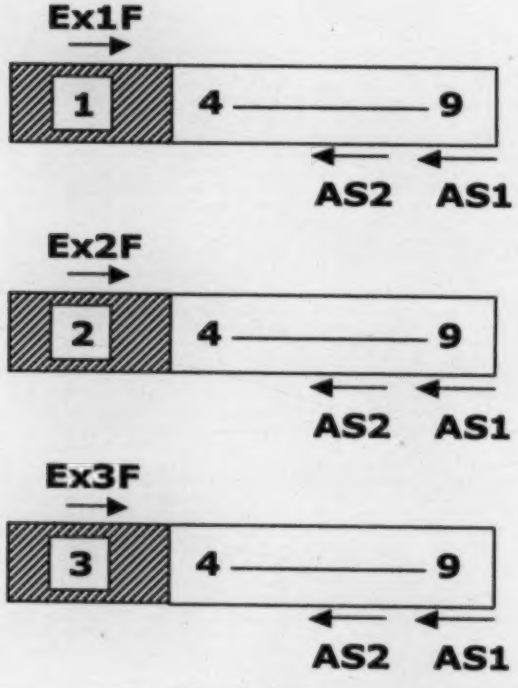

Fig. 2.5 Identification of the Transcription Start Site and Putative Promoter Region of the Major PEMT Transcript.

A. The single amplicon shown was generated from a CapSite cDNA library and includes the transcription start site of the major PEMT transcript. PCR amplification was performed as described in detail in *Materials and Methods.* The PCR product was cloned, and sequenced in both directions to identify the transcription start site.

B. Schematic representation of the 5' region of *PEMT*. Each spliced untranslated exon (crosshatched boxes) is shown in addition to the common exon 4 (filled box) that contains the translation start site. Newly identified sequence from CapSite™ cDNA is represented by the open box of exon 2. The transcription start site of only exon 2-containing transcripts was identified and is indicated with an arrow. Sequences of untranslated exons are enumerated according to their position relative to the first nucleotide of exon 4, which is common to all transcripts. Consensus transcription factor binding sites of the major promoter (promoter B) are indicated.

C. Genomic sequence proximal to the transcription start site of the major PEMT mRNA. Transcription start site is indicated with an asterisk. Proximal sequence is enumerated with reference to the first nucleotide of exon 4, which is common to all transcripts. Common sequence at the 5'end of exon 4 is highlighted in bold. Putative transcription factor-binding sites are underlined and labeled. The boxed ATG denotes the translation initiation site.

A.

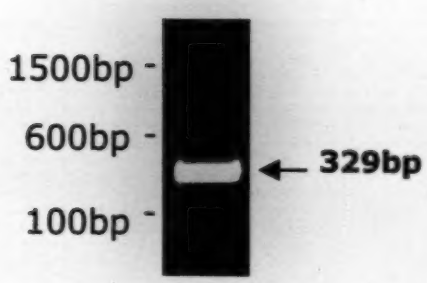

B.

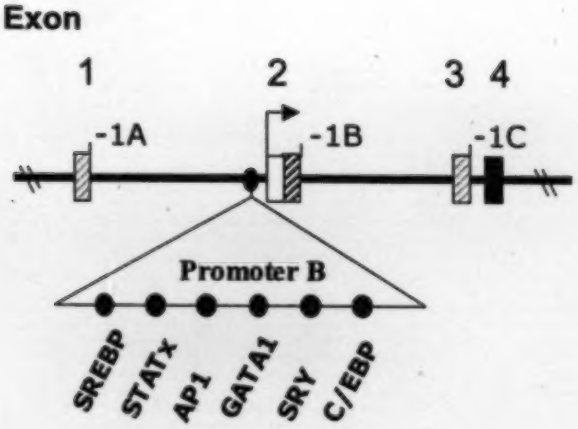

C.

```
GAGATGGAGTCTCGCTCTGTCATCCAGGCTGGAGTGCAGTGGCATGATCT -750B
                    SREBP
CGGCTCACTGCAACCTCTGCCTCCCAGGTTCAAGTGATTCTTCTGCCTCA -700B

GCCTCCCCAGTAGCTGGGACTACAGTCGTGCACCACCATGTCCAGCTAAT -650B

TTTTGTATTTTTAGTAGAAACGGGGTTTCACCATATTGGCCAGGCTGATC -600B
  AP1
TCTGACTCCTGGCCTTGTGATCCGCCTGCCTAGGCCTCCCAAAGTGCTGG -550B
                                        STATx
GATTACGGGGGTGAGCCATCGCGCCCGGCCCAGAGAATAAACTTAGAGGA -500B

AAAAGACTCTGGCACACTCATCCTTATGTCTTTGTGCCAGGCACAGGGCT -450B
                              AP1
CTAACCCAAAGTTGCCGTAAATAAACGTTACCCGAGTCAGCTTATGGTGC -400B

CAGGGCATGAGGGCAGCTCTGGGGGCAGTGGGGGCTGCAGCGCTGCAGGC -350B
 GATA1
AGATTCTGCAGGGGTGATGGATCCCAGGAGGACCTTGTCCCCTTCTCCAG -300B

CAAGCCCCCCACCCATTCCCGTGCCCTTTGTTGTGTGTGGTGTGTGGCCT -250B
                        SRY
GGAATCGATGTGACTTTGCCTGTCCAGGCCTGCTGTTTGTCCATGTGTCA -200B
                                              *
CAATGTGACATGTTGACCCACTGCAGATCATTCCCTGACCACAGAGCGTT -150B
                              C/EBP
GATCCCGAGAACCCTGCACCCCTCAATGGAGTAAATTACCATAAAGCCTC -100B

TTCCTTACCCATGCTTTGGGGTGTTAACAGCTGAGGCTATTCGTCGGTGA -50B
                C/EBP
CCTGTGGGACTCGAGCTATTCCTGCAGCTCAGCAGACCTCCTGGCCGTGG +1

CAGACTTCTGCGTTATG
```

References

1. Kent, C. (1997) *Biochim. Biophys. Acta.* **1348**, 79-90.

2. Mathur, S. N., Born, E., Murthy, S., and Field, F. J. (1996) *Biochem. J.* **314**, 569-75.

3. Agellon, L. B. (2002) in *Biochemistry of Lipids, Lipoproteins and Membranes* (Vance, D. E., and Vance, J. E., eds), 4 Ed., pp. 433-448, Elsevier, Amsterdam

4. Exton, J. H. (1994) *Biochim. Biophys. Acta.* **1212**, 26-42.

5. Vance, D. E. (2002) in *Biochemistry of Lipids, Lipoproteins and Membranes* (Vance, D. E., and Vance, J. E., eds), 4 Ed., pp. 205-232, Elsevier, Amsterdam

6. Vance, D. E., and Ridgway, N. D. (1988) *Prog. Lipid. Res.* **27**, 61-79

7. Sundler, R., and Akesson, B. (1975) *J. Biol. Chem.* **250**, 3359-67.

8. Reo, N. V., and Adinehzadeh, M. (2000) *Toxicol. Appl. Pharmacol.* **164**, 113-26.

9. DeLong, C. J., Shen, Y. J., Thomas, M. J., and Cui, Z. (1999) *J. Biol. Chem.* **274**, 29683-8.

10. Vance, J. E., and Vance, D. E. (1986) *J. Biol. Chem.* **261**, 4486-91.

11. Nishimaki-Mogami, T., Suzuki, K., and Takahashi, A. (1996) *Biochim. Biophys. Acta.* **1304**, 21-31.

12. Nishimaki-Mogami, T., Suzuki, K., Okochi, E., and Takahashi, A. (1996) *Biochim. Biophys. Acta.* **1304**, 11-20.

13. Agellon, L. B., Walkey, C. J., Vance, D. E., Kuipers, F., and Verkade, H. J. (1999) *Hepatology* **30**, 725-9.

14. Verma, A., Ahmed, H. A., Davis, T., Jazrawi, R. P., and Northfield, T. C. (1999) *J. Hepatol.* **31**, 852-9.

15. Cui, Z., Vance, J. E., Chen, M. H., Voelker, D. R., and Vance, D. E. (1993) *J. Biol. Chem.* **268**, 16655-63.

16. Cui, Z., Shen, Y. J., and Vance, D. E. (1997) *Biochim. Biophys. Acta.* **1346**, 10-6.

17. Panagia, V., Ganguly, P. K., and Dhalla, N. S. (1984) *Biochim. Biophys. Acta.* **792**, 245-53.

18. Prasad, C., and Edwards, R. M. (1981) *J. Biol. Chem.* **256**, 1300-3.

19. Nieto, A., and Catt, K. J. (1983) *Endocrinology* **113**, 758-62.

20. Sarzale, M. G., and Pilarska, M. (1976) *Biochim. Biophys. Acta* **441**, 81-92

21. Houweling, M., Cui, Z., Tessitore, L., and Vance, D. E. (1997) *Biochim. Biophys. Acta.* **1346**, 1-9.

22. Tessitore, L., Cui, Z., and Vance, D. E. (1997) *Biochem. J.* **322**, 151-4.

23. Tessitore, L., Dianzani, I., Cui, Z., and Vance, D. E. (1999) *Biochem. J.* **337**, 23-7.

24. Walkey, C. J., Donohue, L. R., Bronson, R., Agellon, L. B., and Vance, D. E. (1997) *Proc. Natl. Acad. Sci. U S A.* **94**, 12880-5.

25. Walkey, C. J., Yu, L., Agellon, L. B., and Vance, D. E. (1998) *J. Biol. Chem.* **273**, 27043-6.

26. Zeisel, S. H., and Blusztajn, J. K. (1994) *Annu. Rev. Nutr.* **14**, 269-96

27. Waite, K. A., Cabilio, N. R., and Vance, D. E. (2002) *J. Nutr.* **132**, 68-71.

28. Walkey, C. J., Shields, D. J., and Vance, D. E. (1999) *Biochim. Biophys. Acta.* **1436**, 405-12.

29. Walkey, C. J., Cui, Z., Agellon, L. B., and Vance, D. E. (1996) *J. Lipid. Res.* **37**, 2341-50.

30. Wang, Y., Newton, D. C., Robb, G. B., Kau, C. L., Miller, T. L., Cheung, A. H., Hall, A. V., VanDamme, S., Wilcox, J. N., and Marsden, P. A. (1999) *Proc. Natl. Acad. Sci. U S A.* **96**, 12150-5.

31. Yu, G. S., Lu, Y. C., and Gulick, T. (1998) *J. Biol. Chem.* **273**, 32901-9.

32. Ha, J., Daniel, S., Kong, I. S., Park, C. K., Tae, H. J., and Kim, K. H. (1994) *Eur. J. Biochem.* **219**, 297-306.

33. Panagia, V., Taira, Y., Ganguly, P. K., Tung, S., and Dhalla, N. S. (1990) *J. Clin. Invest.* **86**, 777-84.

34. Guan, Z. Z., Wang, Y. N., Xiao, K. Q., Hu, P. S., and Liu, J. L. (1999) *Neurochem. Int.* **34**, 41-7.

35. Gingras, A. C., Raught, B., and Sonenberg, N. (1999) *Annu. Rev. Biochem.* **68**, 913-63

36. Mount, S. M. (1982) *Nucleic. Acids. Res.* **10**, 459-72.

Chapter 3

Membrane Topography of Human Phosphatidylethanolamine N-Methyltransferase

A version of this chapter was accepted for publication in *J. Biol. Chem.* (2003)

3.1 Introduction

All eukaryotic cells synthesize phosphatidylcholine (PC), which has an integral role in membrane ultrastructure and intracellular signaling (1,2). In hepatocytes, an additional and substantial demand is imposed on the PC pool by the liver-specific functions of production and secretion of bile and very low density lipoprotein (VLDL) particles (3,4). The phosphatidylethanolamine *N*-methyltransferase (PEMT) and CDP-choline biosynthetic pathways mediate continual replenishment of the hepatic PC pools (5). The liver is the primary site of PEMT activity whereas the enzymes of the CDP-choline pathway are active in all nucleated cells (2,6).

PC biosynthesis is clearly essential to liver function, but why that synthesis must be conducted through two distinct pathways is less evident. Recent studies investigating the proportion of hepatic PC that is derived from each pathway, defined the PEMT-controlled pathway as the source of 30% of hepatic PC with the CDP-choline pathway accounting for 70% (7-9). Significantly perhaps, data from one group also revealed that the PEMT pathway is a metabolically channeled process suggesting that PEMT-derived PC may be destined for a specific function (9).

Given that PEMT is primarily expressed in liver, PEMT-derived PC might be targeted to a liver-specific fate such as VLDL particles or bile (10-13). In efforts to address these hypotheses, studies were recently

conducted using hepatocytes from mice homozygous for a disrupted PEMT allele. The data revealed a defect in the secretion of triacylglycerol and apo B100, key components of VLDL particles, suggesting that PEMT is required for optimal VLDL assembly and/or secretion (14). Additional studies investigating a role for PEMT in bile production or secretion are currently in progress.

Metabolic channeling is central to several metabolic processes including glycolysis and glycogenolysis, and involves the retention of metabolites in a specific microenvironment to promote consecutive enzymatic reactions and hence efficient energy utilization (15). For metabolic channeling to be effective, however, spatial organization is requisite. Thus, not only should enzymes and substrates be localized in the same cellular sub-compartment, but enzymes must also be topographically organized such that key catalytic residues or motifs are correctly oriented.

Liver is the primary site of human PEMT expression, with extra-hepatic PEMT accounting for a mere fraction of corporeal expression (6,16-20). Herein, biochemical analysis of human liver reveals that PEMT is primarily localized to the endoplasmic reticulum (ER) and a subfraction of ER membranes that co-fractionate with mitochondria: mitochondria associated membranes (MAM). However, the exact topography of the enzyme within those membranes has not been determined. Resolution of the topographical orientation of PEMT will permit further analysis of the role

of metabolic partitioning in PC biosynthesis. Moreover, it will provide the basis for in depth exploration of the mechanism by which PEMT becomes rate limiting in the secretion of VLDL particles.

Bioinformatic analysis predicts that PEMT is a polytopic membrane protein with four transmembrane domains, and thus yields a model that positions the N- and C-termini of the enzyme in the same intracellular compartment (21). However, *in silico* analysis cannot resolve whether the end termini of PEMT reside in the cytosol or in the microsomal lumen.

Here, we detail the biochemical validation of a topographical model of PEMT, using endoproteinase protection analysis of functional epitope-tagged derivatives of the enzyme. These studies will provide the basis for detailed structural and functional characterization of the human enzyme.

3.2 Materials and Methods

3.2.1 Reagents

Dulbecco's modified Eagle's medium (DMEM), fetal bovine serum, restriction endonucleases and Platinum Pfx DNA polymerase were from Invitrogen Life Technologies. Oligonucleotides for mutagenesis and epitope tagging were synthesized at the DNA core facility in the Dept. of Biochemistry, University of Alberta. Fugene transfection reagent was from Roche Molecular Biochemicals. *S*-adenosyl-L-[*methyl*-^{3}H]methionine (15 Ci/mmol) was obtained from Amersham Biosciences. Non-radiolabeled *S*-adenosyl-L-methionine, anti-HA monoclonal antibody (clone HA-7) and endoproteinase Lys-C were from Sigma Chemical Co. Rabbit polyclonal anti-protein disulphide isomerase (PDI) antibody was from Stressgen Biotech. Goat anti-rabbit and goat anti-mouse secondary antibodies were purchased from Pierce. All other reagents were of the highest standard commercially available.

3.2.2 Subcellular Fractionation

Adult human liver samples were obtained from the Dept. of Surgery at the University Of Alberta Hospital and were snap-frozen in liquid nitrogen at resection. Differential subcellular fractionation was performed according to the procedure of Croze and Morre as modified by Vance, yielding fractions

corresponding to ER, nucleus, plasma membrane, mitochondria, MAM and Golgi apparatus (22,23). Protein concentrations of individual fractions were measured by the Bradford method, using albumin as standard.

Microsomes for protease protection analysis were prepared by a modified version of the method of Graham (24). Briefly, 24 h post-transfection with the various human PEMT (hPEMT) recombinant plasmids, Cos-7 cells were washed, harvested into phosphate buffered saline and pelleted at 1000 *g*. The pellet was resuspended in buffer A (50 mM Tris, pH 7.4, 250 mM sucrose, 1 mM EDTA), sonicated for 5 s, and centrifuged at 6000 *g* for 15 min to pellet nuclei, heavy mitochondria, plasma membrane, Golgi and cell debris. The resulting supernatant was then centrifuged for 45 min, at 99,000 rpm at 4°C. The pellet was resuspended in 75 µl of Tris-buffered saline by pipetting gently 20 times. Protein concentrations of the prepared microsomes were determined by the Bradford method. Integrity of the microsomes was verified by immunoblotting with a polyclonal antibody against the ER luminal marker, protein disulfide isomerase (PDI).

3.2.3 Bioinformatic analysis

Hydropathy analysis, based on the method of Kyte and Doolittle was performed on the predicted human PEMT amino acid sequence (accession number, NP_009100), using the Grease program of the San Diego Supercomputer Center Biology Workbench (workbench.sdsc.edu) (25). The

TMAP program in the Biology Workbench was employed to predict the position and length of individual transmembrane domains (26).

3.2.4 Recombinant Plasmid Construction

All plasmids were constructed using the wildtype hPEMT-pCI plasmid as template (21). This plasmid consists of the human PEMT open reading frame cloned 5' to 3' into the *Xho*I and *Xba*I sites, respectively, of the pCI mammalian expression vector polylinker (Promega). Transcription is under the control of a CMV promoter. Using PCR, an oligonucleotide encoding a HA (YPYDVPDYA) tag epitope was appended to the 5' end of hPEMT to generate the plasmid, HA-hPEMT. PCR products were blunt-end ligated to *Sma*I-cut pBluescript II (KS) (Stratagene), and recloned into pCI using *Xho*I and *Xba*I restriction sites. Mutant PEMT derivatives for protease protection analysis were generated by the "splice by overlap extension" PCR mutagenesis method, using the HA-hPEMT plasmid as template (27). Full-length mutant products were subcloned into the pCI expression vector as detailed above. All constructs were sequenced to confirm fidelity of PCR and orientation of the insert, at the Molecular Biology Services Unit, University of Alberta.

To mutagenize the two lysines at positions 38 & 41 in loop A to arginine residues, generating the HA-tagged double mutant HA-AK2R2, PCR

A was performed with oligonucleotides 1 (5'-CTCGAGATGTATCCATATGATGTTCCAGATTATGCTACCCGGCTGCTGGGCTACG TGGACCCCCTG-3') and 2 (5'-TGTTCCCATCGTGCAACCACATTCCAG-3'), PCR B with oligonucleotides 3 (5'-GTGGTTGCACGATGGGAACACAGGACCCGCAGG CTGAGCAGGGCCTTCG-3') and 4 (5'-TCTAGATCAGCTCCTCTTGTGGGACCCGG AGGCT-3'), and PCR C, to generate the full-length mutant product, with oligonucleotides 1 and 4, using amplicons from PCR A & B as templates. To mutate the two C terminal lysines at positions 191 & 197 to arginine residues, and generate the HA-tagged double mutant HA-CK2R2, PCR D was performed with oligonucleotides 1 and 5 (5'-TCTAGATCAGCTCCTCCTGTGGGACCCGGAGGCTCTCTGCCG-3'). To insert a novel endoproteinase Lys-C cleavage site into loop B, the arginine residue at position 80 was mutated to a lysine, generating the plasmid HA-R80K. This was achieved as follows: PCR E was performed with oligonucleotides 1 and 6 (5'-GGCTGGCTCAGCATGGCCTG-3'), PCR F was performed with oligonucleotides 7 (5'-CAGGCCATGCTGAGCCAGCCCAAGATGGAGAGCCTGGA C-3') and 4, and the full-length product, using PCR products E & F as template, was generated using oligonucleotides 1 and 4. Each full-length mutant amplicon was recloned into pCI as described.

3.2.5 Cell culture and Transfections

Cos-7 cells, obtained from the American Type Culture Collection repository, were maintained in Dulbecco's modified Eagle's medium, 10%

fetal bovine serum, 100 units/ml penicillin and 100 µg/ml streptomycin sulfate, at 37°C, 5% CO2. On day 0, cells were plated at a confluency of 1.75×10^6 cells/60 mm dish. After an overnight incubation, cells were transfected with test plasmids or mock transfected with empty pCI expression vector using Fugene transfection reagent as per the manufacturer's protocol. Specifically, we used 5 µl Fugene/3 µg DNA plasmid per 60 mm dish. Cells were harvested 24 h later and treated as described in the Figure Legends.

3.2.6 Phosphatidylethanolamine N-Methyltransferase Activity Assays

PEMT activity assays were performed as described previously (28). Briefly, 24 h after transfection, Cos-7 cells were washed with and harvested into phosphate buffered saline, pelleted at 1000 g and resuspended in buffer B (10 mM Tris, pH 7.4, 150 mM NaCl, 1 mM EDTA, 1mM DTT, 0.1 mM PMSF). Following homogenization by sonication, protein homogenates (50 µg) were assayed for PEMT activity using phosphatidylmonomethylethanolamine (Avanti Polar Lipids, Alabaster, AL) as a methyl acceptor and *S*-adenosyl-L-[*methyl*-^{3}H]methionine as the methyl group donor.

3.2.7 Immunoblot analysis

Cell homogenate proteins (25 µg) were separated by Tris-Glycine SDS-polyacrylamide electrophoresis, on 12.5% polyacrylamide gels calibrated with prestained molecular weight standards (Bio-Rad). Following electrophoresis, proteins were transferred to PVDF membranes and immunoblotted with primary antibodies at the indicated concentration. Protein-antibody complexes were detected by enhanced chemiluminescence with horseradish peroxidase-conjugated secondary antibody using the ECL reagent (Amersham Pharmacia Biosciences) as directed. Membranes were exposed to Biomax MR film (Kodak) for the indicated time at room temperature.

3.2.8 Endoproteinase Lys-C Protection Assays

Endoproteinase protection analyses were performed on microsomes prepared from transfected Cos-7 cells as described above. Briefly, microsomal proteins (50 µg) were incubated with 1% Triton X-100 or 100 mM Tris-HCl, pH 8.5, on ice for 30 min. Endoproteinase Lys-C (0, 0.1, or 1 µg) was added to the mixture (final reaction volume: 20 µl) and incubated at 37°C for 3 h. Each reaction was stopped by the addition of buffer C (5x: 60 mM Tris-HCl, pH 6.8, 25% glycerol, 2% SDS, 715 mM β-mercaptoethanol, 0.1% bromophenol blue) and boiled for 10 min. Endoproteinase cleavage products were separated by Tris-Glycine SDS-polyacrylamide gel electrophoresis on 15% polyacrylamide gels and

immunoblotted as described above. Integrity of the microsomes was validated by immunoblotting with a monoclonal anti-PDI antibody.

3.3 Results

3.3.1 Subcellular Localization of PEMT

Early studies on human PEMT identified the liver as the primary site of expression, which parallels the expression pattern of PEMT in rodents (6,29). Although the rat PEMT activity is distributed between ER and MAM, only the isoform designated PEMT2, in the MAM fraction, is immunoreactive with an antibody raised against a C-terminal rat PEMT peptide (16). To determine if the human enzyme displays similar disparity in the localization of enzymatic activity and immunoreactivity, subcellular fractionation of human liver was performed. Similar to rodents, the human PEMT activity is primarily localized to ER and MAM (Fig. 3.1A), but unlike rodents the human PEMT enzyme is also immunoreactive to the anti-PEMT peptide antibody in both ER and MAM (Fig. 3.1B). Immunoblotting with anti-PDI confirmed that the fractions representing ER and MAM (which is a subfraction of ER) were of ER origin (Fig. 3.1C). As the activity and immunoreactivity of human PEMT are superimposable, it appears that the differential subcellular localization of PEMT isoforms, as observed in the rat, has not been conserved in evolution.

3.3.2 Predicted Membrane Topography of PEMT

Purification of PEMT revealed the enzyme to be an integral membrane protein (30). To gain insight into the topography of PEMT in the membranes of ER/MAM, the deduced amino acid sequence was examined *in silico* using the method of Kyte and Doolittle (25). The hydropathy profile of PEMT shown in Fig. 3.2A predicts the presence of four hydrophobic regions. Each hydrophobic region exceeds 20 amino acids in length and registers a value of >2 units on the hydropathy plot, two properties strongly indicative of a transmembrane domain. A polytopic model based on four transmembrane alpha helical domains colocalizes the N- and C- termini on one side of the membrane plane, suggesting that PEMT adopts one of two opposing topographical orientations (both termini in the lumen or both termini in the cytosol).

To investigate which of the two possible topographical models is valid, intact microsomes were prepared from transfected cells and subjected to endoproteinase digestion in the absence or presence of detergent. In the absence of detergent, proteolysis is expected to occur only at exposed cleavage sites on the microsomal exterior and the luminally-oriented sites should remain protected. Cleavage of protected luminally oriented sites should occur only in the presence of detergent. The protease utilized in these studies, endoproteinase Lys-C, specifically cleaves at the C-terminus of lysine residues, and given the position of the lysine residues within the PEMT amino acid sequence, was expected to yield an informative proteolytic pattern (Fig's 3.2B and 3.2C).

3.3.3 Characterization of HA-tagged PEMT Protein

To perform the topographical analyses, an antibody capable of detecting proteolytic cleavage products was required. An antibody against a peptide corresponding to an epitope at the extreme C-terminus of PEMT was raised previously, but this epitope contains two lysine residues (endoproteinase Lys-C cleavage sites) with the consequence that proteolysis would result in cleavage at these residues and destruction of the epitope. Therefore, although this antibody is informative for the localization of the C-terminus, it would not be expected to yield interpretable results for the remainder of the protein.

To circumvent this problem a haemagglutinin (HA) tag, which does not contain lysine residues, was appended to the N-terminus of PEMT. Hydropathy analysis of the epitope-tagged protein sequence did not predict changes in the number or length of the predicted transmembrane domains. Furthermore, the HA-tagged PEMT expressed in Cos-7 cells is enzymatically active (Fig. 3.3A). Immunoblotting verified the production of recombinant proteins (Fig. 3.3B) and faithful recognition of the HA antigen tag by the anti-HA antibody (Fig. 3.3C).

3.3.4 Protease Protection Analysis of Epitope-tagged PEMT

To analyze which one of the two possible membrane topography models of PEMT is valid, a plasmid encoding HA-tagged PEMT was transfected into Cos-7 cells. Subsequently, microsomes were prepared, incubated with various concentrations of endoproteinase Lys-C in the absence or presence of Triton X-100, and the resultant proteolytic products were separated by SDS-polyacrylamide gel electrophoreses and analyzed by immunoblotting (Fig. 3.4A). In microsomes incubated without protease, an immunoreactive band corresponding to the epitope-tagged PEMT was detectable at ~22 kDa in the absence or presence of Triton X-100 (Fig. 3.4A, lanes 1, 2).

In the presence of endoproteinase, but in the absence of Triton X-100, the ~22 kDa band was replaced by one of increased electrophoretic mobility (Fig. 3.4A, lanes 3 and 5). This is indicative of cleavage at the C-terminal lysine residues, which generates a truncation product lacking the final eight residues of the epitope-tagged protein. As proteolysis occurred in the absence of detergent, this result suggests that the C-terminus of PEMT is localized external to the microsomes.

To confirm that the endoproteinase was functional in the absence of Triton X-100, and hence that the electrophoretic shift observed in Fig. 3.4A (lanes 3-6) was due to proteolytic cleavage, duplicate proteolytic products were immunoblotted with a rabbit polyclonal anti-PEMT antibody. Protease treatment, in the absence or presence of Triton X-100 resulted in

destruction of the C-terminal PEMT epitope and consequently, a loss of immunoreactivity, confirming that the protease remained active (Fig. 3.4B, lanes 3-6).

In the presence of Triton X-100, the C-terminal truncation product was again evident but a reduction in intensity resulted as protease concentrations increased (Fig. 3.4A, lanes 4 and 6). This was due to proteolysis at the previously inaccessible luminal cleavage sites. Digestion in the presence of Triton X-100 also resulted in the appearance of a fast migrating band of ~5.2 kDa (Fig. 3.4A, lanes 4 and 6). This band corresponds to the expected proteolytic product resulting from cleavage at the lysine residues in loop A. The diffuse appearance of the 5.2 kDa immunoreactive band is probably due to the high concentration of proteolytic fragments in this region of the gel. Given the appearance of this immunoreactive band only in the presence of detergent, loop A appears to reside in the ER lumen.

To verify the integrity of the prepared microsomes, duplicate proteolysis products were immunoblotted with an antibody against the ER luminal marker, PDI (Fig. 3.4C). In the absence of detergent, a 57 kDa immunoreactive band was detectable, indicating protection of the epitope and thus demonstrating the integrity of the microsomes (Fig. 3.4C, lanes 1, 3 and 5). In the presence of detergent, proteolysis abolished the immunoreactivity of PDI, demonstrating that the detergent permeabilized

the microsomes and that the protease was active (Fig. 3.4C, lanes 4 and 6). These data support the validity of a topographical model that localizes both termini external to the microsomes (Fig. 3.4D).

3.3.5 Evaluation of HA-tagged PEMT mutants

Further analysis of the proposed topography of PEMT required the design of three novel HA-tagged PEMT derivatives. To confirm the specificity of cleavage at the lysine residues in the C-terminus (Fig. 3.4A), both residues were mutated to arginine residues to generate the plasmid, HA-CK2R2. To evaluate the proposed cytosolic localization of loop B, a mutant version of PEMT was generated in which a lysine residue and hence endoproteinase site was engineered into loop B, resulting in the plasmid, HA-R80K. To confirm the specificity of cleavage at the two lysine residues in Loop A, and to investigate the orientation of loop C, a third plasmid, HA-AK2R2, was generated in which both lysine residues in loop A were mutated to arginine residues. To ensure that the mutant constructs retained PEMT activity, each construct was transfected into Cos-7 cells and activity assays were performed. Cells transfected with each mutant construct displayed equal (HA-AK2R2) or greater (HA-CK2R2, HA-R80K) PEMT activity compared to cells expressing the unmodified HA-tagged PEMT enzyme (Fig. 3.5A), signifying that the structure and topography required for enzymatic activity are retained. Immunoblots demonstrated similar levels of expression of the recombinant proteins (Fig. 3.5B).

3.3.6 Protease Protection Analysis of HA-tagged PEMT Mutants

In the next set of experiments, the plasmid HA-CK2R2, encoding an hPEMT derivative that lacks the C-terminal proteolysis sites (Fig. 3.6A), was transfected into Cos-7 cells to evaluate the specificity of endoproteinase cleavage at the C-terminal lysine residues. Microsomes were prepared from the transfected cells and protease protection experiments were conducted as before. Digestion of the microsomes with various concentrations of the protease, in the absence of Triton X-100, did not change the electrophoretic mobility of the ~22 kDa band that corresponds to the full-length tagged mutant protein (Fig. 3.6B, lanes 1-6). This contrasts with data obtained from the HA-hPEMT proteolysis experiments (Fig. 3.4A, lanes 3-6), in which the C-terminal lysine residues are intact and cleavage results. This result supports the notion that the C-terminus of PEMT resides in the cytosol, validating our earlier findings and one portion of our predicted model (Fig. 3.4D). As anticipated, proteolytic products from microsomes treated with protease in the presence of detergent (Fig. 3.6B, lanes 4 and 6), were similar to those generated from protection experiments on HA-hPEMT (Fig. 3.4A, lanes 4 and 6). Reprobing of the membranes with an anti-PDI antibody verified the integrity of the microsomal membranes (Fig. 3.6C).

The topographical model in Fig. 3.4D postulated that loop B is exposed to the cytosol. To examine this hypothesis, Cos-7 cells were

transfected with the plasmid HA-R80K, which contains an engineered endoproteinase site in loop B. Proteolysis in the absence of detergent was predicted to yield a novel immunoreactive proteolytic fragment reflecting cleavage at the exposed loop B site. However, cleavage did not occur in the absence of detergent (results not shown), suggesting that the engineered cleavage site is protected and that loop B is localized proximate to, or embedded in, the membrane. Alternatively, loop B may adopt a structural conformation, external to the microsomes, that renders the cleavage site inaccessible to the endoproteinase. Given the length and hydrophobicity of each predicted transmembrane domain, a bitopic model based on two transmembrane domains that would orient loop B into the ER lumen is unlikely. Thus, although the topography of loop B remains indeterminate, a model positioning the hydrophilic connecting loop contiguous with the external leaflet of the membrane bilayer is favored.

In the final set of experiments, the plasmid HA-AK2R2, in which the cleavage sites in loop A are abolished (Fig. 3.7A), was transfected into Cos-7 cells and protease protection analysis was performed. As anticipated, results from the protease protection experiments conducted in the absence of Triton X-100 (Fig. 3.7B, lanes 1, 3, 5), were similar to those from similar experiments on HA-hPEMT (Fig. 3.4A, lanes 1, 3, 5). However, in the presence of detergent, addition of protease failed to yield a proteolytic fragment of ~5.2 kDa (Fig. 3.7B, lanes 4 and 6), confirming that the 5.2 kDa fragment generated following cleavage of HA-hPEMT was a result of

specific proteolysis at the lysine residues in loop A (Fig. 3.5B, lanes 4 and 6). Hence, the predicted luminal localization of loop A is supported.

Furthermore, proteolysis in the presence of Triton X-100 yielded a fragment of ~15 kDa as postulated (Fig. 3.7B, lanes 4 and 6). Previously, this product was not generated due to the presence of the loop A cleavage sites within the 15 kDa fragment. However, following ablation of the loop A sites, the 15 kDa proteolytic product was generated following cleavage at the lysine residue in Loop C. Given that the appearance of this product occurs in the presence of detergent, our notion of a luminal orientation for loop C is supported. Immunoblotting with an anti-PDI antibody confirmed the integrity of the microsomes and thus the interpretation of our results (Fig. 3.7C).

3.4 Discussion

Expression of the human *PEMT* gene is greatest in the liver and here we demonstrate that the encoded PEMT protein is enriched subcellularly in both the ER and MAM subcompartments (Fig. 3.1). This contrasts with findings in rats where two isoforms of PEMT exist that are distinguishable on the basis of immunoreactivity with an antibody raised against a rat PEMT C-terminal peptide; PEMT1 is localized to the ER while PEMT2 is confined to the MAM (16). However, in humans, PEMT activity and immunoreactivity are detectable in both the ER and MAM suggesting that the differential subcellular localization of PEMT isoforms may be confined to rodents (Fig. 3.1).

Although the localization of PEMT within the human hepatic ultrastructure has now been revealed, factors that direct PEMT to the specific subcellular compartment remain to be identified. Targeting of ER membrane proteins is a well-defined process that is modulated by specific retention or retrieval signals (31,32). Whereas the first transmembrane segment of some polytopic proteins serves to "retain" the protein in the ER membrane, a C-terminal dilysine motif (KKxx or KxKxx) can similarly confer ER localization, albeit through retrieval from an intermediate compartment (31,32). A C-terminal dilysine motif is present in the yeast PEM2 amino acid sequence, but this motif is not conserved in the higher eukaryotes. However, a hybrid xHKRx motif is conserved in the rat, mouse and human

amino acid sequences. Moreover, in certain instances, it has been demonstrated that mutagenesis of one lysine in the dilysine motif to an arginine or a histidine residue can occur without detriment to ER targeting (33). Since histidine and arginine residues flank the C-terminal lysine residue, one of several amino acid combinations could potentially mediate ER targeting of human PEMT. For a dilysine motif to be functional as an ER targeting signal, a cytosolic orientation is requisite. Our proposed topographical model for PEMT in which the C-terminal is localized to the cytosol conforms to this requirement. Further analysis would be required to determine the relative contribution of the xHKRx motif to the subcellular distribution of PEMT.

Elucidation of the subcellular distribution of the integral membrane protein, PEMT, prompted an investigation of the topographical orientation of PEMT in the microsomal membranes. While early trypsin-proteolysis studies suggested that certain domains of PEMT were localized external to the microsomal membranes, the specific membrane topography of PEMT had until now, remained elusive (34). Here, we present data that are consistent with the tetra-span membrane topography model of PEMT shown in Fig. 3.2B.

Bioinformatic analysis of the PEMT amino acid sequence revealed the presence of four regions of hydrophobicity that varied in length between 23 and 29 amino acids. Separating the putative transmembrane alpha helical

regions are short hydrophilic loops (A, B and C) that range from 8 to 29 residues in length. While the exact functional significance of the length of the short loops remains undefined, this structural organization may facilitate juxtaposition of distinct functional domains from the adjoining transmembrane alpha helices. Such an alignment is not without precedent, as the topography of two enzymes central to cellular cholesterol homeostasis (i.e., sterol regulatory element binding protein cleavage-activating protein and 3-hydroxy-3-methylglutaryl CoA reductase), feature a series of five closely aligned transmembrane domains that together, constitute a conserved sterol-sensing domain (35,36).

Since each hydrophobic region of the PEMT protein exceeds the minimum length considered necessary for the formation of a transmembrane segment (20 aa) and because of the relative hydrophobicity (>2 units) of each segment, a membrane topography based on four transmembrane domains is proposed (Fig. 3.2B) (37). In contrast, while the yeast orthologue (PEM2) is proposed to be similarly polytopic, one portion of the yeast protein contains a hydrophobic stretch of 31 amino acids which intriguingly, is the minimum length required for the formation of a helical hairpin (helix-turn-helix) in the membrane (38). Moreover, a pair of residues with helix turn-inducing propensity (lysine-proline) is centrally located in the 31 residue hydrophobic segment (39,40). However, as each putative transmembrane domain of the human protein ranges in length from 23-29 amino acids, and is thus below the minimum requirement for the

formation of a helical hairpin, the four human transmembrane alpha helical regions are not predicted to reorient within the membrane plane.

Protease protection analysis of epitope-tagged PEMT in intact microsomes revealed that the C-terminus is sensitive to proteolytic digestion and hence is exposed to the cytosol, while both hydrophilic loops A and C are protease resistant and are thus predicted to reside in the lumen (Fig. 3.4A, Fig. 3.6B, Fig. 3.7B). Although the orientation of loop B and the N-terminus of PEMT were not resolved unequivocally in the present studies, a hydropathy profile that is strongly indicative of a tetra-spanning topography combined with the orientation of loops A, C and the C-terminus, suggests that both loop B and the N-terminal domain are cytosolically oriented. Furthermore, as the hydropathy profile of PEMT is highly conserved in species from *Rattus norvegicus* to *Homo sapiens*, the elucidated membrane topography of the human enzyme should prove representative of the higher eukaryotic PEMT family.

Recent data from experiments utilizing isotopic labeling and NMR spectroscopy suggest that channeling of metabolites occurs in the PEMT pathway (9). Identification of residues essential for binding of the methyl group donor, AdoMet, combined with the current data on the subcellular localization and topographical orientation of PEMT, should provide the clearest insight yet into the specific role of metabolic channeling in this pathway.

Approximately 85% of methylation reactions occur in the liver and AdoMet is the most widely utilized methyl group donor (41,42). Although several consensus AdoMet-binding motifs have been identified that are conserved in the majority of AdoMet-dependent methyltransferases, a small fraction of AdoMet-dependent methyltransferases including the eukaryotic PEMT family of enzymes lack these motifs (43). Cellular AdoMet is concentrated predominantly in the cytosol, with a smaller fraction present in mitochondria (44). Thus, we posit that residues essential for binding of the AdoMet moiety are localized in the cytosolically disposed hydrophilic loop (B) or at the cytosolic face of the transmembrane alpha helices. Elucidation of the topographical organization of PEMT should therefore accelerate the identification of residues that are important for binding AdoMet.

In summary, we describe the first experimental resolution of the topography of an enzyme that catalyzes the synthesis of PC. Data from the current studies should provide the impetus for detailed structural analysis of PEMT, which in turn should yield evidence for a definitive topographical model of this AdoMet-dependent methyltransferase. Elucidation of the topographical organization of PEMT will enable detailed analysis of the spatio-temporal organization of residues essential for the binding of AdoMet, and hence promote a mechanistic understanding of the methylation-dependent biosynthesis of PC.

Fig. 3.1 Subcellular Localization of PEMT in Human Liver.

Human liver samples, snap-frozen at resection, were subjected to differential subcellular fractionation (22,23).

A. PEMT specific activity in individual fractions. Homogenates of each fraction, 50 μg protein, were assayed for PEMT activity. ER, endoplasmic reticulum; PM, plasma membrane; MAM, mitochondria associated membranes; Mito, mitochondria.

B. Immunoblot with anti-PEMT antibody using 25 μg of protein homogenates for each fraction.

C. Immunoblot with anti-PDI antibody using 25 μg of protein homogenates for each fraction.

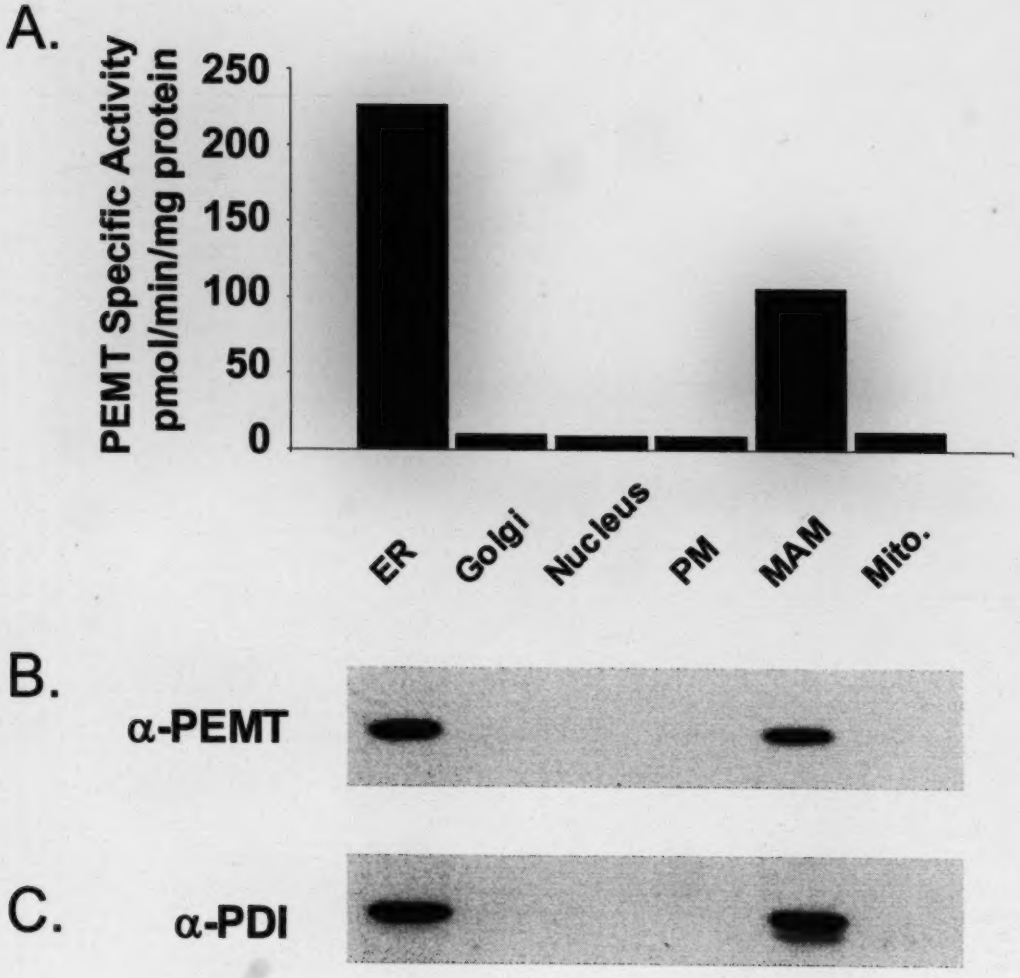
A.
PEMT Specific Activity
pmol/min/mg protein
250
200
150
100
50
0
ER
Golgi
Nucleus
PM
MAM
Mito.
B.
α-PEMT
C.
α-PDI

Fig. 3.2 Hydropathy Plot and Predicted Membrane Topography of PEMT.

A. Hydropathy plot of the human PEMT amino acid sequence, as determined by the Grease program (based on the method of Kyte and Doolitle), at the San Diego Supercomputer Center Biology Workbench (25).

B. Working model for PEMT topography. Hydrophilic connecting loops are labeled A, B and C. Arrows indicate endoproteinase Lys-C cleavage sites.

C. Shaded and unshaded regions in the PEMT amino acid sequence denote predicted transmembrane alpha helices and hydrophilic connecting loops respectively. Asterisks indicate the position of lysine residues (endoproteinase Lys-C cleavage sites).

A.

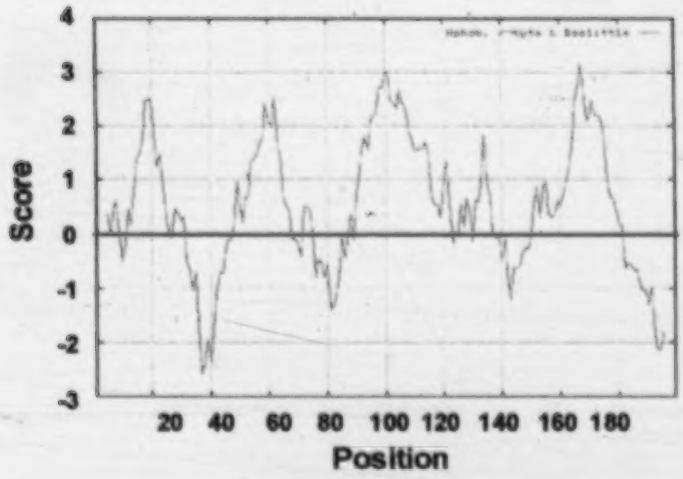

B.

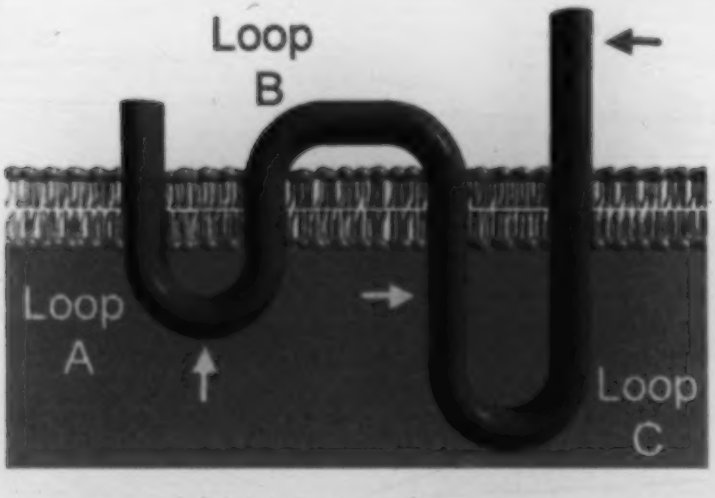

C.

MTRLLGYVDP LDPSFVAAVI TITFNPLYWN VVARWEHKTR KLSRAFGSPY

LACYSLSVTI LLLNFLRSHC FTQAMLSQPR MESLDTPAAY SLGLALLGLG

VVLVLSSFFA LGFAGTFLGD YFGILKEARV TVFPFNILDN PMYWGSTANY

LGWAIMHASP TGLLLTVLVA LTYIMALLYE EPFTAEIYRQ KASGSHKRS

Fig. 3.3 Epitope-Tagged PEMT Protein is Enzymatically Active in Transfected Cos-7 Cells.

Cos-7 cells were transiently transfected with 3 μg of plasmids containing wildtype PEMT or epitope tagged PEMT derivatives, or mock transfected with empty pCI vector.

A. Cellular homogenates, 50 μg protein, were assayed for PEMT activity. The results are expressed as the mean of three separate experiments, each performed in duplicate, ± S.E.M, relative to the values obtained for similar assays on cells transfected with wildtype PEMT.

B. Immunoblot with anti-PEMT antibody using 25 μg protein of transfected cellular homogenates.

C. Immunoblot with anti-HA antibody using 25 μg protein of transfected cellular homogenates

A.

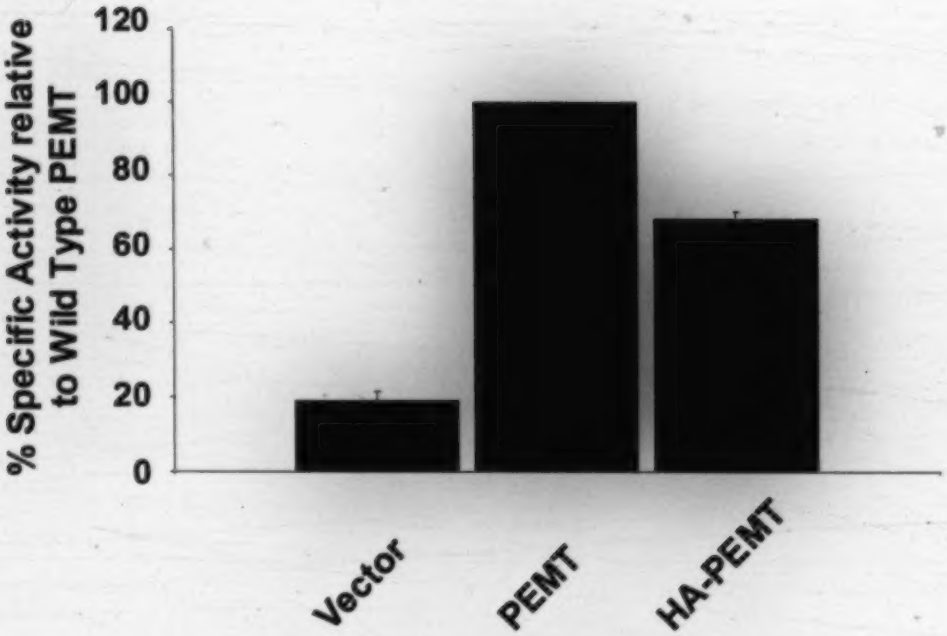
% Specific Activity relative to Wild Type PEMT
120
100
80
60
40
20
0
Vector
PEMT
HA-PEMT

B.

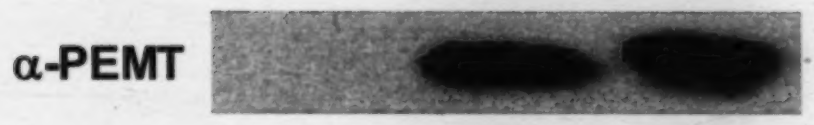
α-PEMT

C.

α-HA

Fig. 3.4 Luminal orientation of loop A and cytosolic orientation of the C-terminus as determined by protease protection analysis.

A. Microsomes were prepared from transfected cells as described in Experimental Procedures. Aliquots, 50 µg protein, were incubated with various concentrations of endoproteinase (+ = 0.1 µg, ++ = 1 µg) at 37°C for 3 h, in the absence or presence of 1% Triton X-100. Reactions were stopped by the addition of electrophoretic loading buffer and boiling at 100°C for 10 min. Samples were separated by SDS-polyacrylamide gel electrophoresis, transferred to PVDF membranes and immunoblotted with anti-HA antibody. The film was exposed at room temperature for 30 s.

B. Replicate membranes of protease protection products, generated as described above, were immunoblotted with an anti-PEMT antibody.

C. Replicate membranes of protease protection products, generated as described above, were immunoblotted with an anti-PDI antibody to confirm the integrity of the microsomes. Representative immunoblots are shown. Each protease protection experiment was repeated at least three times with similar results.

D. Predicted membrane topography model of PEMT. Endoproteinase Lys-C cleavage sites are denoted by arrows and the length of cleavage fragments generated from proteolysis at each site, as measured from the N-terminal HA-tag epitope are indicated in kDa.

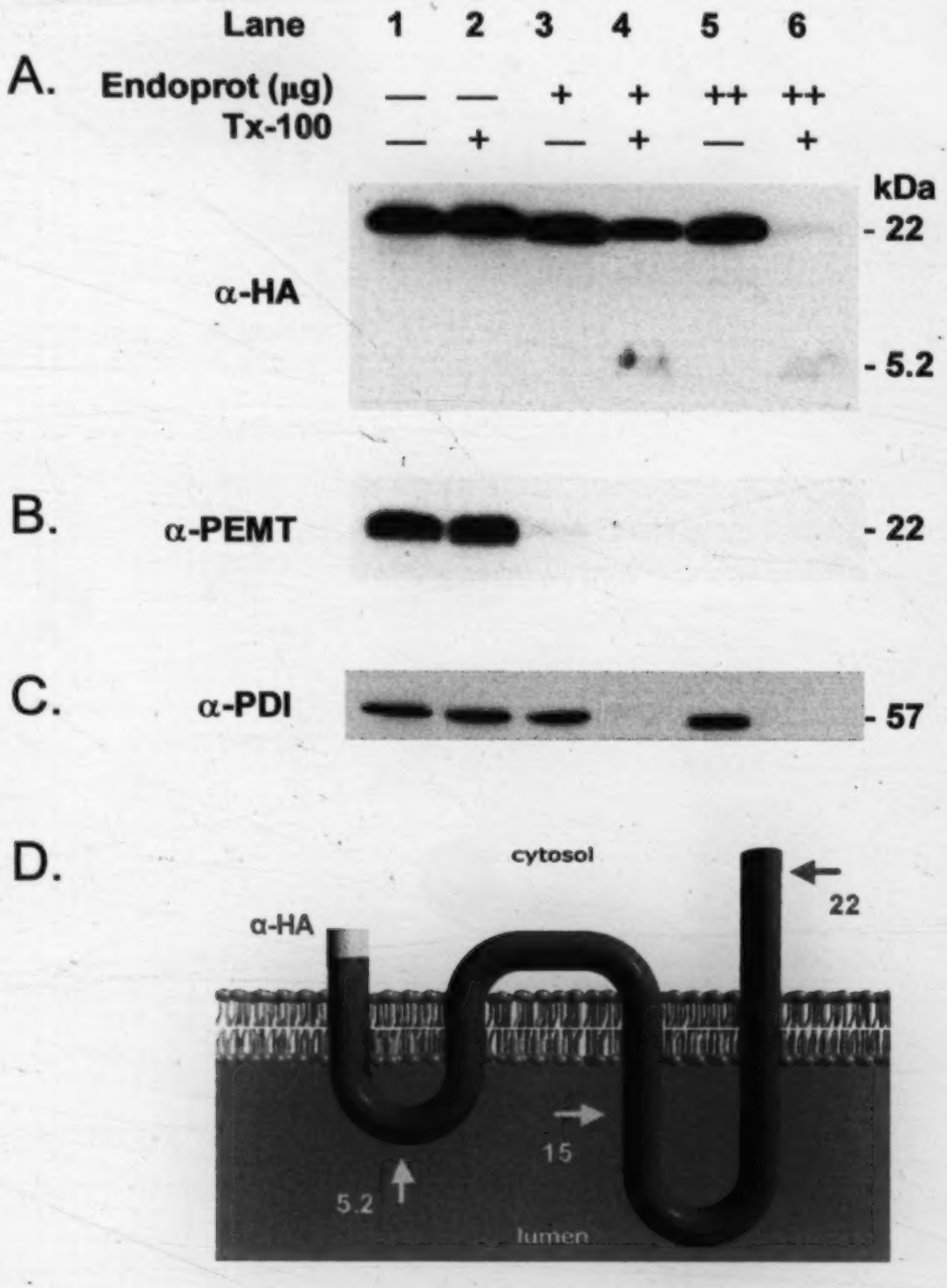
Lane 1 2 3 4 5 6
A.
Endoprot (µg) — — + + ++ ++
Tx-100 — + — + — +
kDa
- 22
α-HA
- 5.2
B.
α-PEMT
- 22
C.
α-PDI
- 57
D.
cytosol
22
α-HA
15
5.2
lumen

Fig. 3.5 Epitope-tagged mutant PEMT derivatives retain enzymatic activity in transfected Cos-7 cells.

Cos-7 cells, set up as described in *Materials and Methods*, were transiently transfected with 3 µg of plasmids containing epitope-tagged PEMT or epitope-tagged mutant PEMT derivatives, or mock transfected with empty pCI vector.

A. Cellular homogenates, 50 µg protein, were assayed for PEMT activity. The results are expressed as the mean of three separate experiments, each performed in duplicate, ± S.E.M, relative to the values obtained for similar assays on cells transfected with HA-tagged PEMT.

B. Cellular homogenates, 25 µg protein, were immunoblotted with anti-HA antibody.

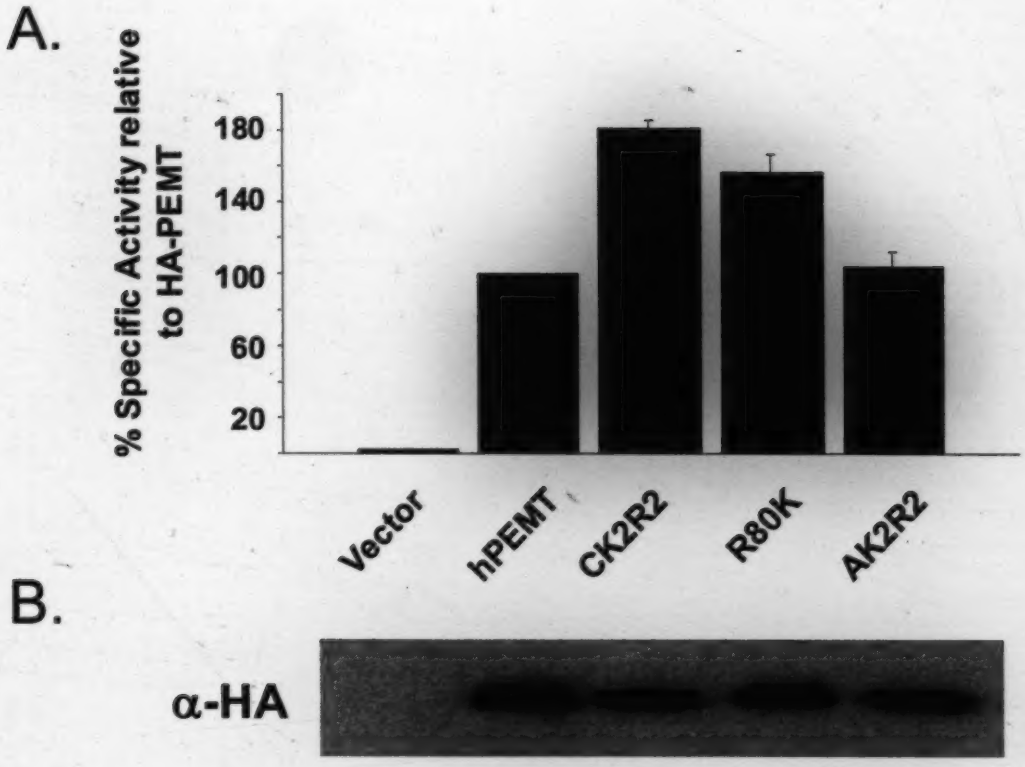
A.
% Specific Activity relative to HA-PEMT
180
140
100
60
20
Vector
hPEMT
CK2R2
R80K
AK2R2
B.
α-HA

Fig. 3.6 Protease Protection Analysis of the PEMT Mutant CK2R2 Confirms the Cytosolic Orientation of the C-terminus.

A. Predicted membrane topography model of PEMT. Endoproteinase Lys-C cleavage sites are denoted by arrows and the length of cleavage fragments generated from proteolysis at each site, as measured from the N-terminal HA-tag epitope are indicated in kDa. Ablation of the C-terminal endoproteinase cleavage sites is indicated.

B. Microsomes were prepared from transfected cells as described in *Materials and Methods*. Aliquots, 50 μg protein, were incubated with various concentrations of endoproteinase (+ = 0.1 μg, ++ = 1 μg) at 37°C for 3 h, in the absence or presence of 1% Triton X-100. Reactions were stopped by the addition of electrophoresis loading buffer and boiling at 100°C for 10 min. Samples were separated by SDS-polyacrylamide gel electrophoresis, transferred to PVDF membranes and immunoblotted with anti-HA antibody. The film was exposed at room temperature for 30 s.

C. Duplicate membranes of protease protection products, generated as described above, were immunoblotted with an anti-PDI antibody to confirm the integrity of the microsomes. Representative immunoblots are shown. Each protease protection experiment was repeated at least three times with similar results.

A.

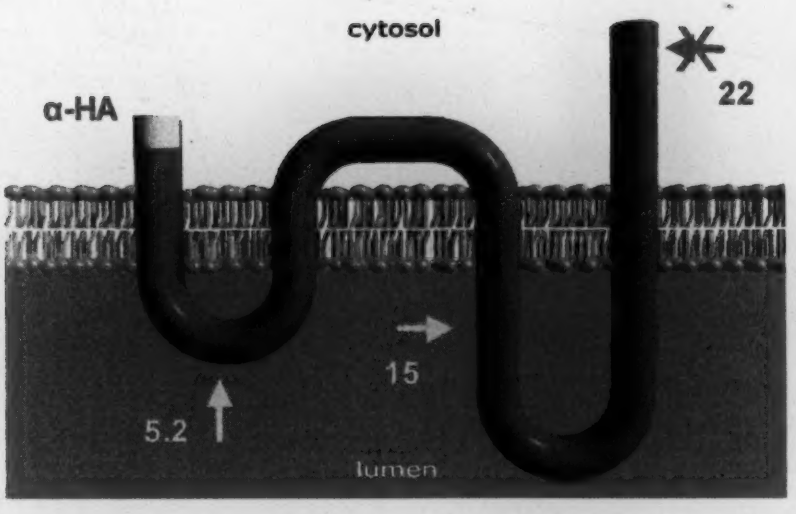

Lane	1	2	3	4	5	6
Endoprot (μg)	—	—	+	+	++	++
Tx-100	—	+	—	+	—	+

B.

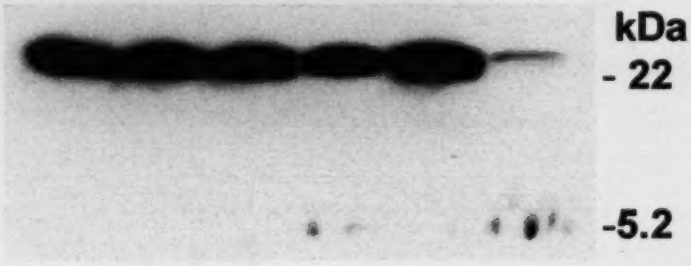

C.

Fig. 3.7 Luminal Orientation of Loops A and C Demonstrated by Protease Protection Analysis of PEMT Mutant, AK2R2.

A. Predicted membrane topography model of PEMT. Endoproteinase Lys-C cleavage sites are denoted by arrows and the length of cleavage fragments generated from proteolysis at each site, as measured from the N-terminal HA-tag epitope are indicated in kDa. Ablation of the Loop A endoproteinase cleavage sites is indicated.

B. Microsomes were prepared from transfected cells as described in *Materials and Methods*. Aliquots, 50 μg protein, were incubated with various concentrations of endoproteinase (+ = 0.1 μg, ++ = 1 μg) at 37°C for 3 h, in the absence or presence of 1% Triton X-100. Reactions were stopped by the addition of electrophoresis loading buffer and boiling at 100°C for 10 min. Samples were separated by SDS-polyacrylamide gel electrophoresis, transferred to PVDF membranes and immunoblotted with anti-HA antibody. The film was exposed at room temperature for 30 s.

C. Duplicate membranes of protease protection products, generated as described above, were immunoblotted with an anti-PDI antibody to confirm the integrity of the microsomes. Representative immunoblots are shown. Each protease protection experiment was repeated at least three times with similar results.

A.

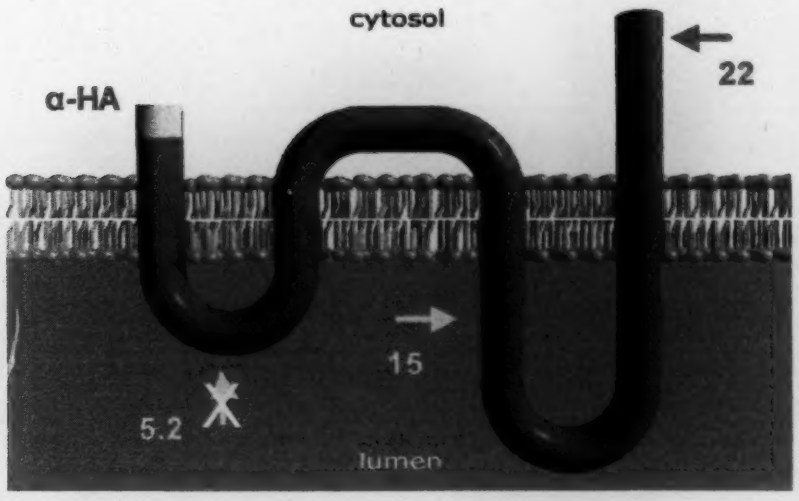

Lane	1	2	3	4	5	6
Endoprot (μg)	—	—	+	+	++	++
Tx-100	—	+	—	+	—	+

B.

C.

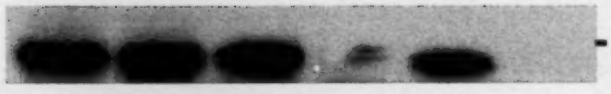

References

1. Exton, J. H. (1994) *Biochim. Biophys. Acta.* **1212**, 26-42.

2. Kent, C. (1997) *Biochim. Biophys. Acta.* **1348**, 79-90.

3. Agellon, L. B. (2002) in *Biochemistry of Lipids, Lipoproteins and Membranes* (Vance, D. E., Vance, J.E., ed), 4 Ed., pp. 433-448, Elsevier, Amsterdam

4. Mathur, S. N., Born, E., Murthy, S., and Field, F. J. (1996) *Biochem. J.* **314**, 569-75.

5. Vance, D. E. (2002) in *Biochemistry of Lipids, Lipoproteins and Membranes* (Vance, D. E., Vance, J.E., ed), 4 Ed., pp. 205-232, Elsevier, Amsterdam

6. Vance, D. E., and Ridgway, N. D. (1988) *Prog. Lipid. Res.* **27**, 61-79

7. DeLong, C. J., Shen, Y. J., Thomas, M. J., and Cui, Z. (1999) *J. Biol. Chem.* **274**, 29683-8.

8. Reo, N. V., and Adinehzadeh, M. (2000) *Toxicol. Appl. Pharmacol.* **164**, 113-26.

9. Reo, N. V., Adinehzadeh, M., and Foy, B. D. (2002) *Biochim. Biophys. Acta.* **1580**, 171-88.

10. Vance, J. E., and Vance, D. E. (1986) *J. Biol. Chem.* **261**, 4486-91.

11. Nishimaki-Mogami, T., Suzuki, K., and Takahashi, A. (1996) *Biochim. Biophys. Acta.* **1304**, 21-31.

12. Nishimaki-Mogami, T., Suzuki, K., Okochi, E., and Takahashi, A. (1996) *Biochim. Biophys. Acta.* **1304**, 11-20.

13. Agellon, L. B., Walkey, C. J., Vance, D. E., Kuipers, F., and Verkade, H. J. (1999) *Hepatology* **30**, 725-9.

14. Noga, A. A., Zhao, Y., and Vance, D. E. (2002) *J. Biol. Chem.* **In Press**

15. Al-Habori, M. (1994) *Intl. J. Biochem. Cell Biol.* **27**, 123-132

16. Cui, Z., Vance, J. E., Chen, M. H., Voelker, D. R., and Vance, D. E. (1993) *J. Biol. Chem.* **268**, 16655-63.

17. Panagia, V., Ganguly, P. K., and Dhalla, N. S. (1984) *Biochim. Biophys. Acta.* **792**, 245-53.

18. Prasad, C., and Edwards, R. M. (1981) *J. Biol. Chem.* **256**, 1300-3.

19. Nieto, A., and Catt, K. J. (1983) *Endocrinology* **113**, 758-62.

20. Sarzale, M. G., and Pilarska, M. (1976) *Biochim. Biophys. Acta* **441**, 81-92

21. Walkey, C. J., Shields, D. J., and Vance, D. E. (1999) *Biochim. Biophys. Acta.* **1436**, 405-12.

22. Croze, E., and Morre, D. J. (1984) *J. Cell. Physiol.* **119**, 46-57

23. Vance, J. E. (1990) *J. Biol. Chem.* **265**, 7248-56.

24. Graham, J. M. (1997) in *Subcellular Fractiionation: a practical approach* (Graham, J. M., Rickwood, D., ed), pp. 205-242, Oxford University Press, Oxford

25. Kyte, J., and Doolittle, R. F. (1982) *J. Mol. Biol.* **157**, 105-132

26. Persson, B., and Argos, P. (1994) *J. Mol. Biol.* **237**, 182-192

27. Ho, S. N., Hunt, H. D., Horton, R. M., Pullen, J. K., and Pease, L. R. (1989) *Gene* **77**, 51-9.

28. Ridgway, N. D., and Vance, D. E. (1992) *Methods Enzymol* **209**, 366-74

29. Shields, D. J., Agellon, L. B., and Vance, D. E. (2001) *Biochim. Biophys. Acta.* **1532**, 105-14.

30. Ridgway, N. D., and Vance, D. E. (1987) *J. Biol. Chem.* **262**, 17231-9.

31. Teasdale, R. D., and Jackson, M. R. (1996) *Annu. Rev. Cell. Dev. Biol.* **12**, 27-54

32. Nilsson, T., and Warren, G. (1994) *Curr. Opin. Cell. Biol.* **6**, 517-21.

33. Hardt, B., and Bause, E. (2002) *Biochem. Biophys. Res. Commun.* **291**, 751-7.

34. Audubert, F., and Vance, D. E. (1984) *Biochim. Biophys. Acta.* **792**, 359-62.

35. Nohturfft, A., Brown, M. S., and Goldstein, J. L. (1998) *J. Biol. Chem.* **273**, 17243-50.

36. Olender, E. H., and Simoni, R. D. (1992) *J. Biol. Chem.* **267**, 4223-35.

37. Van Geest, M., and Lolkema, J. S. (2000) *Microbiol. Mol. Biol. Rev.* **64**, 13-33.

38. Monne, M., Nilsson, I., Elofsson, A., and von Heijne, G. (1999) *J. Mol. Biol.* **293**, 807-14.

39. Romano, J. D., and Michaelis, S. (2001) *Mol. Biol. Cell.* **12**, 1957-71.

40. Monne, M., Hermansson, M., and von Heijne, G. (1999) *J. Mol. Biol.* **288**, 141-5.

41. Finkelstein, J. D., and Martin, J. J. (1986) *J. Biol. Chem.* **261**, 1582-7.

42. Fauman, E. B., Blumenthal, R.M., Cheng, X. (1999) In *S-Adenosylmethionine-Dependent Methyltransferases: Structures and Functions* (Cheng, X., Blumenthal, R.M., ed), pp. 1-32, World Scientific Publishing, Singapore

43. Kagan, R. M., and Clarke, S. (1994) *Arch. Biochem. Biophys.* **310**, 417-27.

44. Farooqui, J. Z., Lee, H. W., Kim, S., and Paik, W. K. (1983) *Biochim. Biophys. Acta.* **757**, 342-51.

Chapter 4

Molecular Dissection of the AdoMet binding site of Phosphatidylethanolamine *N*-methyltransferase

4.1 Introduction

PEMT catalyzes the sequential transfer of three methyl groups from *S*-adenosylmethionine (AdoMet) to phosphatidylethanolamine (PE) to generate the essential phospholipid, phosphatidylcholine (PC) (1). Concomitant production of one *S*-adenosylhomocysteine (AdoHcy) molecule occurs with each methylation step (1). The liver is the primary site of PEMT activity and the PEMT-controlled pathway accounts for approximately 30% of hepatic phosphatidylcholine biosynthesis (1-4). The enzymes of the CDP-choline pathway, which are active in all nucleated cells, catalyze the remaining 70% of PC biosynthesis in the liver (2-5).

In addition to being a key modulator of PC biosynthesis, the liver is the site of approximately 85% of all methylation reactions (6). AdoMet, the primary methyl group donor, is utilized by at least 39 mammalian methyltransferases, including DNA, RNA, protein, lipid and small molecule methyltransferases (7,8). Each AdoMet-dependent transmethylation reaction generates AdoHcy, which in turn is hydrolyzed to yield adenosine and the non-protein amino acid, homocysteine (Hcy) (9). Since mild hyperhomocysteinemia is an independent risk factor for cardiovascular and atherosclerotic disease, circulating plasma homocysteine levels are of significant clinical interest (10).

Previous studies on PEMT focused on the PC biosynthetic function of the enzyme, and in particular, whether PEMT-derived PC was targeted to a specific hepatic fate such as very low density lipoprotein particles or bile (11-14). Recently however, phenotypic analysis of mice homozygous for a disrupted PEMT allele revealed a novel role for PEMT in the regulation of plasma Hcy levels (15). Although the liver is the site of numerous AdoMet-dependent methylation reactions, each of which contributes to the Hcy pool, genetic ablation of the *PEMT* gene alone resulted in a 50% decrease in circulating Hcy levels (15). Furthermore, hepatoma cells transfected with a cDNA encoding PEMT secreted more Hcy than mock-transfected cells (15). Combined, these results suggest a key, yet previously unknown role for PEMT in the regulation of hepatic one-carbon metabolism.

To gain further insight into the PEMT transmethylation reaction and the mechanism by which this enzyme modulates plasma Hcy levels, we sought to identify residues that are required to bind AdoMet. A plethora of enzymes bind AdoMet and/or AdoHcy, including the AdoMet-dependent methyltransferases, AdoMet synthetase, AdoMet decarboxylase and AdoHcy hydrolase (16). Comparative amino acid sequence analysis previously identified several conserved motifs that bind the AdoMet/AdoHcy moieties, but a small number of methyltransferases including the eukaryotic PEMT family of enzymes do not contain any of these motifs (16-18).

Using bioinformatic analysis, we identified two putative AdoMet binding motifs that are conserved among the eukaryotic PEMT proteins. Here, we describe the biochemical evaluation of the motifs in the human PEMT enzyme. Understanding the nature of the interaction between AdoMet and PEMT will promote resolution of the mechanism by which the enzyme modulates plasma Hcy levels, and facilitate the design of agents for therapeutic intervention in cases of hyperhomocysteinemia.

4.2 Materials and Methods

4.2.1 Reagents

Dulbecco's modified Eagle's medium (DMEM), fetal bovine serum, restriction endonucleases and Platinum Pfx DNA polymerase were from Invitrogen Life Technologies. Oligonucleotides for mutagenesis were synthesized in the DNA core facility at the Dept. of Biochemistry, University of Alberta. Fugene transfection reagent was from Roche Molecular Biochemicals. *S*-adenosyl-L-[*methyl*-^{3}H]methionine (15 Ci/mmol) was obtained from Amersham Biosciences. *S*-adenosyl-L-methionine was from Sigma Chemical Co. HAWP 02500 filters for AdoMet binding assays were from Millipore. Goat anti-rabbit secondary antibodies were purchased from Pierce. All other reagents were of the highest standard commercially available.

4.2.2 Bioinformatic Analysis

The PROWL ProteinInfo sequence analysis program (prowl.rockefeller.edu) was used to screen for putative AdoMet binding motifs in the predicted human PEMT primary structure (accession number, NP_009100). The ALIGN program (based on the ClustalW algorithim) at the San Diego Supercomputer Biology Workbench (workbench.sdsc.edu) was

utilized to analyze the conservation of motifs between orthologous eukaryotic PEMT enzymes (19).

4.2.3 Recombinant Plasmid Construction

Mutant PEMT derivatives for analysis of putative AdoMet binding residues/motifs were generated by the "splice by overlap extension" PCR mutagenesis method, using the wildtype hPEMT-pCI plasmid as template for all reactions (20,21). This plasmid consists of the human PEMT (hPEMT) open reading frame cloned 5' to 3' into the *Xho*I and *Xba*I sites respectively of the pCI mammalian expression vector polylinker (Promega) (21). Transcription is under the control of a CMV promoter. Full-length mutant PCR products were blunt-end ligated to *Sma*I-cut pBluescript II (KS) (Stratagene), and recloned into the pCI expression vector using *Xho*I and *Xba*I restriction sites. All constructs were sequenced to confirm fidelity of amplification and orientation of the insert, at the Molecular Biology Services Unit, University of Alberta.

Plasmids encoding conservative GxG motif mutants were generated as follows. To mutagenize the glycine residue at the first position in the GxG tripeptide motif to an alanine residue and generate the plasmid, hP-G98A, PCR A was performed with oligonucleotide (oligo) 1 (5'-CTCGAGATGACCCGGCTGCTGGGCTAC-3') and oligo 2 (5'-CAGGAGCGCGAGG

CCCAGGCTG-3'), PCR B with the mutant oligo 3 (5'-AGCCTGGGCCTCGCGCTCCTGGCACTGGGCGTCGT-3') and oligo 4 (5'-TCTAGGATCAGCTCCTCTTGTGGGAC-3'), and PCR C, to generate the full-length mutant product, with oligo's 1 and 4, using amplicons from PCR A & B as templates. Each of the other mutant plasmids was produced by the same protocol but using a different mutant oligo (#3) for the construction of each PEMT derivative. To mutagenize the glycine residue at the second position in the GxG tripeptide motif, to an alanine residue, and generate the plasmid, hP-G100A, oligo 3 was: (5'-AGCCTGGGCCTCGCGCTCCTGGGACTGGCCGTCGT-3'). To mutagenize both glycine residues in the GxG tripeptide motif to alanine residues and generate the plasmid, hP-G2A2, (5'-AGCCTGGGCCTCGCGCTCCTGGCACTGGCCGTCGT-3') was the mutant oligo. For construction of the single and combinatorial non-conservative GxG mutant plasmids, the mutant oligonucleotides were as follows; hP-G98E, (5'-AGCCTGGGCCTCGCGCTCCTGGAACTGGGCGTCGT-3'); hP-G100D, (5'-AGCCTGGGCCTCGCGCTCCTGGGACTGGACGTCGT-3'; hP-GEGD, (5'-AGCCTGGGCCTCGCGCTCCTGGAACTGGACGTCGT-3').

Plasmids encoding the di-glutamate motif mutants, E180D and E181D, were generated as follows. To mutate the glutamate at position 180 to an aspartate residue and generate the plasmid, hP-E180D, PCR A was performed with oligonucleotide 1 (as above) and oligo, 5 (5'-ATAGGAGAGCCATTATGTAGGTG-3'), PCR B with the mutant oligo 6 (5'-

CTACATAATGGCTCTCCTATACGACGAGCCCTTCACCGCTGAGATC-3') and 4 (as above), and PCR C, to generate the full-length mutant product, with oligonucleotides 1 and 4, using amplicons from PCR A & B as templates. To mutate the glutamate at position 181 to an aspartate residue and generate the plasmid, hP-E181D, a similar protocol was followed except the mutant oligo was (5'-CTACATAATGGCTCTCCTATACGAAGATCCCTTCACCGCTGAGATC -3').

4.2.4 Cell culture and Transfections

Cos-7 cells, obtained from the American Type Culture Collection repository, were maintained in Dulbecco's modified Eagle's medium, 10% fetal bovine serum, 100 units/ml penicillin and 100 µg/ml streptomycin sulfate, at 37°C, 5% CO_2. Transfection of various plasmids encoding PEMT and mutant PEMT derivatives was performed using the Fugene reagent as described previously (22).

4.2.5 PEMT Activity Assays and Immunoblots

PEMT activity assays were performed as described previously using phosphatidylmonomethylethanolamine as the methyl acceptor and *S*-adenosyl-L-[*methyl*-^{3}H]methionine as the methyl group donor (23). Immunoblots of the recombinant PEMT protein and mutant derivatives were

performed as described previously using an anti-PEMT peptide antibody at the indicated concentrations (22).

4.2.6 S-Adenosylmethionine Binding Assays

Binding assays were performed on microsomes prepared from transiently transfected Cos-7 cells. Microsomes were prepared as described previously except the resultant microsomal pellet was resuspended in 75 µl of Buffer X (50 mM Tris HCl, pH 9.5, 5 mM DTT) (22). Binding assays were carried out according to a modified version of the method of Zhu et al (24). Briefly, 50 µg of microsomal protein was incubated with 10 µCi of *S*-adenosyl-L-[*methyl*-^{3}H]methionine (15 Ci/mmol) in Buffer X for 10 min at 37°C (total assay volume, 30 µl). The binding assay mixture was passed over a HAWP 02500 filter (Millipore) on a filtration funnel and unbound *S*-adenosyl-L-[*methyl*-^{3}H]methionine was removed by washing with 100 ml of Buffer X. Filters were dried and bound *S*-adenosyl-L-[*methyl*-^{3}H]methionine was quantitated by liquid scintillation spectrometry.

Similar assays were performed in the absence of microsomal protein to account for non-specific binding of *S*-adenosyl-L-[*methyl*-^{3}H]methionine to the filter. Binding assays on microsomes from mock-transfected cells quantitated AdoMet bound by microsomal components other than PEMT. Binding activities of microsomes from cells expressing mutant PEMT proteins

were expressed relative to the binding activity of microsomes from cells expressing the unmodified enzyme.

4.3 Results

4.3.1 Identification of a Putative AdoMet-Binding Motif

PEMT-catalyzes a series of AdoMet-dependent methylation reactions to produce PC and the byproduct, AdoHcy (Fig. 4.1). Three AdoMet binding motifs (I, II and III) are conserved in the majority of non-DNA AdoMet-dependent methyltransferases (Fig. 4.2A (i)), but a small number of methyltransferases including the enzymes of the eukaryotic PEMT family do not contain the three motifs (16).

However, using bioinformatic analysis, we identified a partial motif I consensus sequence that is conserved among the eukaryotic PEMT orthologues (Fig. 4.2B & 4.2C)(25). Furthermore, this partial motif (GxG, where x is any amino acid) is similar to a DNA methyltransferase AdoMet-binding motif, one of the AdoMet binding motifs of AdoMet synthetase, as well as a nucleotide-binding motif found in protein kinases and other nucleotide binding proteins such as the NAD-binding proteins (Fig. 4.2A (ii), Fig. 4.2A (iii) & Fig. 4.2A (iv))(17,26-28).

4.3.2 Conservative Mutagenesis of the GXG Motif

To probe the role of the conserved glycine residues in binding of the AdoMet moiety, each glycine residue of the GxG motif was individually

mutated to an alanine residue (encoded by the mutant PEMT plasmids, hP-G98A and hP-G100A. To evaluate the effect of conservative mutagenesis of each glycine residue on PEMT activity, Cos-7 cells were transfected with plasmids encoding wildtype PEMT or the mutant PEMT derivatives, or mock transfected with empty vector, and cell homogenate protein was assayed for PEMT activity. Mutagenesis of ^{98}G to an alanine residue decreased PEMT activity by approximately 25%, whereas mutagenesis of ^{100}G completely abolished PEMT activity in the Cos-7 cell homogenates (Fig. 4.3A). Immunoblots with an anti-PEMT peptide antibody demonstrated similar levels of abundance of the recombinant proteins (Fig. 4.3B).

4.3.3 Conservative Mutagenesis of ^{100}G Abolishes AdoMet Binding Activity

To determine if the changes in PEMT activity were specifically due to decreased AdoMet binding activity, we transfected Cos-7 cells with the wildtype or mutant PEMT plasmids, or mock transfected with empty vector. Microsomes were prepared for AdoMet binding assays. The microsomal fraction was utilized for AdoMet binding assays as we have previously demonstrated that PEMT activity is enriched in the microsomal subcompartment (22).

Microsomes from cells expressing the mutant hp-G98A protein, displayed a reduction of approximately 20% in AdoMet binding activity,

compared with the unmodified enzyme (Fig. 4.3C). In contrast, conservative mutagenesis of ^{100}G completely abolished the AdoMet binding activity of the mutant enzyme. These results suggest that the altered enzymatic activity of the mutant recombinant PEMT proteins was a consequence of a direct effect on AdoMet binding activity. Thus, a specific role for ^{100}G in binding to the AdoMet moiety is supported.

4.3.4 Non-conservative and Combinatorial Mutations of the GXG Motif

To further investigate the role of the glycine residues in the putative AdoMet binding motif, we performed non-conservative mutagenesis of each glycine residue to glutamate or aspartate residues, to yield the mutant plasmids, hP-G98E and hP-G100D, respectively. Additionally, combinatorial mutant plasmids were generated in which both glycine residues were mutated to alanine residues (hP-GAGA) or to glutamate and aspartate residues (hP-GEGD). To assess the PEMT activity of the non-conservative and combinatorial mutants, Cos-7 cells were transiently transfected with wildtype or mutant plasmids, or mock transfected with empty vector. Cellular homogenates were assayed for PEMT activity.

Cells expressing the non-conservative mutant PEMT derivatives (hP-G98E, hP-G100D) were completely inactive as compared with mock-transfected cells (Fig. 4.4A). In the case of hP-G98E, this was in contrast to

the conservative G98A mutation, which only caused a decrease of 20% in PEMT activity (Fig. 4.3A). Cells expressing the combinatorial mutant PEMT derivatives were similarly devoid of PEMT activity (Fig. 4.4A). Immunoblots with an anti-PEMT peptide antibody confirmed the expression of each PEMT derivative Fig. 4.4B).

4.3.5 Non-Conservative Mutagenesis of ^{98}G Reduces AdoMet Binding Activity

In the next series of experiments, we resolved the issue of whether the lack of PEMT activity in the non-conservative and combinatorial GxG mutants was due to a specific decrease in the AdoMet binding activity of the recombinant mutant proteins. Cos-7 cells were transfected and microsomal AdoMet binding assays were performed as described.

Although, cells expressing the mutant hP-G98E protein did not display any significant PEMT activity (Fig. 4.4A), the mutant protein retained approximately 55% of AdoMet binding activity as compared with the unmodified enzyme (Fig. 4.4C). Combined, these results suggest that while the mutant protein is partially capable of binding AdoMet, the bound AdoMet moiety is not available for PEMT-catalyzed transmethylation (i.e. the mutant PEMT enzyme is unable to transfer the methyl group from the bound AdoMet moiety). This may arise because AdoMet is bound in such a conformation that the methyl group is not accessible to the

transmethylation machinery. Furthermore, since mutagenesis of ^{98}G to the small amino acid, alanine, had only minimal effects on both PEMT activity and binding activity (Fig. 4.3A & 4.C), but mutation to the larger and charged glutamate residue caused a significant decrease in binding activity (Fig. 4.4A & 4.4C), ^{98}G may serve to structurally position ^{100}G for optimal binding activity rather than actually bind to AdoMet itself.

As expected, the hp-G100D mutant protein and the combinatorial mutant PEMT derivative, hP-GEGD did not bind AdoMet, whereas the mutant PEMT protein, hP-GAGA, retained only fractional activity (Fig. 4.4C). Taken together, these results strongly suggest that both glycine residues of the conserved GxG motif have an integral role in the binding of AdoMet by PEMT.

4.3.6 Identification of a Second Putative AdoMet Binding Motif

A number of AdoMet-dependent methyltransferases do not contain the classical AdoMet binding motifs (16,17,26). Analysis of enzymes that lack the three classical AdoMet-binding motifs (including the yeast *PEM2*-encoded PEMT orthologue) identified a novel tripartite motif (Fig. 4.5A)(18) referred to in abbreviated form as the "RHPxY –hyd- EE" motif. This motif consists of two regions of homology (Region A & Region B) separated by a hydrophobic region of ~30 residues (18). To determine if the tripartite motif is conserved among the higher eukaryotic PEMT enzymes, we

performed feature analysis of the aligned amino acid sequences. Although the greater part of Regions A and B do not exist in human PEMT, two specific portions of the motifs, which flank the hydrophobic region, are conserved, i.e. PxY –hydrophobic region- EE, where x represents any amino acid (Fig. 4.5A, 4.5B and 4.5C).

We recently demonstrated that PEMT is a quatrotopic ER membrane enzyme that adopts a topographical orientation, which localizes both termini external to the ER subcompartment (Chapter 3)(22). Such a topographical orientation would localize the PxY motif in the ER lumen and the di-glutamate motif on the external surface of the ER membrane. Since, AdoMet is most concentrated in the cytosolic compartment, we hypothesize that of the two motifs the di-glutamate motif is more likely to function in an AdoMet binding capacity in human PEMT (29).

4.3.7 Mutagenesis of the Di-glutamate Motif Decreases PEMT Activity

To examine the role of the conserved di-glutamate motif in binding to AdoMet, we mutated each glutamate residue to an aspartate residue to generate the mutant PEMT plasmids, hP-E180D and hP-E181D. To evaluate the conservative glutamate mutants, we assayed PEMT activity in homogenates from cells that express the recombinant PEMT derivatives. Mutagenesis of ^{180}E to an aspartate residue completely abolished PEMT activity whereas similar mutagenesis of ^{181}E resulted in a 70% decrease in

PEMT activity (Fig. 4.6A). Immunoblots with an anti-PEMT peptide antibody demonstrated the production of the recombinant proteins to similar levels (Fig. 4.6B).

4.3.8 Mutagenesis of the Di-glutamate Motif Diminishes AdoMet Binding Activity

To elucidate if the changes in PEMT activity were specifically due to a reduction in AdoMet binding activity, we performed microsomal AdoMet binding assays on transfected cells. Mutation of ^{180}E to an aspartate residue abolished the AdoMet binding capacity of the recombinant mutant enzyme (Fig. 4.6C). Similar mutagenesis of ^{181}E generated a protein that exhibited a 55% decrease in binding of the AdoMet moiety (Fig. 4.6C). As the changes in binding activity (Fig. 4.6C) are proportionally similar to the changes in enzymatic activity (Fig. 4.6C), it appears that mutagenesis of the di-glutamate motif diminished the PEMT activity by altering the AdoMet binding activity of the enzyme. Thus, a functional role for the di-glutamate motif in the AdoMet binding activity of the human PEMT enzyme is supported.

4.4 Discussion

AdoMet is the most commonly used cofactor after ATP (7). The AdoMet moiety is required for the synthesis of several essential biomolecules including PC, creatine and epinephrine, as well as for the methylation of DNA and RNA (30). A measure of the importance of AdoMet is perhaps best illustrated in that the only known genome that lacks the gene encoding AdoMet synthetase is that of the obligate intracellular parasite, *Chlamydia trachomatis* (31). Furthermore, the AdoMet molecule is intrinsically linked with the non-protein amino acid, Hcy. Elevated plasma Hcy concentrations are considered an independent risk factor for cardiovascular disease (10).

To understand how genetic ablation of PEMT can cause decreased circulating plasma homocysteine levels, we examined the role of specific PEMT amino acid residues in the binding of AdoMet. We have now identified two distinct motifs that are required for PEMT to bind the methyl donor.

Three AdoMet-binding motifs are conserved in the majority of the AdoMet-dependent methyltransferases but these motifs are absent from several enzymes including those of the eukaryotic PEMT family and the isoprenylcysteine carboxyl methyltransferase (ICMT) family of enzymes (Fig. 2A (i))(16,18). The ICMT enzymes constitute part of a post-translational modification process, in which proteins that terminate in a CaaX motif, such

as Ras, undergo isoprenylation, C-terminal proteolytic cleavage and carboxyl methylation (10). Although absent from all eukaryotic PEMT enzymes, the three classical AdoMet binding motifs are present in the prokaryotic *Rhodobater sphaeroides* PEMT orthologue, encoded by the *pmtA* gene (16,32). However, this enzyme is a soluble cytosolic protein that has little homology with the higher eukaryotic, membrane-bound PEMT orthologues (32,33).

A partial consensus AdoMet binding motif (^{98}Gx^{100}G) is conserved in the eukaryotic PEMT enzymes and site-directed mutagenesis of each glycine residue demonstrated their importance in the AdoMet binding activity of PEMT (Fig. 2C & Fig. 3C). Whereas ^{100}G is essential for binding of the AdoMet moiety, ^{98}G may serve in a structural capacity, as conservative mutagenesis of the residue was quite well tolerated (Fig. 3A & Fig. 3C). Moreover, significant binding activity was retained even when ^{98}G was substituted with a glutamate residue (Fig. 4C).

Our data do not allow us to exclude the possibility that the glutamate residue is also mediating the binding of AdoMet, especially since we have demonstrated the role of other PEMT glutamate residues in AdoMet binding (Fig. 6C). However, since the AdoMet binding function of ^{100}G has been clearly demonstrated, and the replacement of ^{98}G with an alanine residue had little impact on AdoMet binding, insertion of a glutamate residue, combined with an intact ^{100}G might be expected to result in enhanced

AdoMet binding. As this was not the case, we favor a structural role for ^{98}G in the AdoMet binding activity of the human PEMT enzyme.

To further define the AdoMet binding site of human PEMT, we examined a novel, recently proposed, AdoMet-binding motif (RHPxY-hyd-EE) (18). This non-classical motif was derived following alignment-based analyses of the ICMT family of enzymes, homologs thereof, the yeast PEM2 enzyme, and several sterol reductases (18). By *in silico* analysis, we determined that the consensus motif is also partially conserved in the rat, mouse and human PEMT orthologues.

Topographical analysis of Ste14p, a member of the ICMT family of methyltransferases, indicated that the enzyme is oriented in the ER membrane such that the two flanking regions of the motif are colocalized on the external face of the membrane (18). Such an orientation might be possible because the intervening hydrophobic domain is predicted to "double back" within the membrane plane through the use of a helical hairpin (18). The C-terminal transmembrane domain of the yeast PEM2 enzyme is proposed to adopt a similar structural conformation (18).

In contrast, the corresponding transmembrane domain in the human PEMT enzyme is shorter than the minimum length (31 amino acids) necessary for helical hairpin formation and a topographical model based on four transmembrane domains has been elucidated (22). Such a

topographical structure would position the two flanking segments of the motif on opposite sides of the ER membrane. Hence, in this model, the N-terminal portion of the motif (PxY) is lumenally oriented, and therefore diametrically opposed to the AdoMet-rich cytosol (22,29). While we have not eliminated the possibility that the lumenally oriented PxY motif might still have a role in the AdoMet binding activity of PEMT, our working hypothesis is that the cytosolically localized di-glutamate motif is the functional AdoMet binding portion of the "RHPxY-hyd-EE" motif, in the human PEMT enzyme.

Mutagenesis of the di-glutamate motif coupled with AdoMet binding assays verified the importance of the glutamate pair, with ^{180}E in particular, being essential to the AdoMet binding activity of PEMT (Fig. 6C). Nucleotide-binding proteins such as p21, contain a GxGxxG motif and an invariant acidic residue that are separated by ~20 amino acids (34). Hydrogen bonding between the acidic residue and the 2'-hydroxy group of the adenosine ribose has been demonstrated (34). Thus, either or both glutamate residues in the conserved di-glutamate motif of PEMT, may bind the AdoMet moiety through hydrogen bonding. Mutagenesis of each glutamate residue to an aspartate residue reduced AdoMet binding activity. Although aspartate residues may also form hydrogen bonds, the shorter length of the aspartate side-chain may impair the AdoMet binding capacity of the residues, in this region of the human PEMT enzyme.

From the topographical orientation of the PEMT enzyme, and the predicted length of the transmembrane domains, we envision a model that would position the conserved GxG and di-glutamate motifs towards the cytosolic face of the third and fourth transmembrane helices respectively (Fig. 7). This would provide optimal access to the AdoMet pool in the cytosol (29). Moreover, as the third and fourth transmembrane helices are adjacent domains, the conserved GxG and di-glutamate motifs may be juxtaposed (Fig. 7). Furthermore, *S*-adenosylhomocysteine hydrolase, which hydrolyzes AdoHcy to Hcy and adenosine, is also localized in the cytosol (35). Combined, the topographical organization of these disparate elements may provide the basis of a mechanism that links the AdoMet-dependent PEMT reaction to circulating Hcy levels.

In summary, we identified two closely oriented amino acids motifs in the human PEMT enzyme that are essential for binding of AdoMet. The AdoMet binding site of PEMT is unique in that it conforms to neither the classical nor non-classical binding motifs, but rather is a novel combination of both classes. Since PEMT has been shown to modulate circulating plasma Hcy levels, the enzyme represents a novel target for therapeutic intervention in patients with hyperhomocysteinemia. Resolution of key motifs that bind AdoMet will greatly accelerate the design of such therapeutic agents.

Figure 4.1 Interrelationships Between the PEMT-Catalyzed Biosynthesis of PC and Hcy Metabolism

PEMT catalyzes the synthesis of PC via three AdoMet-dependent transmethylation reactions. AdoHcy is produced with each methylation step (1). Hydrolysis of AdoHcy yields Hcy and adenosine in a reaction catalyzed by the enzyme AdoHcy hydrolase (9). Hcy may be directed to the irreversible trans-sulfuration pathway to generate cysteine, reincorporated to the methionine cycle for regeneration of AdoMet or transported from the cell (35).

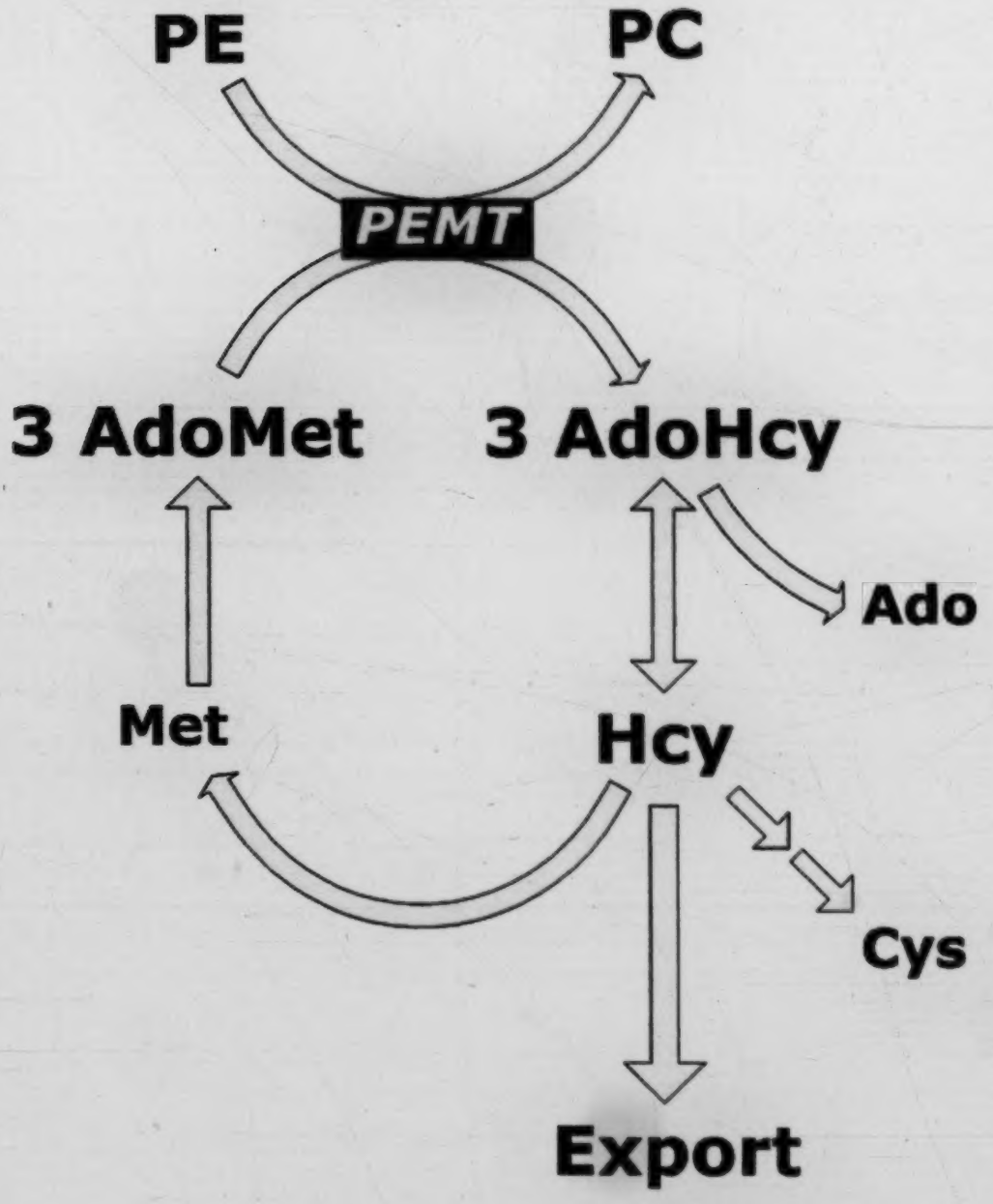
PE
PC
PEMT
3 AdoMet
3 AdoHcy
Ado
Met
Hcy
Cys
Export

Figure 4.2 A Putative AdoMet Binding Motif (GXG) is Conserved in PEMT Orthologues

A. Alignment of conserved AdoMet/nucleotide binding motifs. (i) Three conserved AdoMet-binding motifs found in the majority of non-nucleic acid AdoMet-dependent methyltransferases. (ii) Motif I of the conserved nucleic acid AdoMet binding site. (iii) Motif I of the AdoMet synthetase AdoMet binding site. (iv) ATP-/nucleotide-binding motif of protein kinases and other nucleotide-binding proteins, such as the NAD-binding proteins. The shaded box indicates conservation of the GXG motif in disparate motifs.

B. Linear schematic map of the human PEMT enzyme indicating the position of the conserved GXG motif.

C. Amino acid sequence alignment of PEMT orthologues. The shaded box indicates conservation of the GXG motif in PEMT enzymes from different species. GenBank accession numbers for each protein are included.

A.

	Motif I	Motif II	Motif III
(i)	hh(D/E)hGxGxG	PQFDAIFC	LLRPGGRLLI
(ii)	hh(D/S)(L/P)FxGxG		
(iii)	GxGDxG		
(iv)	GxGxxG		

B.

C.

					98		100				
Human	CTC	GCG	CTC	CTG	GGA	CTG	GGC	GTC	GTG	CTC	GTG
NP_009100	*L*	*A*	*L*	*L*	*G*	*L*	*G*	*V*	*V*	*L*	*V*
Mouse	CTT	GCA	TTC	CTA	GGT	TGG	GGA	TTC	GTG	TTT	GTG
Q61907	*L*	*A*	*F*	*L*	*G*	*W*	*G*	*F*	*V*	*F*	*V*
Rat	CTT	GCA	CTC	CTG	GGC	TGG	GGA	CTC	GTG	TTT	GTG
A47353	*L*	*A*	*L*	*L*	*G*	*W*	*G*	*L*	*V*	*F*	*V*
Yeast	GTG	GCT	CTC	TTT	GGT	TTG	GGG	CAA	GTG	CTT	GTT
P03575	*V*	*A*	*L*	*F*	*G*	*L*	*G*	*Q*	*V*	*L*	*V*

Figure 4.3 Conservative Mutagenesis of the GXG motif Alters PEMT Specific Activity and AdoMet-Binding Activity

Cos-7 cells were transiently transfected with plasmids (3 μg) containing wildtype PEMT or epitope tagged PEMT derivatives, or mock transfected with empty pCI vector.

A. Cell homogenates (50 μg protein) were assayed for PEMT activity. The results are expressed as the mean of three separate experiments, each performed in duplicate, ± S.E.M, relative to the values obtained for similar assays on cells transfected with wildtype PEMT. Asterisk signifies $P<0.05$.

B. Immunoblot with anti-PEMT antibody using 25 μg protein of transfected cell homogenates.

C. Microsomes (50 μg protein) prepared from transfected cells, were assayed for AdoMet binding activity. The results are expressed as the mean of three separate experiments, each performed in duplicate, ± S.E.M, relative to the values obtained for similar assays on microsomes from cells transfected with wildtype PEMT. Asterisk signifies $P<0.05$. Binding assays on microsomes from mock-transfected cells quantitated AdoMet bound by microsomal components other than PEMT. Binding activities of microsomes from cells expressing mutant PEMT proteins were expressed relative to the binding activity of microsomes from cells expressing the unmodified enzyme.

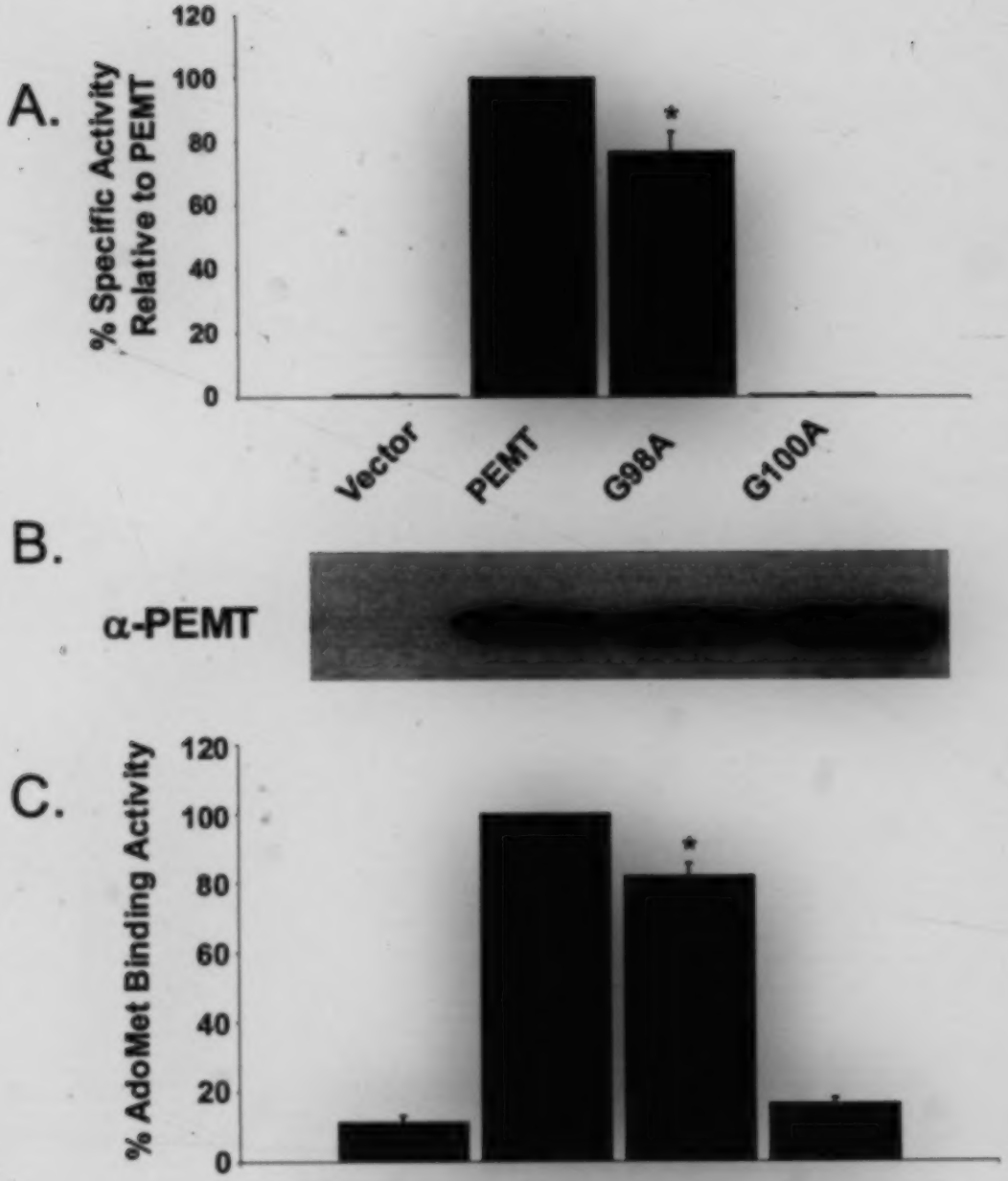
A.
% Specific Activity Relative to PEMT
120
100
80
60
40
20
0
*
Vector
PEMT
G98A
G100A
B.
α-PEMT
C.
% AdoMet Binding Activity
120
100
80
60
40
20
0
*

Figure 4.4 Non-Conservative and Combinatorial Mutagenesis of the GXG Motif Decreases PEMT Specific Activity and AdoMet-Binding Activity

Cos-7 cells were transiently transfected with plasmids (3 μg) containing wildtype PEMT or epitope tagged PEMT derivatives, or mock transfected with empty pCI vector.

A. Cell homogenates (50 μg protein) were assayed for PEMT activity. The results are expressed as the mean of three separate experiments, each performed in duplicate, ± S.E.M, relative to the values obtained for similar assays on cells transfected with wildtype PEMT.

B. Immunoblot with anti-PEMT antibody using 25 μg protein of transfected cell homogenates.

C. Microsomes (50 μg protein) prepared from transfected cells, were assayed for AdoMet binding activity. The results are expressed as the mean of three separate experiments, each performed in duplicate, ± S.E.M, relative to the values obtained for similar assays on microsomes from cells transfected with wildtype PEMT. Binding assays on microsomes from mock-transfected cells quantitated AdoMet bound by microsomal components other than PEMT. Binding activities of microsomes from cells expressing mutant PEMT proteins were expressed relative to the binding activity of microsomes from cells expressing the unmodified enzyme.

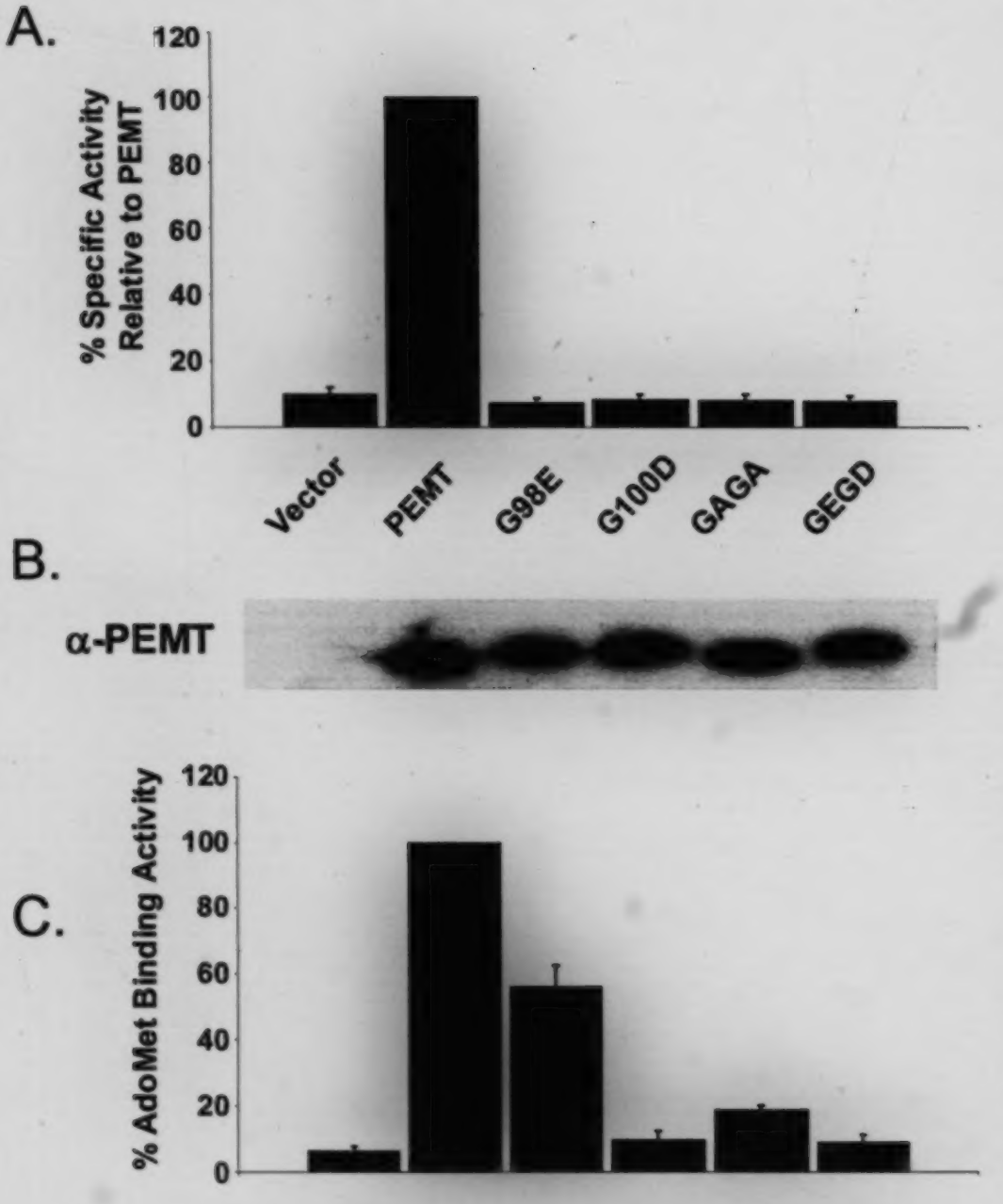
A.
% Specific Activity Relative to PEMT
120
100
80
60
40
20
0
Vector
PEMT
G98E
G100D
GAGA
GEGD
B.
α-PEMT
C.
% AdoMet Binding Activity
120
100
80
60
40
20
0

Fig. 4.5 A Putative AdoMet-binding Motif (EE) is Conserved in PEMT Orthologues

A. A tripartite putative AdoMet-binding motif is conserved in several methyltransferases that lack the classical AdoMet-binding motifs. Two regions of homology (Regions A and B) are separated by a hydrophobic region (hyd.) of ~30 amino acids. The shaded boxes indicate regions that are conserved in PEMT orthologues.

B. Linear schematic map of the human PEMT enzyme indicating the position of the conserved di-glutamate motif.

C. Amino acid sequence alignment of PEMT orthologues. The shaded box indicates conservation of the di-glutamate motif in PEMT enzymes from different species. GenBank accession numbers for each protein are included.

A.

Region A	Hyd.	Region B
...GxY(x3)RHPxYxG	-hydrophobic-	xR(x3)EE(x2)...

B.

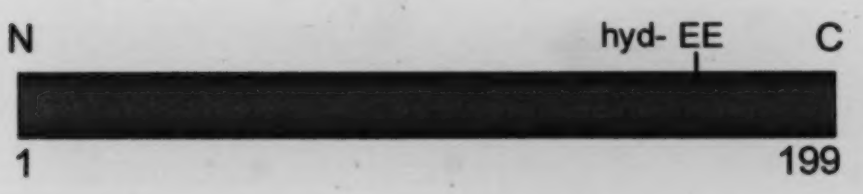

C.

		180	181		
Human		GAA	GAG	CCC	TTC
NP_009100	-hydrophobic-	E	E	P	F
Mouse		GAA	GAG	CCC	TTC
Q61907	-hydrophobic-	E	E	P	F
Rat		GAA	GAG	CCC	TTC
A47353	-hydrophobic-	E	E	P	F
Yeast		GAA	GAA	CCT	TTT
P03575	-hydrophobic-	E	E	P	F

Fig. 4.6 Site-Directed Mutagenesis of the Di-Glutamate Motif Decreases the Enzymatic and AdoMet-binding Activities of PEMT.

Cos-7 cells were transiently transfected with plasmids (3 µg) containing wildtype PEMT or epitope tagged PEMT derivatives, or mock transfected with empty pCI vector.

A. Cell homogenates (50 µg protein) were assayed for PEMT activity. The results are expressed as the mean of three separate experiments, each performed in duplicate, ± S.E.M, relative to the values obtained for similar assays on cells transfected with wildtype PEMT.

B. Immunoblot with anti-PEMT antibody using 25 µg protein of transfected cellular homogenates.

C. Microsomes (50 µg protein) prepared from transfected cells, were assayed for AdoMet binding activity. The results are expressed as the mean of three separate experiments, each performed in duplicate, ± S.E.M, relative to the values obtained for similar assays on microsomes from cells transfected with wildtype PEMT. Binding assays on microsomes from mock-transfected cells quantitated AdoMet bound by microsomal components other than PEMT. Binding activities of microsomes from cells expressing mutant PEMT proteins were expressed relative to the binding activity of microsomes from cells expressing the unmodified enzyme.

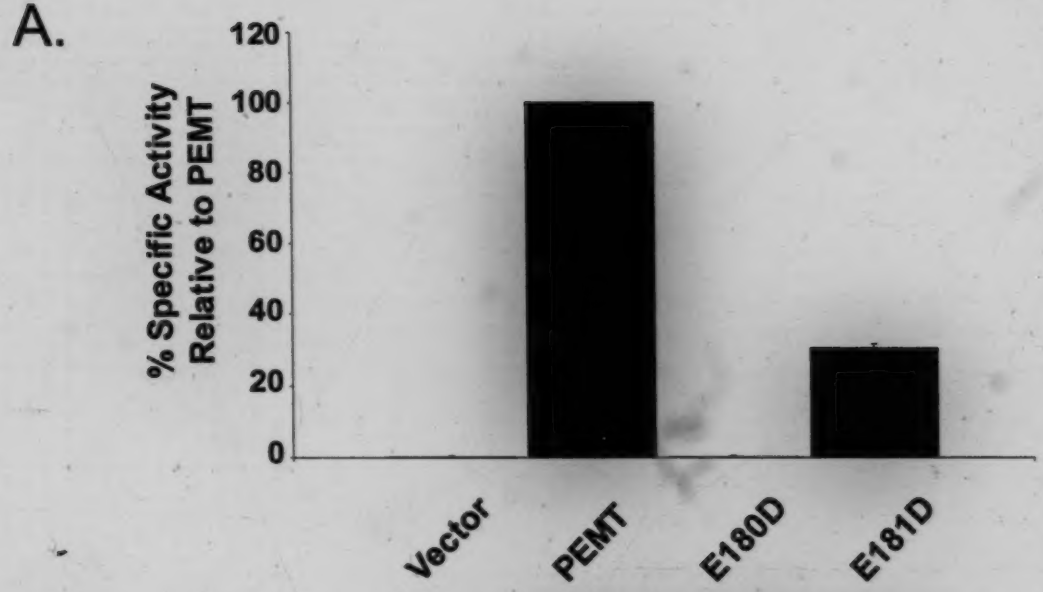
A.
% Specific Activity Relative to PEMT
120
100
80
60
40
20
0
Vector
PEMT
E180D
E181D

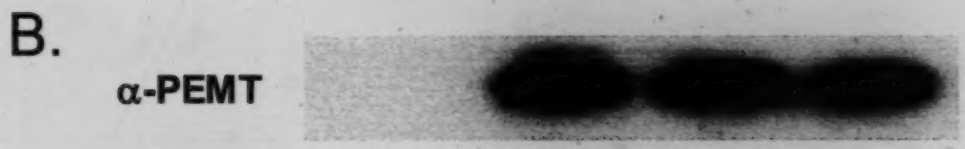
B.
α-PEMT

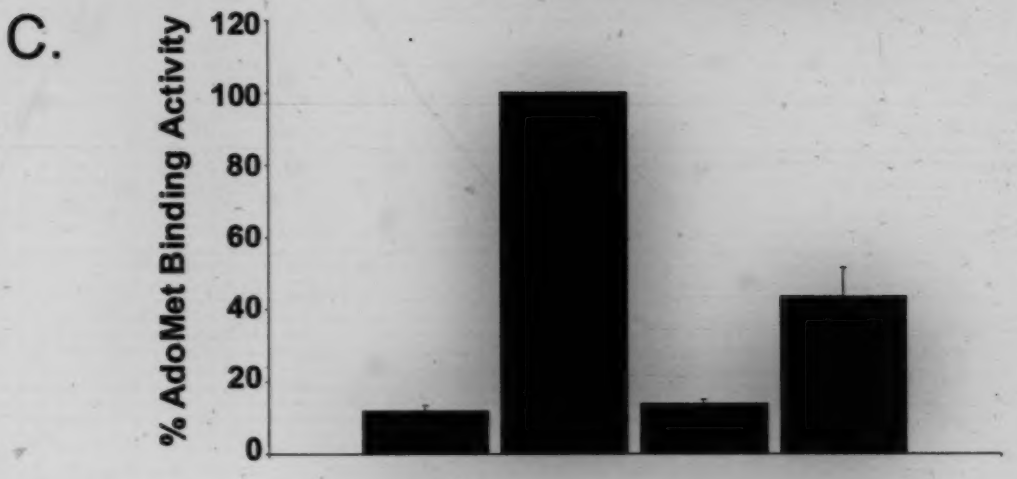
C.
% AdoMet Binding Activity
120
100
80
60
40
20
0

Fig. 4.7 Model of the Topographical Organization of the AdoMet Binding Site of PEMT.

Topographical model of PEMT is based on data from previous studies (22). Four transmembrane domains span the ER membrane in an orientation that positions the N and C termini external to the ER membrane. The positions of the GXG and di-glutamate motifs are indicated.

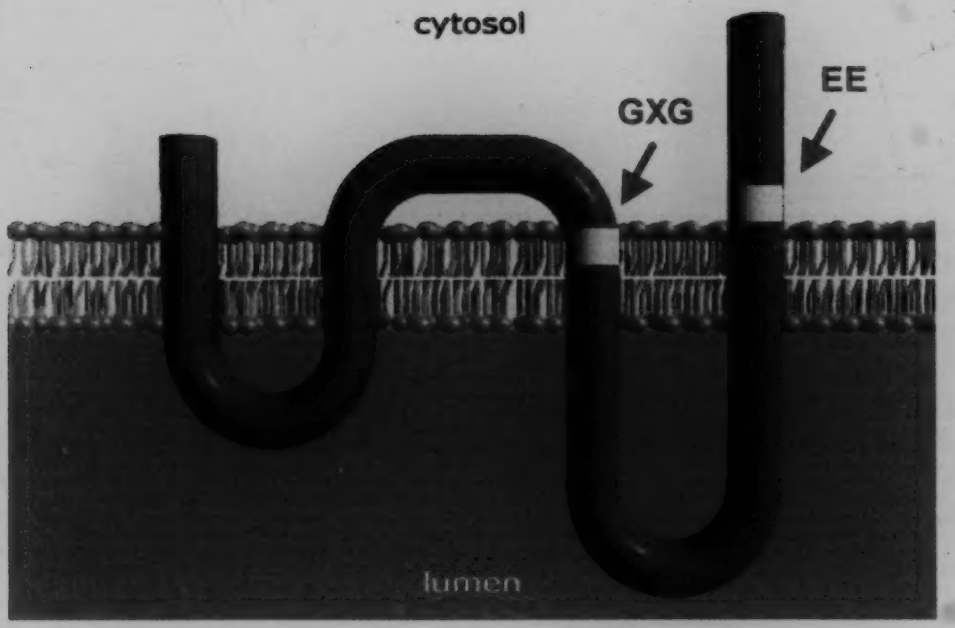
cytosol
GXG
EE
lumen

References

1. Vance, D. E., and Ridgway, N. D. (1988) *Prog. Lipid. Res.* **27**, 61-79

2. DeLong, C. J., Shen, Y. J., Thomas, M. J., and Cui, Z. (1999) *J. Biol. Chem.* **274**, 29683-8.

3. Reo, N. V., and Adinehzadeh, M. (2000) *Toxicol. Appl. Pharmacol.* **164**, 113-26.

4. Reo, N. V., Adinehzadeh, M., and Foy, B. D. (2002) *Biochim. Biophys. Acta.* **1580**, 171-88.

5. Kent, C. (1997) *Biochim. Biophys. Acta.* **1348**, 79-90.

6. Finkelstein, J. D., and Martin, J. J. (1986) *J. Biol. Chem.* **261**, 1582-7.

7. Fauman, E. B., Blumenthal, R.M., Cheng, X. (1999) in *S-Adenosylmethionine-Dependent Methyltransferases: Structures and Functions* (Cheng, X., Blumenthal, R.M., ed), pp. 1-32, World Scientific Publishing, Singapore

8. Fujioka, M. (1992) *Int. J. Biochem.* **24**, 1917-24.

9. Finkelstein, J. D. (1998) *Eur. J. Pediatr.* **157 Suppl 2**, S40-4.

10. Refsum, H., and Ueland, P. M. (1998) *Curr. Opin. Lipidol.* **9**, 533-9.

11. Vance, J. E., and Vance, D. E. (1986) *J. Biol. Chem.* **261**, 4486-91.

12. Nishimaki-Mogami, T., Suzuki, K., Okochi, E., and Takahashi, A. (1996) *Biochim. Biophys. Acta.* **1304**, 11-20.

13. Nishimaki-Mogami, T., Suzuki, K., and Takahashi, A. (1996) *Biochim. Biophys. Acta.* **1304**, 21-31.

14. Agellon, L. B., Walkey, C. J., Vance, D. E., Kuipers, F., and Verkade, H. J. (1999) *Hepatology* **30**, 725-9.

15. Noga, A. A., Stead, L. M., Zhao, Y., Brosnan, M. E., Brosnan, J. T., and Vance, D. E. (2003) *J. Biol. Chem.* **In Press**

16. Kagan, R. M., and Clarke, S. (1994) *Arch. Biochem. Biophys.* **310**, 417-27.

17. Posfai, J., Bhagwat, A. S., Posfai, G., and Roberts, R. J. (1989) *Nucleic. Acids. Res.* **17**, 2421-35.

18. Romano, J. D., and Michaelis, S. (2001) *Mol. Biol. Cell.* **12**, 1957-71.

19. Thompson, J. D., Higgins, D. G., and Gibson, T. J. (1994) *Nucleic. Acids. Res.* **22**, 4673-80.

20. Ho, S. N., Hunt, H. D., Horton, R. M., Pullen, J. K., and Pease, L. R. (1989) *Gene* **77**, 51-9.

21. Walkey, C. J., Shields, D. J., and Vance, D. E. (1999) *Biochim. Biophys. Acta.* **1436**, 405-12.

22. Shields, D. J., Lehner, R., Agellon, L. B., and Vance, D. E. (2003) *J. Biol. Chem.* **In Press**

23. Ridgway, N. D., and Vance, D. E. (1992) *Methods. Enzymol.* **209**, 366-74

24. Zhu, Y., Qi, C., Cao, W. Q., Yeldandi, A. V., Rao, M. S., and Reddy, J. K. (2001) *Proc. Natl. Acad. Sci. U.S.A.* **98**, 10380-5.

25. Cui, Z., Vance, J. E., Chen, M. H., Voelker, D. R., and Vance, D. E. (1993) *J. Biol. Chem.* **268**, 16655-63.

26. Lauster, R., Trautner, T. A., and Noyer-Weidner, M. (1989) *J. Mol. Biol.* **206**, 305-12.

27. Saraste, M., Sibbald, P. R., and Wittinghofer, A. (1990) *Trends. Biochem. Sci.* **15**, 430-4.

28. Scrutton, N. S., Berry, A., and Perham, R. N. (1990) *Nature* **343**, 38-43.

29. Farooqui, J. Z., Lee, H. W., Kim, S., and Paik, W. K. (1983) *Biochim. Biophys. Acta.* **757**, 342-51.

30. Clarke, S., and Banfield, K. (2001) in *Homocysteine in health and disease* (Carmel, R., and Jacobsen, D. W., eds), Cambridge University Press, 63-78

31. Stephens, R. S., Kalman, S., Lammel, C., Fan, J., Marathe, R., Aravind, L., Mitchell, W., Olinger, L., Tatusov, R. L., Zhao, Q., Koonin, E. V., and Davis, R. W. (1998) *Science* **282**, 754-9.

32. Arondel, V., Benning, C., and Somerville, C. R. (1993) *J. Biol. Chem.* **268**, 16002-8.

33. Cain, B. D., Donohue, T. J., Shepherd, W. D., and Kaplan, S. (1984) *J. Biol. Chem.* **259**, 942-8.

34. Wierenga, R. K., and Hol, W. G. (1983) *Nature* **302**, 842-4.

35. Ueland, P. M., Berge, R. K., Saebo, J., and Farstad, M. (1979) *FEBS. Lett.* **101**, 184-186

36. Finkelstein, J. D. (2001) in *Homocysteine in health and disease* (Carmel, R., and Jacobsen, D. W., eds), Cambridge University Press, 92-99

Chapter 5

Summary and Future Directions

Significant advances have been made recently in the field of methylation based PC biosynthesis. Purification of PEMT has been completed, enabling detailed study of the enzyme, and the encoding genes have been identified, characterized and even disrupted in the case of the mouse (1-7). However, the *Homo sapiens* orthologue has not been afforded such detailed analysis and consequently, research on PEMT in our species has been significant only by its absence. Thus, the overall goal of this thesis was to provide the first in depth examination of human PEMT.

In preliminary studies of human PEMT we cloned three cDNAs, each of which has a different 5' untranslated region (5'UTR). To determine the origin of PEMT splice variants and to investigate expression of the gene in human liver, we isolated a bacterial artificial chromosome (BAC) clone containing the full-length human gene. Nine exons were defined in a gene that spans ~85 kB of a region on the antisense strand of chromosome 17p11.2. Each of the three unique untranslated first exons is present in a contiguous array in the 5' region of the gene, confirming the integrity of the cDNAs and alternative processing of PEMT transcripts.

Human liver, heart and testis contain the highest levels of PEMT transcripts and of these, liver has the greatest PEMT expression. Furthermore, each of the three PEMT transcripts is present in varying abundance in liver whereas heart and testis contain only one and two transcripts, respectively. Thus, we demonstrated that differential promoter

usage in the human *PEMT* gene generates three unique transcripts and confers a tissue-specific expression pattern. In addition to being the first investigation of a gene encoding an enzyme of human phospholipid biosynthesis, this study also provided the impetus for the re-examination of the murine *Pemt* gene locus. Subsequently, alternate PEMT transcripts were identified in the mouse (Leiter, E., personal communication).

Although we demonstrated differential abundance of the three PEMT transcripts in the liver, precise quantitation of the transcripts remains to be completed. Additional future studies should focus on the tissue-specific transcriptional regulation of human PEMT. Three putative promoter regions have been identified, as well as several consensus transcription factor-binding sites, for factors implicated in tissue-specific gene expression. Combined, this data represent a definitive starting point for these studies. The differences between fetal and adult PEMT expression may also be the subject of further investigation. Alternate studies may include *in situ* hybridization and *in situ* PCR of human liver samples. This would resolve whether zonation of PEMT transcripts exists in human liver and may provide additional insight into the raison d'être of PEMT, as different regions of the liver are associated with distinct hepatic functions (8).

Once the liver was identified as the primary site of human PEMT expression, we attempted to characterize the enzyme at the subcellular level. PEMT has long been recognized as an integral membrane protein but

the structural organization of the enzyme within the membrane had not been elucidated. Biochemical analysis of human liver revealed that the PE-methyltransferase activity is primarily localized to the endoplasmic reticulum and mitochondrial-associated membranes. Bioinformatic analysis of the predicted amino acid sequence suggested that the enzyme adopts a polytopic conformation in those membranes.

Data from endoproteinase-protection analysis studies suggest a topographical model of PEMT; four transmembrane regions span the membrane such that both the N and C termini of the enzyme are oriented towards the cytosol. Two hydrophilic connecting loops protrude into the lumenal space of the microsomes whereas a corresponding loop on the cytosolic side remains proximate to the membrane. Alternatively, the external loop may simply adopt a conformation that renders the endoproteinase cleavage site inaccessible to digestion. As the primary structure, and in particular the predicted transmembrane regions, are highly conserved, this model may prove representative of the mammalian PEMT enzymes.

Although PEMT is localized in the ER and MAM membranes, factors mediating the targeting of PEMT to a specific subcellular localization remain to be identified. Initial studies in this area may focus on the C-terminal region of the enzyme that contains a putative ER retention motif (xHKRx).

Additionally, factors that mediate the topogenesis of PEMT in the ER and MAM membranes are as yet unresolved.

Analysis of mice lacking a functional *PEMT* gene revealed a severe reduction in plasma homocysteine levels. Homocysteine is generated by the hydrolysis of AdoHcy, which is a product of the PEMT reaction. To gain insight into the mechanism by which PEMT regulates homocysteine levels, we sought to define the residues required for binding of the methyl group donor, AdoMet. Using bioinformatic analysis of the predicted amino acid sequence of human PEMT, we identified two putative AdoMet binding motifs (^{98}Gx^{100}G & ^{180}E^{181}E).

Site-directed mutagenesis experiments demonstrated the requirement of the conserved motifs for PEMT specific activity. Analysis of the AdoMet binding ability of mutant recombinant PEMT derivatives established a role for the motifs in binding of the AdoMet moiety. Whereas the residues, ^{98}G and ^{181}E influenced enzymatic efficiency, the residues ^{100}G and ^{180}E are absolutely essential for the AdoMet binding activity of the human PEMT enzyme. A model of PEMT based on our data juxtaposes the two separate AdoMet binding motifs, at the cytosolic side of the endoplasmic reticulum membrane.

Combined, the data from our topographical and AdoMet studies provide insight into the orientation of the putative AdoMet binding site

relative to the ER lumen and cytosol. This suggests a model for the mechanism by which PEMT gains access to the methyl group donor required for the generation of the essential biomolecule, PC.

While additional residues may be required for binding the AdoMet moiety, future investigations should include the search for residues that bind the PEMT substrate, PE. Bioinformatic analysis of the enzymes that bind PE should prove invaluable with regard to the identification of candidate residues for evaluation. Identification of the PE binding site(s) will enable the formulation of an enzymatic model for the PEMT-catalyzed transmethylation reaction.

In conclusion, this thesis describes a tri-faceted investigation of PEMT in the human species. Whereas certain findings may be exclusive to the human PEMT orthologue, such as the tissue-specific processing of transcripts, data on the topography and AdoMet binding site of PEMT could prove invaluable to the study of all mammalian PEMT enzymes. Definitive characterization of the role of PEMT in humans may now begin in earnest.

References

1. Ridgway, N. D., and Vance, D. E. (1987) *J. Biol. Chem.* **262**, 17231-9.

2. Ridgway, N. D., and Vance, D. E. (1988) *J. Biol. Chem.* **263**, 16864-71.

3. Ridgway, N. D., and Vance, D. E. (1988) *J. Biol. Chem.* **263**, 16856-63.

4. Ridgway, N. D., Yao, Z., and Vance, D. E. (1989) *J Biol Chem* **264**, 1203-7.

5. Kanipes, M. I., Hill, J. E., and Henry, S. A. (1998) *Genetics* **150**, 553-62.

6. Walkey, C. J., Cui, Z., Agellon, L. B., and Vance, D. E. (1996) *J. Lipid. Res.* **37**, 2341-50.

7. Walkey, C. J., Donohue, L. R., Bronson, R., Agellon, L. B., and Vance, D. E. (1997) *Proc. Natl. Acad. Sci. U S A.* **94**, 12880-5.

8. Jungermann, K., and Kietzmann, T. (1996) *Annu. Rev. Nutr.* **16**, 179-203